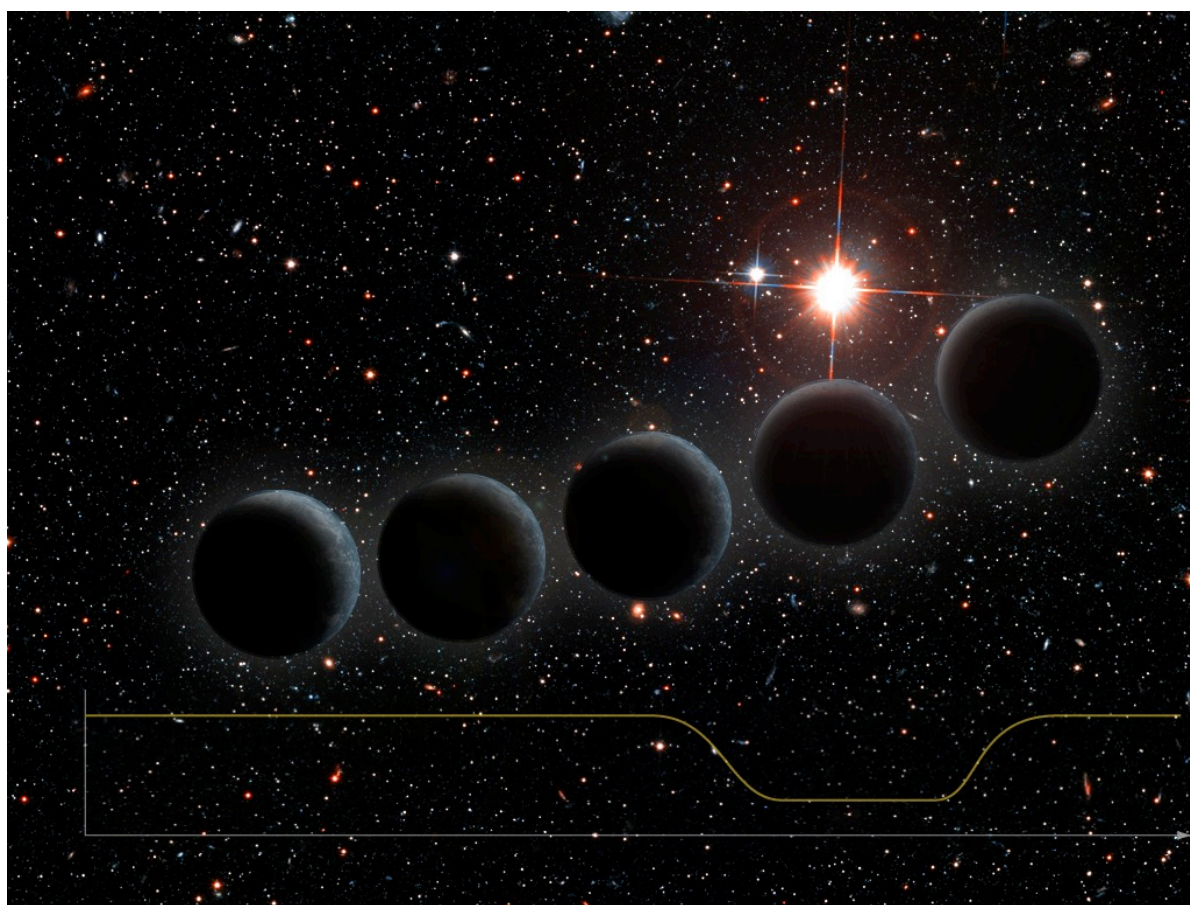


PLATO

Next-generation planet finder



Assessment Study Report

PLATO – the exoplanetary system explorer

Table 1-1: Summary of CV 2015-2025 candidate mission PLATO.

Science:			
Key scientific objectives	<ul style="list-style-type: none"> - Simultaneous detection and characterization of exoplanetary systems of all kinds, including both the planets and their host stars, reaching down to small, terrestrial planets in the habitable zone; - Identification of suitable targets for future, more detailed characterization, including spectroscopic search for biomarkers in nearby habitable exoplanets. 		
Observational concept	<ul style="list-style-type: none"> - Ultra-high precision, long (few years), uninterrupted photometric monitoring in the visible band of very large samples of bright stars. These samples, with m_V between 8 and 11, is the backbone of the PLATO mission, and is considered as the highest priority objective. - Ground-based follow-up programme, in particular very precise radial velocity monitoring 		
Mission concept:			
Primary data product	Very accurate optical light curves and centroid curves of large numbers of bright stars		
Payload concept	Ensemble of many wide-field co-aligned telescopes, each telescope with its own CCD-based focal plane array		
Observing plan	Two long monitoring phases (3 years and 2 years), each one with a single field monitored One-year additional "step & stare" phase with several successive fields monitored for a few months each		
Duty cycle	≥ 95%		
Launch and orbit:			
	<ul style="list-style-type: none"> • Launch by Soyuz-Fregat 2B1 from Kourou in 2017 • Transfer to L2, then large amplitude libration orbit around L2; elliptical (a=500k km, b=400k km) • Eclipse-free 		
Mission lifetime:			
	<ul style="list-style-type: none"> • 2 years (goal 3) observation of sky region 1 • 2 years (goal 3) observation of sky region 2 • 2 years observation on step& stare mode 		
Radiation environment:			
	<ul style="list-style-type: none"> • Sun-Earth L2 – relatively benign environment 		
Spacecraft specifications:			
Stabilisation	3-axis		
Telemetry band	X-band (10 MHz maximum bandwidth)		
Average downlink capacity	109Gb per day (Assumption: ground station contact for 4 hours per day, 3.5 hours for data downlink with a data downlink rate of 8.7 Mbps)		
Pointing stability	0.2 arcsec rms over 14 hours		
Mass	Concept A	Concept B	Concept C
Payload incl. 20% system margin	1174 kg	1164 kg	1379kg
Platform incl. 20% system margin	744 kg (incl. 118 kg sun shield)	605 kg	n/a
Total dry mass incl. 20% system margin, excl. launch adapter	1918 kg	1925 kg (incl. 156 kg sun shield)	n/a
Antenna	2 steerable	1 fixed	1 fixed TBD

Power			
Solar array mounting	Deployable with 1 degree of freedom steerable mechanism	body mounted	body mounted TBD
Solar array size	8 m ²	13.2 m ²	n/a
Power consumption (incl. 20% system margins)	1.4 kW average 1.5 kW peak	1.7 kW average 1.7 kW peak	n/a n/a
Payload specifications:			
	Concept A	Concept B	Concept C
Optical system	2 mirrors/telescope	6 lenses per telescope (all spheric)	6 lenses per telescope (4 spheric and 2 aspheric)
Total number of telescopes	12	54	42
Total number of CCDs	176	120	168
Instantaneous field of view	2×900 deg ²	625 deg ²	1800 deg ²
Collecting area per target	0.15m ²	0.29 m ²	0.12/0.24/0.48 m ² depending on the location in the field
Focal planes	176 CCDs with 2080×2574 27µm pixels	120 CCDs with 3000×6000 18µm pixels	168 CCDs with 3584×3584 18µm pixels
Pointing strategy	one 180 deg rotation around the line of sight every 6 months	one 30 deg rotation around the line of sight every month	one 90 deg rotation around the line of sight every 3 months
Key mission drivers:			
	<ul style="list-style-type: none"> • Parts procurement (lenses, CCDs,...) • Integration and verification (AIV) of large number of telescopes, lenses, focal plane arrays • Payload accommodation (mass and volume) 		
Key technology development:			
	<ul style="list-style-type: none"> • Deployable sunshield for Concept A • CCD pre-development for all designs • Telescope prototype needed for all designs 		

Foreword

The PLATO mission was proposed in 2007 as a medium class candidate in response to the first call for missions of the Cosmic Vision 2015-2025 program. The proposal was submitted by Dr. Claude Catala (Observatoire de Paris) on behalf of a large consortium of more than 150 scientists from laboratories all across Europe. Following favorable reviews by ESA's scientific advisory bodies, PLATO was selected in 2007 as one of the missions for which an assessment study has been carried out in 2008 and 2009 by ESA, supported by the PLATO Study Science Team (PSST).

Its scientific objectives are to detect and characterize transiting exoplanetary systems of all kinds (including both the exoplanets and their host stars), in particular small, telluric planets in their habitable zones. PLATO will perform a detailed seismic analysis of the planet host stars, allowing a precise determination of their radii, masses and ages, from which the radii, masses and ages of the exoplanets will be derived. This will provide a complete characterization of the exoplanetary systems, including their evolutionary status, and enabling us to deduce the nature of the planetary bodies (e.g. ocean or rocky planets etc). These objects will be prized targets for future more detailed characterization, including the search for biomarkers in their atmospheres.

These goals will be achieved by highly accurate time-resolved photometry of a large number of bright and nearby stars, coupled to a vigorous ground-based follow-up programme. The initial PLATO proposal included two concepts: the 'staring' concept whereby a wide field-of-view was continuously monitored for several years by a fixed instrument composed of a large number of co-aligned small telescopes; and the 'spinning' concept consisting of a spinning satellite scanning a great circle of the sky.

In a first phase of the study (2007), the staring concept was selected by the PSST as the most efficient one to reach the science objectives, and the mission was further studied within the ESA Concurrent Design Facility (CDF) in 2007/2008, leading to a design suitable for feasibility assessment and production of an Invitation to Tender (ITT) toward Industry. Consequently, two concurrent industrial contracts for a study of the full mission were issued in 2008. At the same time, a consortium consisting of scientists from ESA member states (PLATO Payload Consortium, PPLC) was initiated to make an independent study of the payload alone, under leadership of Dr. Claude Catala (Observatoire de Paris, France). All three studies have been running in parallel and were completed simultaneously at the end of summer, 2009.

The three concepts resulting from these studies differ significantly from one another, but all three studies conclude that the PLATO mission is technically fully feasible, at no technological risk.

A PLATO Science Consortium (PSC) was also set up in 2008, in parallel to the PPLC, under leadership by Dr. Don Pollacco (Queens University, Belfast, UK), and has been actively working on the scientific preparation of the PLATO mission.

This report describes the results of all these various studies, both on the scientific and technical points of view. It results from a vast team effort, involving many different parties (ESA CDF, PSC, PPLC, industrial companies), under general supervision by the PLATO study science team (PSST) and the ESA study team.

The members of the ESA PLATO Science Study Team (PSST) were:

C. Catala Observatoire de Paris, France
J.M. Mas-Hesse CAB (CSIC-INTA) Madrid, Spain
G. Micela INAF, Osservatorio di Palermo, Italy
E. Poretti INAF-Osservatorio di Brera, Merate, Italy
D. Pollaco Queens University, Belfast, United Kingdom
H. Rauer DLR, Berlin, Germany
I. Roxburgh Queen Mary University of London, London, UK
S. Udry Geneva Observatory, Geneva University, Switzerland
C. Aerts University of Leuven, Belgium (until December 2008)
T. Arentoft University of Aarhus, Aarhus, Denmark (until June 2009)

The team members from the ESA Directorate of Science and Robotic Exploration were:

M. Fridlund Study Scientist
R. Lindberg Study Manager
D. Lumb Payload Manager (until February 2009)
A. Stankov Payload Manager (from February 2009)
P. Gondoin Assistant study manager during CDF phase

Members of the ESA planning and coordination office during the study have been: M. Coradini, P. Escoubet, F. Favata and T. Prusti

Additional contributions to this study were made by:

C. Afonso, Heidelberg, D, **Y. Alibert**, Besancon, F, **S. Aigrain**, Oxford, UK, **M. Barbieri**, Padova, I, **Willy Benz**, Bern, CH, **J. Cabrera**, Berlin, D, **Sz. Csizmadia**, Berlin, D, **J. Christensen Dalsgaard**, Aarhus, DK, **H. Deeg**, Tenerife, E, **M. Deleuil**, Marseille, F, **S. Desidera**, Padova, I, **X. Dumusque**, CAUP, Porto, P, **R. Dvorak**, Wien, A, **A. Erikson**, Berlin, D, **L. Gizon**, Katlenburg-Lindau, D, **L. Grenfell**, Berlin, D, **H. Lammer**, Graz, A, **R. Neuhäuser**, Jena, D, **A. Hatzes**, Tautenburg, D, **I. Pagano**, Catania, I, **G. Piotto**, Padova, I, **R. Ragazzoni**, Padova, I, **A. Smith**, MSSL, UK, **F. Sohl**, Berlin, D **D. Walton**, MSSL, UK, **W.W. Weiss**, Wien, A, **W. Zima**, Leuven, B

Important contributions to the mission design were made by Astrium Satellites, Thales Alenia Space, E2V, LIDAX.

Executive summary

Main goals of PLATO

PLATO is the next generation planetary transit experiment; its objective is to characterize exoplanets and their host stars in the solar neighbourhood. While it builds on the heritage from CoRoT and Kepler, the major breakthrough to be achieved by PLATO will come from its strong focus on bright targets, typically with $m_v \leq 11$. The PLATO targets will also include a large number of *very bright and nearby stars*, with $m_v \leq 8$.

The prime science goals of PLATO are:

- the detection and characterization of exoplanetary systems of all kinds, including both the planets and their host stars, reaching down to small, terrestrial planets in the habitable zone;
- the identification of suitable targets for future, more detailed characterization, including a spectroscopic search for biomarkers in nearby habitable exoplanets.

These ambitious goals will be reached by ultra-high precision, long (few years), uninterrupted photometric monitoring in the visible band of very large samples of (pre-selected, low activity) bright stars, which can only be done from space. The resulting high quality light curves will be used on the one hand to detect planetary transits, as well as to measure their characteristics, and on the other hand to provide a seismic analysis of the host stars of the detected planets, from which precise measurements of their radii, masses, and ages will be derived. For the brightest targets, planets are also expected to be detectable through the modulation of stellar light reflected on the planet surface, and/or through the astrometric wobble induced on the star by the planet orbital motion.

The PLATO space-based data will be complemented by ground-based follow-up observations, in particular very precise radial velocity monitoring, which will be used to confirm the planetary nature of the detected events and to measure the planet masses.

The full set of parameters of the systems with detected exoplanets will thus be measured, including all characteristics of the host stars and their orbits, radii, masses, and ages of the planets. Measurements of the radii and masses will be used to derive the planet mean densities and therefore will give insight on their internal structure and composition. The orbital parameters, together with the precise knowledge of all characteristics of the host star, will enable us to estimate the temperature and radiation environment of the planets. Finally, the knowledge of the age of the exoplanetary systems will allow us to put them in an evolutionary perspective.

PLATO in the wider context

PLATO will address the basic question of the existence, distribution, evolutionary state, and characteristics of exoplanets in the solar neighbourhood. Answers to these questions are essential to understand how planetary systems, including our own, are formed and evolve, and also as a first and necessary step to understand whether life can exist elsewhere in the Universe, and locate potential sites for life. Since the discovery of the first exoplanet in 1995, this field has seen a remarkable development, with about 400 exoplanets known as of the end of October 2009. Most of these objects are giant planets in close-in orbits, but continuous progress in the precision of radial velocity observations is now enabling the detection of "super-Earths", with masses just a few times that of the Earth.

Exoplanet discovery has been recently boosted with the launch of the CoRoT satellite in December 2006, followed by that of *Kepler* in March 2009. The discovery of CoRoT-7b, the very first small telluric, rocky planet with measured radius and mass, and therefore with a known density, has opened up a new era, in which the CoRoT extended mission and *Kepler* are now playing a major role.

Both CoRoT and *Kepler* target rather faint stars, up to $m_v = 15$ and beyond. Their ground-based follow-up, in particular in radial velocity monitoring, is made difficult by this relative faintness. As a consequence, ground

confirmation and mass measurements are restricted to the largest of the CoRoT and *Kepler* planets, which severely impacts the scientific return of these two missions. While we can today with CoRoT, and soon with NASA's *Kepler* mission, detect the passage of a planet the size of our own world, *it is impossible to confirm the presence of such an object found by either spacecraft with the required precision*. Moreover, even in cases where radial velocities can be measured to the required precision to confirm the planetary nature of the detected event and measure the planet-to-star mass ratio, our knowledge of the faint host stars is still too poor to allow us to derive estimates of the planet radii, masses and ages to a sufficient accuracy to significantly constrain their structure and state of evolution.

The main goal of PLATO is to alleviate these severe difficulties by focusing on bright stars, typically 3 to 4 magnitudes brighter than CoRoT and *Kepler*, and also by including in its target list a large sample of very bright ($m_v \leq 8$) and nearby stars. This will bring three decisive advantages:

- the ground-based follow-up observations will be greatly facilitated, and the required precision will be reached to confirm small, terrestrial planets in the habitable zone and to determine their masses;
- the host stars of the detected planets will be studied in detail, in particular via seismic analysis using the PLATO data themselves; seismic analysis, *i.e.* the measurement of stellar oscillations, will be used to probe the internal structure of these stars, and determine their radii, masses, and ages in a precise and reliable way;
- the detection of exoplanets orbiting very bright and nearby stars will allow us to identify the best targets for subsequent detailed follow-up observations, both from space (*e.g.* JWST) and from the ground (*e.g.* E-ELT), including in particular spectroscopy of their surfaces and atmospheres, in the search for biomarkers.

PLATO additional science

PLATO will deliver a database of stellar variability, with time scales ranging from minutes to years, with photometric precisions well below one millimag, on several hundreds of thousands of stars. In addition to the primary science goals, the PLATO data will therefore allow a variety of other scientific programs to be carried out, in various areas of stellar physics, stellar formation, as well as in solar-system studies.

PLATO observation strategy

The basic PLATO science product will be a very large sample of ultra-high precision stellar light curves, obtained on very long time intervals (up to 3 years) and with very high duty cycle ($\geq 95\%$). The main requirement is to obtain a photometric precision better than 2.7×10^{-5} in one hour for more than 20,000 cool dwarfs and subgiants brighter than approximately $m_v=11$, and 8.0×10^{-5} in one hour for 250,000 stars down to $m_v=13-14$.

In order to reach this goal, PLATO will monitor two successive very wide fields, one for 3 years, the other one for 2 years (goal 3 years). These two long monitoring sequences will be followed by a one- or two-year step-and-stare phase, during which a number of fields will be monitored for several months each. This step-and-stare phase will bring flexibility to the mission, allowing for instance to survey a very large fraction of the whole sky (up to 42% depending on the selected concept), as well as to re-visit particularly interesting targets identified during the long monitoring phases.

The spacecraft is intended to be launched in late 2017 on a Soyuz-Fregat rocket for injection into a Lissajous Orbit around the L2 Lagrangian point. This will give a nominal lifetime of 6 years, which is compatible with the example observation strategy outlined above.

PLATO payload

The PLATO mission was subject to three independent studies, two by industrial contractors and one by the PLATO PayLoad Consortium (PPLC). All three studies have been running in parallel and were completed simultaneously at the end of summer, 2009. The outcome is reported in the present document and forms, together with the documentation provided by the three study entities, the basis for the evaluation of the mission for the future.

The three concepts resulting from these studies differ significantly from one another, but have in common optical designs with very wide fields-of-view, and overall large collecting areas. Wide fields-of-view are

required to obtain large samples of bright stars, while large collecting areas are necessary to reach the desired photometric precision. In all three concepts, this is achieved by using a collection of small, optically fast, wide-field telescopes, each with its own CCD-based focal plane. The light and centroid curves from each individual telescope unit are transmitted to the ground at the required cadence, where they are co-added to reach the desired precision.

In concept A, the chosen solution has 12 reflective telescopes with a field-of-view of about 1800 deg², and a total collecting area for each observed star of 0.15 m², while concept B is using 54 refractive telescopes with a field-of-view of 625 deg², and a total collecting area for each observed star of 0.29 m². Concept C proposes a different arrangement with 42 refractive telescopes. In the two first solutions, all telescopes are pointed in the same direction and are covering the same field. Concept C instead has the telescopes grouped in 4 sections, each section having its line of sight offset from the next one by one-half of the field-of-view. This overlapping line-of-sight arrangement results in a total surveyed field of about 1800 deg², each star being observed either by 10, 20, or 40 telescopes, with a resulting collecting area of 0.12, 0.24, or 0.48 m², depending on the star's position in the field.

All three designs are shown to be compliant with the science requirements, and to be feasible at no technological risk. The reliability of the PLATO concept is supported by the fact that three viable optical solutions have been found, which can be traded off against one another before the start of the definition phase.

Operations and data policy

The PLATO Science Operation Centre (SOC) will be responsible for producing and distributing the validated light curves, which are the basic PLATO science products. Further scientific treatment and exploitation of these data, leading to high scientific added-value products, will be performed in one or several nationally funded PLATO data centre(s).

It is foreseen that most PLATO data produced by the SOC will be made public immediately after their validation, with no proprietary time. However, a small number of light curves, of the order of a few hundreds out of the several hundreds of thousands available targets, will remain propriety of the co-Is for one year after validation of the corresponding data. These proprietary targets will be selected prior to the launch.

Conclusions

PLATO will discover and characterize exoplanetary systems, including both the planets and their host stars, in the solar neighbourhood. PLATO will be the next generation mission in this area, building on the experience accumulated in Europe with the CoRoT satellite, and in the US with the *Kepler* mission. By focusing on bright and nearby targets, it will provide a full census of exoplanets down to small, low mass, terrestrial planets, orbiting their host stars in the habitable zone, *i.e.* in principle able to sustain life. Due to the brightness of the planet host stars, the full and exquisite knowledge that will be gained on them, including *via* seismic analysis using PLATO data, will allow us to fully characterize the detected exoplanetary systems.

PLATO will therefore represent a crucial step forward after the CoRoT and *Kepler* missions. It will capitalize on the strong European expertise in the field of exoplanet science, accumulated through the development and exploitation of the CoRoT mission, as well as through many years of ground-based efforts. It will also benefit from the outstanding achievements of asteroseismology, where European scientists are playing a leading role, in particular through their involvement in CoRoT and the seismology program of *Kepler*.

More generally, the efforts of the European scientific community in the fields of stellar and exoplanetary astrophysics, in particular in space with missions such as Hipparcos, CoRoT, the aborted Eddington mission, the strong European involvement in the *Kepler* asteroseismic program, and with the upcoming Gaia mission, constitute a powerful and very convincing roadmap to a full understanding of planetary and stellar evolution.

The PLATO mission, with its strong synergy with Gaia, clearly represents a natural and unique opportunity to continue on this same road, and bring European lead in these areas to full fruition. It will open the way for future space missions and ground-based facilities that will aim at exploring in detail exoplanets, especially Earth-like ones, and search for signatures of life in the Universe.

Table of content

1	INTRODUCTION	12
2	SCIENTIFIC OBJECTIVES	16
2.1	Very low-mass planets are common around solar-type stars	16
2.2	PLATO main science goals	18
2.3	Tools at our disposal to reach PLATO's goals	19
2.3.1	Wide-field, long, continuous and high-precision photometric monitoring	20
2.3.2	Precise radial velocity measurements	23
2.3.3	The determination of precise stellar parameters	24
2.3.4	Difficulties and challenges	25
2.4	Characterization of exoplanet host stars	26
2.4.1	Stellar radii from Gaia	26
2.4.2	Determination of stellar masses and ages	26
2.4.3	Basic principles of asteroseismology	27
2.4.4	Model independent inversions for the stellar mass	28
2.4.5	Model fitting to get masses and ages	29
2.4.6	Seismic achievements from CoRoT	30
3	SCIENTIFIC REQUIREMENTS	31
3.1	Basic observation strategy	31
3.2	Star counts	32
3.3	PLATO high level science requirements	34
3.3.1	Required noise levels and monitoring durations	34
3.3.2	Basic measurement principle; PLATO products	34
3.3.3	Surveyed field	34
3.3.4	Stellar samples and photometric noise level	35
3.3.5	Duration of monitoring	36
3.3.6	Time sampling	36
3.3.7	Photon noise versus non-photonic noise	36
3.3.8	Overall duty cycle	36
3.3.9	Colour information	37
3.3.10	The need to go to space	37
4	EXPECTED PERFORMANCES	39
4.1	The PLATO end-to-end simulator	39
4.2	Impact of confusion and contamination	40
4.3	Expected noise level	41
4.4	Expected numbers of targets	42
5	GROUND-BASED SUPPORT	44
5.1	Limitations to precise radial velocity follow-up measurements	44
5.2	Timescales of intrinsic variations and optimal observing strategy	46
5.3	Organization of the follow-up	48
5.4	Preparatory observations	50
6	SCIENTIFIC IMPACT OF PLATO	51
6.1	Samples of Exoplanets: from Giants down to Earths	51
6.2	Planet characterisation	52
6.3	Expected number of planet transit detections	54
6.4	Additional Exoplanet Investigations	55
6.4.1	Reflected stellar light	55
6.4.2	Astrometric detection of planets	56
6.4.3	Secondary transits	56
6.4.4	Rings and moons	57
6.4.5	Transit timing variations	57

6.5	PLATO objects as targets for atmospheric studies	57
6.5.1	Follow-up with complementary space facilities	57
6.5.2	Imaging and spectroscopy with the E-ELT	58
6.6	Planet dynamics	58
7	ADDITIONAL SCIENCE	59
7.1	Asteroseismology and stellar evolution	59
7.2	General Astrophysics	61
8	PAYLOAD	62
8.1	Industrial studies – Design Concept A	63
8.1.1	Optical reference design	63
8.1.2	Focal plane instrument	65
8.1.3	Front end electronics	66
8.1.4	Data handling	66
8.1.5	Structures	67
8.1.6	Thermal sub-system	68
8.1.7	Operating Modes	69
8.1.8	Interface requirements	69
8.2	Industrial studies – Design Concept B	70
8.2.1	Optical reference design	70
8.2.2	Focal plane instrument	72
8.2.3	Front end electronics	74
8.2.4	Data handling	74
8.2.5	Structures	74
8.2.6	Thermal sub-system	76
8.2.7	Operating Modes	76
8.2.8	Interface requirements	76
8.3	Design Concept C	77
8.3.1	Optical reference design	78
8.3.2	Focal plane instrument	79
8.3.3	Front end electronics	80
8.3.4	Data handling	80
8.3.5	Structures	81
8.3.6	Thermal sub-system	82
8.3.7	Operating Modes	82
8.3.8	Interface requirements	83
8.4	Instrument Performance Model, Performance Prediction and Compliance	83
8.4.1	Instrument Performance	83
8.4.2	Compliance Matrix	85
9	MISSION DESIGN	87
9.1	Maximising Observed Number of Stars	87
9.2	Mission Profile	87
9.3	Mission Scenario	88
9.4	Design Concept A	89
9.4.1	Observation Strategy	89
9.4.2	Service Module and Spacecraft Sub-systems	89
9.4.3	Structural Design	89
9.4.4	Propulsion and Attitude and Orbit Control Sub-systems	89
9.4.5	Power and Thermal Sub-systems	90
9.4.6	Communications and Data-handling Sub-systems	90
9.5	Design Concept B	91
9.5.1	Observation Strategy	91
9.5.2	Service Module and Spacecraft Sub-systems	91
9.5.3	Structural Sub-system	91
9.5.4	Propulsion and AOCS Sub-systems	92

9.5.5	Power and Thermal Sub-systems	92
9.5.6	Communications and Data-handling Sub-systems	92
9.6	Design Concept C	93
9.6.1	Observation Strategy	93
9.6.2	Service Module	94
9.7	Budgets Summary	94
9.7.1	Mass Budget	94
9.7.2	Power budgets	95
9.7.3	Link budgets	96
9.8	Development Plan	96
9.9	Technology Readiness Level	96
10	MISSION OPERATIONS	98
10.1	Mission Operations Centre	98
10.1.1	Scope	98
10.1.2	Operational Concept Goals	98
10.1.3	Mission Planning, Spacecraft Monitoring and Control	99
10.1.4	Orbit and Attitude Control	100
10.1.5	Communications	100
10.1.6	Ground Segment Design	100
10.2	Science Operations	102
10.2.1	Concept	102
10.2.2	Data products and processing	102
10.2.3	Observing modes	104
10.2.4	Structure of the PDAAS	104
11	MANAGEMENT	107
11.1	Preliminary Procurement Approach	107
11.1.1	Industrial Organisation	107
11.1.2	Payload Procurement	107
11.2	PLATO Schedule	108
11.3	List of acronyms	110
12	REFERENCES	112

1 INTRODUCTION

The question of the existence of life beyond the Earth has been a concern of humanity for several thousand years. In order to understand ourselves better we need to know what our true place is in the Universe, and in the greater scheme of things. Are we just one of many instances of life, evolving on a common class of planet to the point that we have begun to enquire of our origins? Or are we unique? Born in a very special place and under very extraordinary circumstances? We still do not know, but for the first time in the history of mankind we are able to address these questions as we now have the technology to do so.

In this context, significant effort is now being spent at ESA within the Robotic Exploration programme in the search for present or past life on other bodies in the Solar System. Although success in these endeavours would be a great achievement, and would provide us with much needed information, the Solar System is just a miniscule speck in the Cosmos and within the Milky Way galaxy. Furthermore, all of the Solar System originated out of the same primordial nebula at the same time. Thus if any rare and special conditions were relevant to the origin of the Earth and life on it, it would not be strange if the same conditions applied to *e.g.* Mars.

If we want to understand our real place in the Universe, we must thus also look outside the Solar System. As far as we know, life only arises on or near the surface of planets. The first question that must be asked is if planets are common in our Galaxy? This question has recently (in the last 15 years) been answered. Literally one planet orbiting a star other than the Sun is, at the moment, *found every week!*

We thus assume that life in the Universe is intimately connected with planets. Also, although some scientists have suggested ecologies in the atmosphere of Jupiter like planets (*e.g.* Sagan & Salpeter, 1976), the currently held opinion is that in order for life to arise and establish itself, you need a small 'rocky' world with liquid water and thus a benign temperature, just like our own Earth. The search for and study of planetary systems like our own, around other stars, and in particular the search for the signatures of life in exoplanetary systems, is thus a prerequisite towards generalising our understanding about the distribution of life in the Universe and how it may have once arisen on the Earth.

Planet formation and evolution theory is at the centre of this problem. In order to understand the origin of life and to determine where it is most likely to exist in the Universe, a full understanding of planet formation and the evolution of planetary bodies is an absolute necessity. We need to measure accurately the distribution of planet sizes, masses and orbits, at least down to Earth-sized planets, and to determine which of these planets are likely to be habitable. As importantly, we need to determine their age. Only then will we be able to relate all characteristics of the planets to the evolutionary history and age of the exoplanetary systems, and determine under which initial conditions and at what stage of their evolution planets can provide the necessary environment for life.

Terrestrial planets in the habitable zone *i.e.* the region in the stellar environment where physical conditions are such that water can be present in a liquid state, are of particular interest, since they are in principle privileged sites for the development of life. The complete picture of the exoplanet population that we need to obtain in the first place, however, requires a full study of the whole planet size, mass and orbit spectrum.

Although an exoplanetary search programme was described already 60 years ago (Struve, 1952) it took, for technical and sociological reasons, about 40 years before the first systematic search programmes were in place, and then achieved their first successes a few years later. Latham and co-workers (1989) reported 'A Brown Dwarf or even a Planet' of 11 Jupiter masses orbiting the star HD 114762. Then there were surprises! Earth size planets were found orbiting pulsars! They were also not found in any of the exoplanetary search programmes but just by chance during timing studies of the radio signals emanating from the pulsars. Presumably originating in the blast debris resulting from the supernova that the pulsar originates out of, just a few such planets – ranging down to 0.02 Earth masses – have been found (Wolszczan & Frail, 1992).

Following closely behind these surprising discoveries, the first bona fide planet was reported in the autumn of 1995 (Mayor & Queloz, 1995), with others following soon after (Marcy & Butler, 1996). Already these first objects produced surprises for those who had expected that all solar systems would look very much like our own. For example, these giant planets were orbiting very near to their primaries (*only a few stellar radii*

in some cases!). Planets could clearly not have formed where they were found but must have migrated there, and other peculiar bodies such as planets with eccentricities more like comets in our own Solar System were completely unexpected. To a very large extent, these first 'peculiar' planets were the results of the biases created by the technology and methods used for the first searches, which were significantly more sensitive to massive, short period bodies. While the discoveries have continued, at an accelerated rate to date, there has been no system like our own credibly reported.

Since 1995, we have found more than 400 planets orbiting around stars other than the Sun. While the building blocks of our own system appear to be there, like systems with multiple (5 or 6) planets, planets similar to Jupiter, Neptune like planets and now even low-mass 'rocky' worlds like our own (CoRoT-7b: Léger et al., 2009, Queloz et al., 2009; Gliese 581e, Mayor et al., 2009a), they are always found in the wrong location (*e.g.* CoRoT-7b is orbiting only 5 stellar radii away from its solar type star and consequently experience surface temperatures of around 2000K), *i.e.* the structure of the exo-systems do **not** look like our Solar System.

There are several methods that have been used in order to detect exoplanets. The first method to be successfully applied involved measuring the radial velocities of many 'Solar type' stars. As a planet orbits its primary, the star will move back and forth along the line-of-sight due to the gravitational influence of the planet, and the Doppler effect will thus alternately blue- and red-shift the spectral signatures of the star. By measuring a large number of spectral absorption lines (typically several thousand per star) it is possible to measure the position of the line centre to an accuracy of a few parts in a thousand, consequently providing a velocity precision that today can be less than 1 m/s. Assuming enough observations have been made, this results in a usable radial velocity curve with the same precision and the presence of an influencing body can be inferred and its mass determined (actually the minimum mass of the planet unless the inclination of the orbital plane is known by another method – see below). Today, this method enables the detection of small planets (a few Earth masses) to be discovered close to low-mass stars, but the actual Earth orbiting a true sun-analogue would require another order-of-magnitude in precision and this is still some years in the future.

The next method that provided results was the transit method (Charbonneau et al., 2000). If the orbital plane happens to intersect the line-of-sight to the star, the planet will occasionally transit (part of) the stellar surface. The probability of a chance alignment varies between about 0.5% for a $1R_{\oplus}$ planet at 1 AU from a solar type star to several tens of percent for gaseous giant planets that are orbiting very close to red dwarf stars. By observing the light output of the star when the planet is transiting the stellar surface, the shape and depth of the light curve can tell us a lot about the size and other physical parameters of the planet (and of the star). Specifically, the transit constrains the inclination of the exoplanetary orbit so well that the true mass of the planet can be found from the radial velocity curve. By observing both the occultation of part of the light of the star by the planet, as well as the associated radial velocity curve, exact measurements of the planetary mass and diameter allow a determination of the body's average density and thus its mineralogy. Since this method – known most often as the transit method – requires a chance alignment to occur, any systematic investigation calls for the simultaneous observations of a large number of stars during an as long as possible time with an as high as possible duty cycle of the observations.

There are other methods that have had a great impact on the field of exoplanet research, *e.g.* using so-called micro-lensing (gravitational lensing where an intervening body enhances the light from a background object, in such a way that it reveals the presence of any planetary body orbiting the lensing object). This method requires an even larger stellar sample to be observed simultaneously than the transit method, and is thus limited to the observation of very distant objects (with the accompanying problems when one tries to carry out detailed follow-up observations).

The study of exoplanets is one of the fastest growing areas of modern contemporary astronomy. This is being driven by new discoveries that are revealing the large variety and extraordinary complexity of exoplanetary systems. Hardly a week goes by without a new "record" being set (*e.g.* the biggest or the smallest, water/CO in their atmospheres etc) and this in turn is fuelling an immense public interest in exoplanets in particular and astronomy in general. As the study of exoplanets is a new area of activity, it is to be expected that the research proceeds through a phase of discovery and this, in turn, is important as the exoplanet parameter space is mapped out. For example, we have found gas giants of the same mass with more than a factor of two

variation in radii, planets evaporating their atmospheres in gigantic clouds surrounding them, as well as a number of very large planets orbiting low-mass, cool stars. Each of these new discoveries tell us about new and fundamental properties of planets that can help constrain models of their formation etc.

Essentially every new facility being contemplated for astronomy today has to address the issue of exoplanets. The very large ground-based telescopes in the 30 – 40m class, currently being planned all have exoplanets as one of their main rationales for being developed. Therefore, the next 15-20 years will see significant resources being made available on the ground. These resources will nevertheless have limitations because of their position at the surface of our planet. The atmosphere as well as the rotation of the Earth will impose severe limitations in key areas. Therefore, in order to address the *direct* study of Earth-like exoplanets, instruments will need to be deployed in space.

It is clear that the ground- and space-based assets will complement each other depending on the physical parameter one wishes to measure. Two pioneering missions have already been launched. CoRoT, developed by the French space agency CNES with the active partnership of ESA, Austria, Belgium, Brazil, Germany and Spain has already had its first successes (see above) with the detection of the first characterized 'super-Earth' rocky planet. This object is the first planet outside our Solar System that has been demonstrated to have an average density very similar to the one of the terrestrial planets in the Solar System. There is no doubt that CoRoT will make more discoveries over the next few years.

Recently launched, NASA's *Kepler* mission is following in the European footsteps. Over the next few years it could well happen that we will witness the momentous discovery of a candidate rocky planet also in the habitable zone of a star using the already flying space missions like CoRoT or *Kepler*. However, ground-based confirmation of those candidates will be extremely challenging and many, if not all, may prove beyond detailed examination or even confirmation with current facilities. *A next generation mission, allowing us to collect precise and reliable information on the distribution of exoplanets, including, most importantly, planetary radii (required for any type of comparative planetology and thus bringing other sciences into the field), orbits, masses and ages, is therefore clearly needed to progress in this area.* The PLATO mission will provide such information. The targets will consist of a significant portion of the brightest - and nearest - stars in the sky (more than 10% of the surface of the sky will be observed). It will provide a target list for complementary observations of all aspects of exoplanetology and stellar physics.

PLATO will do so by observing a sizable fraction of all bright stars in the sky simultaneous for year-long periods at a time. The stars will be brighter than 11th magnitude (significantly brighter than the samples of CoRoT and *Kepler*) and a large number will even be brighter than 8th magnitude. This will allow the collected ensemble of ground- and space-based auxiliary instrumentation to be brought to bear on any target discovered to have a transiting companion planet. The sensitivity of PLATO will be so high for these objects that – from the same light curve as the transit will be studied – the asteroseismological spectrum will be obtained with unprecedented precision. From this we will learn the structure of the interior of the star, its age, and thereby the history of the complete system. This will allow researchers from a large number of fields to be able to accurately describe other solar systems and compare them with our own. For the first time, one will have access to both the sizes as well as the orbital periods of planets representative for what we find in the inner Solar System.

This will not be the end of this exciting field but only a very strong beginning. Based on the PLATO results, correct design of future missions aimed at the detailed, direct study of individual, Earth-sized planets will be possible. Such missions could range from using again the transit method but this time in order to register spectral information (as has been suggested as a target for the James Webb Space Telescope in the case of nearby red-dwarf stars with transiting planets – if such are found). The direct study of exoplanetary surfaces will require much larger instruments of the next generation like interferometers or large coronagraphs but these instruments will also build on the work of PLATO which will have to find suitable objects before the larger instruments will be actively contemplated.

PLATO will therefore bring in a new era in exoplanetology. Using stellar seismology as an active tool, and thereby forging the star-planet connection – as we are doing just now in the case of the Sun-Earth connection in our active space research programmes, we will enhance our knowledge not only about exoplanets themselves but also about ourselves.

In this report we present the first assessment of PLATO as carried out by industry, which have studied the mission, spacecraft and payload in two parallel contracts during 2008-2009. Simultaneously, a consortium of scientists, have made an independent study of the payload in order to further develop the possibility that this could be provided by nationally funded consortia.

In chapter 2 the Scientific Objectives as well as the actual Scientific tools – photometric transits and asteroseismic analysis – that PLATO will use in order to achieve the former, are described. In chapter 3 we detail the Scientific Requirements of PLATO and in Chapter 4 we present the Expected Performances that we expect will be derived from a successful PLATO mission as well as the simulations that have been carried out during the various studies. Chapter 5 lists the Ground-based support and in Chapter 6 and 7 the Scientific Impact and the Additional Science of the mission.

The Payload as envisaged by the different industrial and scientific institutes & consortia studies is described in Chapter 8 followed by the mission design in Chapter 9, Mission Operations in Chapter 10 and the Management of the mission in Chapter 11.

2 SCIENTIFIC OBJECTIVES

The discovery of extra-solar planets orbiting solar-type stars has been one of the major astronomical breakthroughs of the past 15 years. The regularly increasing number of known extra-solar planets is lending some confidence to observed features in statistical distributions of the planet and primary star properties. These features are thought to keep fossil traces of the processes active during the formation of the system and help constrain the planet formation models. We have learned that planets are common, especially the lower-mass ones, and that Nature is able to produce a surprising variety of configurations. Understanding the physical reasons for such wide variations in outcome remains a central issue in planet-formation and evolution theory, especially in the context of the determination of the conditions for the development of life. Our vision of the Solar System formation and evolution will also be conditioned by a better knowledge of exoplanet systems.

Building from the expertise of the domain accumulated over the past decade from ground-based and space observations, and from progress of theory, PLATO can bring fundamental steps forwards toward the detection and characterization of planets similar to our own.

2.1 Very low-mass planets are common around solar-type stars

An emerging population of super-Earths: The majority of the known exoplanets have been found with the so-called radial velocity technique. Most of these are giant gaseous planets similar in nature to Jupiter. The past few years have, however, seen a breakthrough in the field of extra-solar planets with the detections of light ($2\text{-}20 M_{\text{Earth}}$), solid (rocky/icy) planets around solar-type stars (e.g. Lovis et al. 2006; Bouchy et al. 2009; Mayor et al. 2009b) and M dwarfs (Bonfils et al. 2007; Udry et al. 2007; Mayor et al. 2009a). The first super-Earth planet with measured radius and density was discovered by CoRoT (Léger et al, 2009; Queloz et al, 2009). It was discovered with the transit method.

Results from radial velocity programs suggest that the already published discoveries only represent the tip of the iceberg and that a new population of Neptune-mass and super-Earth planets is emerging (Figs. 2.1 and 2.2 left). In particular, a recent census of planetary candidates among stars of the HARPS-GTO "high-precision" subprogram is revealing that more than 40% of solar-type stars host low-mass planets (Udry et al., in "Towards other Earths" (ESO-CUAP) held at Porto, Portugal October 2009), among which about $30 \pm 10\%$ of close-in ice giants and super-Earths (Lovis et al. 2008; Mayor et al. 2009a). The existence of a large population of super-Earths is supported by discoveries of similar objects at larger separations using the microlensing technique (e.g. Beaulieu et al. 2006; Bennett et al. 2008) and, more importantly, by very recent detections with the Kepler satellite of a large population of close-in, small transiting objects (2 - 4 Earth radii, private communication) awaiting to be confirmed by radial velocity observations. Planet-search surveys are now building up a detailed and unbiased view of planets with masses in the range of super-Earths and Neptunes.

Planet population synthesis models: The present observational findings on super-Earths are also in good agreement with the results of population synthesis models based on the core accretion paradigm for planet formation (Ida & Lin 2004, 2005; Alibert et al 2004, 2005; Mordasini et al. 2009). These models predict the existence of a large number of low-mass objects with a distribution steeply increasing towards the lower masses (Fig.2.2, right), up to an overwhelming proportion of Earth-mass planets. The sharp rise of the number of planets predicted by the simulations below a few Earth masses is still out of the present instrumental sensitivity of radial velocity surveys, but, if real, will provide a fantastic reservoir of candidates to be detected by space transit missions like PLATO.

In addition to predicting a large number of Earth-size planets, interesting ideas, linked to population synthesis models, postulate differences in the internal composition of super-Earths, depending on their formation and evolution history: refractory elements in *born-again embryos* giving birth to a super-Earth through the perturbation of a forming giant planet, or volatile element content for failed cores (Lin, in “Towards other Earths” (ESO-CUAP) held at Porto, Portugal October 2009). Precise measurements of the planet radii are needed to discriminate between these different cases.

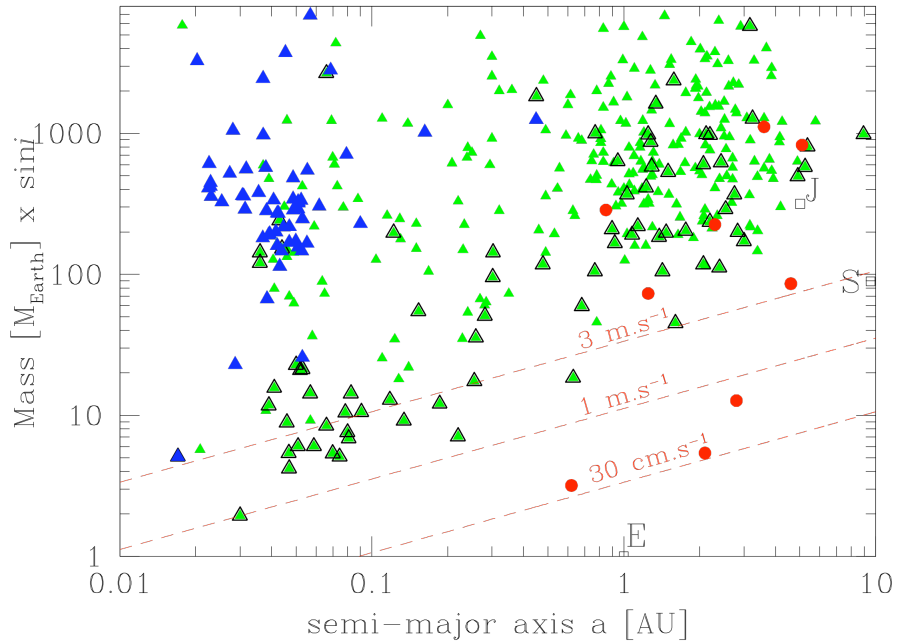


Figure 2.1 Mass-separation distribution for known exoplanets. Transiting planets with accurately determined physical parameters are shown as blue triangles (with CoRoT-7b visible as the lowest point). Planets detected through radial velocity monitoring have undetermined radii and are shown as green triangles, with those detected with HARPS on the ESO 3.6m telescope as larger symbols. The planets from microlensing surveys are represented by red dots. The red dashed lines show the limiting masses of planets around a Sun-mass star detectable with current instrumentation.

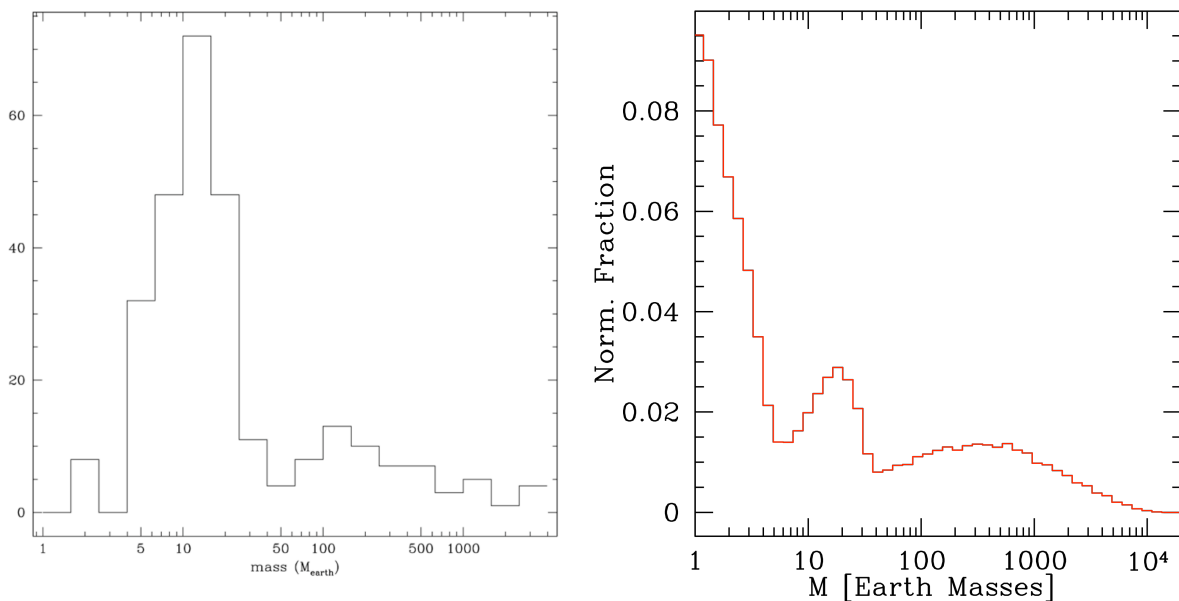


Figure 2.2 Left: Mass distribution of known exoplanets. The low- and high-mass parts of the histogram have been separately normalized taking into account the sample size in the corresponding planet search surveys. Right: Same distribution for the planet population predicted by population synthesis models (Mordasini et al. 2009).

2.2 PLATO main science goals

During the past decade, our understanding of planetary formation had to integrate several new peculiar characteristics of the detected extra-solar systems, leading us to continuously re-examine the statistical properties of the derived orbital elements and stellar-host characteristics, in search for constraints for planet formation and evolution scenarios. Eventually, when a rocky planet at a suitable distance from its star will be detected and coarse spectra of its atmosphere will be obtained, we want to be able to discuss its habitability on solid scientific grounds. At that point, only a complete understanding of how planets form and evolve, and subsequently the knowledge of what material they are made of, will allow us to confidently address this question.

As a first step, suitable candidates have to be detected. On the ground, radial velocity surveys are on good tracks towards the detection of lower and lower mass planets and eventually could find a few Earth analogs in the habitable zone around bright solar-type stars. However, such detections will only provide information on the orbital distance of the planet to the star and on the planet mass (strictly speaking, the fractional mass of the planet compared to its host star), a physical parameter that is necessary but not sufficient to constrain the internal structure and composition of the planet. To obtain this fundamental information we need as a prerequisite to know the radius of the planet. The most precise estimate of planet radii is obtained through photometric measurements of transit events. Due to transit geometrical probability, hundreds of radial velocity candidates will then be required to eventually have one transiting planet. Conversely, projects like COROT and Kepler will find many small-size objects transiting solar-type stars. The candidate hosts will however be faint, making radial velocity observations very difficult and the derivation of the planet mass virtually impossible. *Because of this difficulty, the explicit goal of Kepler, since the beginning of the mission, is to statistically demonstrate that Earth-type planets exist in the habitable zone around solar-type stars, and not to point out which of the candidates host Earth twins.*

To reach the ambitious objective of detecting and characterizing the basic physical properties of Earth-type planets in the habitable zone of solar-type stars, we need a mission able to measure the radius and mass of the planet with exquisite precision. This is possible when coupling a space-based photometric transit search targeting a large number of *bright* late dwarf stars for which state-of-the-art ground-based precise radial velocities can be obtained. Building on cutting-edge advancements of both transit and radial velocity projects, PLATO will bring this approach to another level. The scientific goals of PLATO will then be:

1) The detection of extra-solar planetary systems of all kinds, including small, terrestrial planets in the habitable zone of solar-type stars.

The understanding of how planetary systems form, evolve in time and eventually harbour suitable conditions on the planet surface for life to develop requires a detailed study of each of the mentioned stages, for the different types of low-mass planets. It is thus extremely important to pave the planet physical parameter space, from giant planets down to Earth twins, in a statistically significant way. Although challenged by transit probability and by the difficulty of the radial velocity follow-up, PLATO will follow a sufficiently large number of bright stars to achieve this goal. As a by-product, PLATO will also consolidate with actually *confirmed* planets the occurrence frequency of potentially habitable worlds around solar-type stars.

2) A precise characterization of the basic physical parameters of the detected exoplanets and the host stars: radius, mass, age.

While the actual principles of the determination of the parameters of both planets and stars have been carried out for gaseous giant transiting planets, they have been verified for the first time for a super-Earth with CoRoT. PLATO will mark the beginning of detailed science on exoplanets. The perspective of 'true' comparative planetology, *i.e.* when one begins to compare different planetary systems with a precision in the determination of physical parameters of order 1-2%, coupled with age determinations with a precision of about 200-300 million years, will allow - for the first time - evolutionary sequences for planets to be put together. In order to achieve this, the basic requirements are light curves measured with very high photometric precision, with a high cadence and a very high duty cycle. Further it is necessary to measure very large numbers of bright stars, in order to have enough transiting planets of different types, ages and

stellar primaries, with full physical parameter characterization. PLATO will reach these goals taking the results to an unprecedented level.

3) *The identification of suitable targets for future, more detailed characterization.*

In the past few years we have seen the first attempts to determine the atmospheric constitution of exoplanets. By determining the difference of the star spectra taken before/after and during the transit, a spectrum of the planet can be derived. While systematic effects in the data and the luminosity difference between the star and planet make this extraordinarily difficult to achieve, these studies have led to the first analysis of the planetary atmospheric constitution and height structure which can be compared directly with models. Spitzer and HST/NICMOS observations have led to the detection of, *e.g.* water vapour (Tinetti et al. 2007) and methane (Swain et al. 2008). Earlier molecule abundance determination had also been obtained by simply comparing transit depth at wavelengths corresponding to given species, *e.g.* sodium (Charbonneau et al. 2002), hydrogen (Vidal Madjar et al. 2003), carbon and oxygen (Vidal Madjar et al. 2004).

A better understanding of planet physics is now possible by direct measurement of planetary thermal emission. During occultation phases, when the planet is hidden behind the star, the observed total luminosity of the system (star+planet) is expected to decrease. This effect is very small in the visible but of the order of a few parts per thousand in the infrared. Although, until recently all secondary eclipse detections have been observed from space with the Spitzer space telescope for HD209458 (Deming et al. 2005), TrES-1 (Charbonneau et al. 2005), and even for the Neptune-mass planet around Gl436 (Deming et al. 2007; Gillon et al. 2007), recently ground-based telescopes have also been successful (de Mooij & Snellen 2009, Sing et al. 2009). From the measured thermal emission the planetary effective temperature can be derived. It can then also be compared with models of irradiated planets (*e.g.* Burrows et al. 2006; Charbonneau et al. 2008), bringing strong constraints for these models. Also, outside of the transit, the measurement of orbital phase variations at IR wavelengths can be used to give an estimate of the temperature distribution on the surface of the planet (*e.g.* Knutson et al. 2007). In the future it is likely that ground-based techniques will be refined and secondary eclipse detection more routine - at least for the largest planets, till the installation of the new generation of giant telescopes being now studied.

In practice, almost all that is known about exoplanet atmospheres results from measurements of the brightest objects (primarily HD209458 and HD189733) and this reflects the immense difficulty in obtaining these observations. Planets transiting bright stars are thus eagerly needed to bring advancement in the field. There is no doubt that this area of research will be drastically helped when JWST and the ELT's become operational and additional molecular species are likely to be detectable. The situation with smaller planets is however still somewhat confused. At this point it looks like that only in some favourable cases (super-Earth transiting late-type dwarfs) will atmosphere content characterization be possible with JWST or the ELT's (Palle et al. 2009). It is quite likely that some small planets will not have a measurable atmosphere with the presently foreseen observing facilities. This should by no mean stop our effort. Understanding how atmospheres change when going to lower planet masses and how they evolve in time will prove to be fundamental when analyzing in the future the atmosphere of Earth-type planets in search for biosignatures. The discovery of bright stars hosting Earth twins will also provide a strong push for the development of new initiatives like the former Darwin and TFP projects, with the aim of finding life forms on other Earths, one of the ultimate goals of our field of research, and probably also one of the greater expectation of the general public from science.

2.3 Tools at our disposal to reach PLATO's goals

In a first step, the problem in front of us is now to find smaller and smaller planets orbiting other stars, determining better and better the physical characteristics of these objects and of their host stars, as well as the orbital properties of the detected systems. Remarkably enough, we have to our disposition powerful tools that when combined allow us to achieve these ambitious goals.

2.3.1 Wide-field, long, continuous and high-precision photometric monitoring

Photometric transit. As already mentioned, because of the nature of the method, only the orbital parameters and a lower limit on the planet mass is known from radial velocity measurements alone. Much tighter constraints for planet models are obtained by the observations of a photometric transit of the planet in front of its parent star. Combined with radial velocity measurements such observations yield the exact mass, radius and mean density of the transiting planet, providing priceless constraints for the planet internal structure, as well as for the planet-evolution history.

Planetary transits can be detected through high precision photometric monitoring. A planetary transit in front of a star causes a decrease of the photometric signal $\Delta F = \left(\frac{R_p}{R_*}\right)^2$ where R_p and R_* are the radius of the planet and of the star, respectively. The duration of a transit is given by:

$$d \approx \frac{PR_*}{\pi a} \sqrt{\left(1 + \frac{R_p}{R_*}\right)^2 - \left(\frac{a \cos i}{R_*}\right)^2} \quad (2.3.1)$$

For a star like the Sun, the typical relative variations are $\Delta F = 10^{-4}$ with 13 hour duration for 1AU orbits for Earth-size planets, and $\Delta F = 10^{-2}$ for Jupiter-size bodies. Observations of recurring planetary transits can be used to measure the orbital period P , and therefore the semi-major axis of the orbit, by applying Kepler's third law. In combination with the radial velocity method, the true mass and therefore the planet mean density can be derived.

Giant gaseous planets. Presently, more than 60 such systems are known, with only a handful of them transiting bright stars. They are the most interesting targets for complementary follow-up ground-based or space observations. Remarkably, more than half of the 60 or so currently known transiting planets have been found in the past year. Thus, in 2008, for the first time, the transit method was equally successful as the radial velocity technique. Most of the detected transiting planets have been found by novel, wide-angle ground-based facilities targeting bright stars such as WASP, HAT, TrES and XO projects (Pollacco et al. 2006, Bakos et al. 2004, Alonso et al. 2007, McCullough et al. 2005). For several years there was a dichotomy between the expected and observed detection rates, but a better understanding of systematic noise sources and their effect on photometry has allowed the photometric surveys to start delivering closer to their potential. However, atmospheric limitations make the detection of small planets around solar type stars particularly challenging. Consequently, most known transiting planets have masses and radii comparable to Jupiter but with vastly shorter orbital periods (see Figs. 2.1 and 2.4).

Low mass planets. On the low-mass end of the distribution, the detection of transiting Neptunes and super-Earths will provide fundamental information to constrain the inner composition of these planets as *e.g.* the relative fraction in mass between the iron core, the mantle or the atmosphere of the planet, or the fraction of water/icy among solids. Even if degeneracy probably exists and no unique solution is expected, basic guesses on the chemical species present in the planet could allow to at least partially solving the problem. For example, an extended atmosphere will have a major effect on the radius and it should be possible, directly from the observations, to separate planets with thin and thick atmospheres. This is an important point related to the planet habitability. Up to now, two Neptunes have been found to transit in front of their stars (GJ436b, Gillon et al. 2007; and HAT-P-11, Bakos et al. 2009). For GJ436b, the planet radius, mass, and mean density were then improved thanks to observations with the Spitzer space telescope (Demory et al. 2007).

The prime goal of space missions is to extend the detection range towards small planets. Recently, the CoRoT satellite has opened a new frontier with the discovery of the first transiting planets from space. These discoveries include a number of Jupiter-sized planets (Barge et al. 2008, Alonso et al. 2008, Aigrain et al.

2008, Rauer et al. 2009, Fridlund et al. 2009) as well as the Super-Earth, CoRoT-7b, (Fig. 2.3). This has $R_p = 1.7 R_{\text{Earth}}$ and $M_p = 4.8 M_{\text{Earth}}$ and orbits a G9V star with a period of 0.85 day (Léger et al. 2009, Queloz et al., 2009). Additional CoRoT planets are expected in the near future, but those already detected demonstrate the potential of space observations for planet detection both in term of photometric precision and also duty cycle.

With the realization that rocky planets may well be plentiful around M-dwarf stars, a number of ground-based surveys have started regular monitoring of a significant number of these objects as *e.g.* the M-Earth Project (Irwin et al. 2008) with the expectation that around these small stars, super-Earth (or smaller) planets should be detectable. Given the low luminosity of the star, the habitable zones in these objects are close in, and it is likely that ground-based surveys could well be able to detect planets in these regions within a few years. The faintness of typical M-dwarf host stars will make detailed characterization follow-up really challenging, even with the future giant telescopes or with JWST. Enthusiastically, a first discovery from the M-Earth project (Charbonneau, private communication) is revealing a super-Earth with a mean density very different from the one of CoRoT-7b despite similar masses (Fig. 2.4).

Information from transits. Transit observations have led to some remarkable results. We have found almost a factor of two variations in the size of giant planets of similar masses (with unexplained cause) and begun to study their internal structure through comparison of their bulk density with theoretical models. Although still based on small statistics, the situation seems to be similar for super-Earths, for which the CoRoT and M-Earth candidates present fairly different radii (1.7 and 2.7 Earth radius) despite estimates of their masses that are not very different (4.8 and 5.7 Earth masses, respectively). This demonstrates once more the variety of possible outcome from planet formation processes. Recently, we also have started to gather hints about the orbital dynamical histories of transiting planets through the Rossiter-McLaughlin and Kozai effects. Very surprisingly, it turns out that about 1/3 of the known transiting planets are misaligned (not crossing the stellar disk perpendicularly of the star rotation axis; Collier-Cameron, in “Towards other Earths” (ESO-CUAP) held at Porto, Portugal October 2009), a strong indication of stochastic processes during the planet formation or evolution. It also indicates the presence of further large planets in the system.

Necessity of long monitoring. Observations of transiting planets at large orbital periods are rare due to the decreasing geometrical transit probability ($P_t \propto P^{-2/3}$). A recent highlight is the observation of the primary transit of the 111-day-period Jupiter-like planet HD80606 b (Moutou et al. 2009, Fossey et al. 2009), previously detected by radial velocity observations (Naef et al. 2001). Figure 2.1 shows that although many more planets are known from radial velocity detections, the parameters range is not well sampled for planets with known primary parameters, especially towards long periods or/and small masses, and that long-lived continuous monitoring of bright stars are required to completely characterize planets on wider orbits. The significant bias in the observations toward larger planets, and more importantly the difficulty to confirm the transit candidates with ground-based follow-up for the faint CoRoT and Kepler targets, is likely to preclude any rapid firm conclusion on this issue. In the future, we expect more such detections of giant planets on long-period orbits as radial velocity surveys are extended and Kepler results are followed up. However, small planets in long period orbits will remain extremely difficult for either CoRoT or Kepler with the smallest objects being only accessible to PLATO.

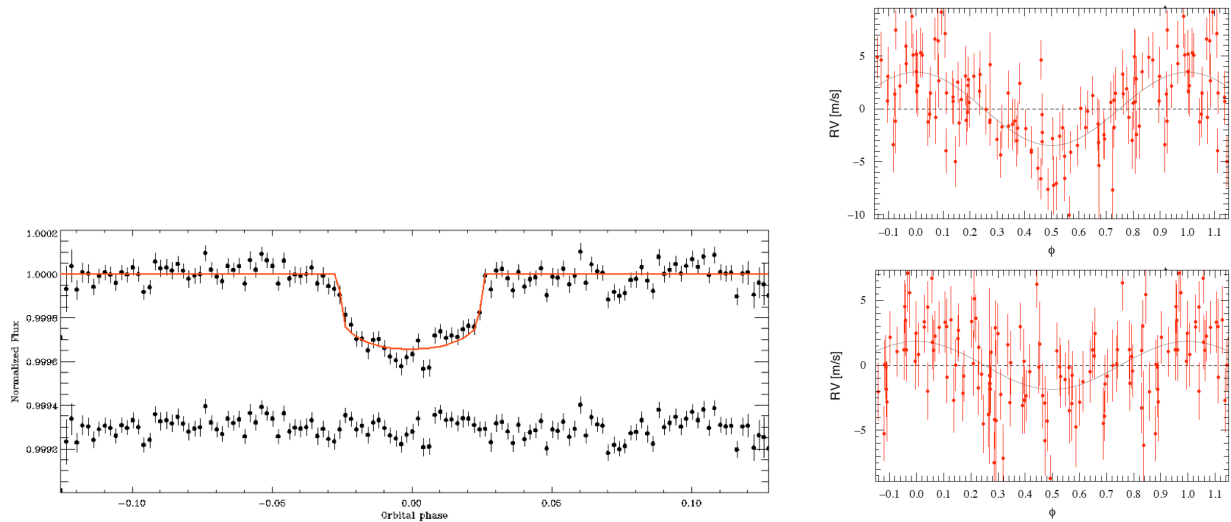


Figure 2.3 Left: Phase-folded light curve of CoRoT-7b (top; Léger et al. 2009), with residuals after subtracting the best fitted model (bottom). Right: Corresponding phase-folded solution for the radial velocity curve of CoRoT-7, including 2 super-Earths in the system (the non transiting CoRoT-7c on top, and CoRoT-7b on the bottom), and after correcting from activity effect by harmonic decomposition (Queloz et al. 2009).

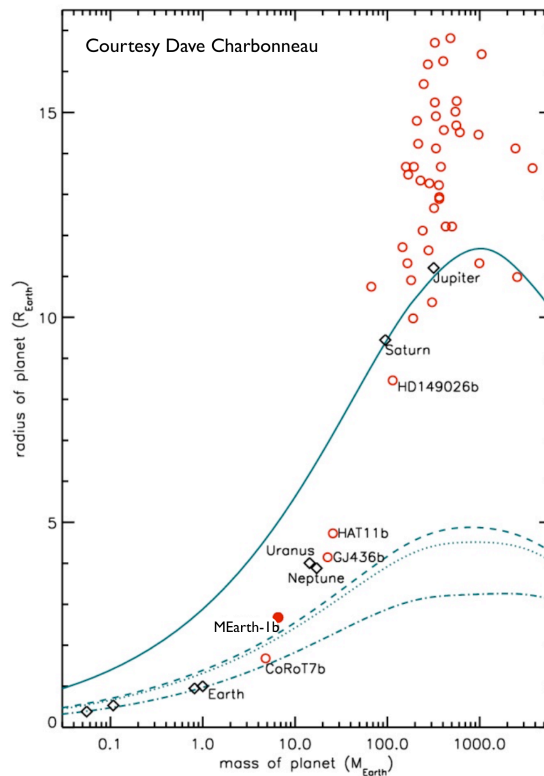


Figure 2.4 Mass-radius diagram for the known extra-solar planets. The large diversity of densities (spread of the points) observed for giant planets seems to be also the rule for super-Earths. Indeed, the 2 presently known candidates, CoRoT-7b (Léger et al. 2009, Queloz et al. 2009) and MEarth-1b (Charbonneau et al., 2009, Nature, submitted), have very different observed radii (1.7 and 2.7 Earth radii) compared to more similar masses (4.8 and 5.7 Earth masses, respectively). Results for the MEarth-1b candidate have been kindly provided in advance of publication for the PLATO YB by the MEarth team.

We clearly need a new set of observations offering a relatively unbiased insight into the distribution of exoplanets in the (radius, semi-major axis) parameter space, down to Earth size planets, and up to at least 1 AU. The main thrust in future exoplanet research will be the detection and characterization of Earth-like planets within the habitable zone of Solar-like stars *i.e.* surveying true Earth analog systems. These observations will be extremely challenging and can only be done from a space-based platform.

2.3.2 Precise radial velocity measurements

In the case of transiting planets, a ground-based radial velocity follow up of the detected candidates is mandatory for several reasons. It will first confirm the planetary nature of the transiting body by providing a direct measure of its mass from the observed amplitude of the radial velocity variation, the orbital inclination being known from the transit light curve. As already mentioned, the mass is a key parameter for the planet physical characterization. Phase coverage of the velocity curve will then confirm the orbital period inferred from the photometric data and allow characterizing the orbital motion of the planet. The shape of the orbit provides important information *e.g.* for habitability questions, the instantaneous energy received by the planet from the central star depending on the position of the planet on an elongated orbit. Orbital shapes can also be indicative of secular evolutionary processes during the life of the system. Finally, high-resolution spectra obtained during the radial velocity campaign will provide exquisite spectra for the spectral analysis of the stellar host. Effective temperature, gravity, chemical composition, rotation and activity level of the stellar host will be precisely defined.

The detections of the large majority of low-mass planets known today (Neptunes and super-Earths) were made possible thanks to the development of new stable and more precise instruments for radial velocity measurements, the most efficient one being the ESO HARPS spectrograph designed for high-precision planet search and capable of reaching long-term repeatable radial velocity precision below 1 m/s (see Fig. 2.1 for an over-view of HARPS detections). The application of a careful observing strategy to help reduce the effects of stellar noise, possibly hiding the tiny planet signal, also plays an important role for the detection of very small velocity variations. Building on the HARPS experience, the state-of-the-art approach to still improve the radial velocity efficiency in detecting even lower-mass planets in the Earth-mass regime is described in more detailed in Sect. 5 discussing the ground-based support aspects for PLATO. For the most challenging low-mass candidates (the effect of the Earth on the Sun is at the level of 9 cm/s), ultra-precise radial velocity measurements will basically require:

- 1) Long-term, ultra-stable, high-resolution spectrographs, with wavelength calibration precise at the level of a few cm/s. These goals are at the heart of the ESPRESSO/VLT and CODEX/E-ELT projects.
- 2) Large telescopes. The radial velocity precision scales with the spectra S/N (or roughly with the telescope diameter), meaning an increase of a factor 100 in flux for a gain in precision of a factor 10 (*e.g.* going from 1 m/s down to 10 cm/s). Scaling from HARPS results and/or using Exposure Time Calculators developed for the different projects, the typical photon-noise limit of 10 cm/s is reached in 15 minutes for a $V=8$ magnitude star on ESPRESSO, and for a $V=11$ on the E-ELT (42-m telescope).
- 3) Quiet stars. Intrinsic stellar variability sets limits for the lower-mass planets detectable by radial velocities of solar-type stars.

The same limitations concerning the estimates of precise radial velocities apply in the case of transiting low-mass planets, with the further disadvantage that we cannot choose in advance the best suitable targets for the measurements. In practice, the more massive planets will be characterized for most of the PLATO targets, whereas for the lower-mass planets (super-Earths and below) the characterization will only be possible for the non-active stars, especially when they are at some distance from their central star. This will restrict a bit further the final output from the survey but realistic simulations (Sect. 6) show that, for the most difficult cases of habitable low-mass planets, several tens of them will still be detected and characterized by radial velocities.

We note here that the photometric detection of the transit itself brings extra confidence to the reality of the radial velocity signal for the most difficult cases, as it was the case for CoRoT-7b (Fig. 2.3). Knowledge of

the photometric period and approximate orbital phase also makes follow-up observations somewhat easier compared to the direct detection of the planet from radial velocity information alone.

2.3.3 The determination of precise stellar parameters.

The key to understanding many aspects of exoplanets is linked to the precise determination of the physical parameters of both the planets and their host stars. Indeed, measurements of the planet parameters is inextricably linked to the knowledge of the host star physical properties as most of the fundamental observables like masses or radii are obtained with regards to the corresponding value for the star. Small errors in stellar parameters translate into relatively large errors on their planets. Star radii, masses and ages are usually estimated by locating the star in the HR diagram, which is imprecise and often unreliable. As demonstrated by CoRoT data, monitoring of the stellar flux at high precision reveals micro-fluctuations in light output caused by acoustic waves travelling between the stellar interior, where energy is produced by thermonuclear reactions, and the photosphere where light escapes into space. These waves carry information from the layers deep down into the star where they penetrate, up to the surface where the power spectrum of the light output produces measurable light variations (if measured with enough precision) that can be used to determine fundamental parameters of the star. This asteroseismology approach is described in more detail in Section 2.4, below.

Planet and star masses. Most planets have been detected through the reflex motion they induce on their host star, but without an estimate of the planet's orbital inclination we cannot confidently determine the mass of the planet. If the inclination can be determined, then Kepler's laws can be solved and the mass function $(M_p / M_*)^{2/3}$ can be accurately derived. Radial velocity techniques, even when the inclination angle is known, provide only the mass function, and a good measurement of stellar mass is needed to derive the planetary mass. Presently, stellar masses can be determined from their spectra and stellar evolution models with a precision of the order of 20%. The asteroseismic analysis of the PLATO light curves will be able to provide 2-4% error in the stellar masses (Sect. 2.4.2), which will lead to an improvement of the precision of planetary masses of about one order of magnitude.

Planet and star radii. Planets that are seen to transit their host star have tightly constrained orbital inclinations and the added benefit that the depth of the eclipse is directly related to the planet and star size, R_p / R_* . If the stellar mass and radius are accurately known then the planetary parameters can be derived and its bulk density estimated. Clearly, knowledge of the star radii is vital to achieving good accuracy for planetary parameters. By combining Gaia data and ground-based spectroscopy, stellar radii can be derived to excellent accuracies, giving an overall improvement of more than 3 in the accuracy of planet radii (see Sect. 2.4.1).

Given this, it is not surprising that the detection of large numbers of transiting planets has become a major goal in recent years. As techniques improve and instrumentation increases in sensitivity, it is likely that there will be a gradual shift in focus towards detailed characterization of the most interesting planets. The mean planet density naturally depends on the planet mass and radius. The above mentioned accuracy improvements will, therefore, lead to an improvement of a factor of 10 to 50 for planet densities. This is extremely important to better constrain the planet internal structure.

Planet and star ages. Finally, the understanding of exoplanetary system evolution requires an estimate of their ages, which can only be determined by a measurement of the age of their central stars. For the next generation transit surveys, like PLATO, it is therefore crucial to take into account also an accurate determination of stellar parameters to better constrain the input for planetary system evolution modelling. For the bright star sample, asteroseismology from PLATO light curves is able to tell us the age and mass of the star in an independent way and with higher precision than available with other methods (see Sect. 2.4 below for a more detailed description of the method).

2.3.4 Difficulties and challenges

Impact of confusion and contamination: Confusion by background faint sources is a potential problem for a mission like PLATO, primarily due to the large size of the PSF on the sky (typically 30 arcsec). However, even if the PSF is indeed rather extended, it is in fact similar to that of CoRoT in its exoplanet field, which uses a dispersive prism. In the case of CoRoT, in spite of this extended PSF, the impact of confusion is minimized by an appropriate choice of photometric mask, while the targets are as faint as $m_V=15$. It is therefore expected that confusion will be an even less serious problem for PLATO, with similar PSF sizes and targets in the range $m_V=11-13$. In order to properly assess the impact of confusion for PLATO, we have used the end-to-end simulator, which is described in Sect. 4. The detailed results of these simulations are presented in Sect. 4, where it is concluded that indeed confusion, although significant, will not be a major concern for PLATO.

Stellar microvariability and transit light curve modelling: At the kind of photometric precision foreseen for PLATO, intrinsic stellar microvariability, associated with oscillations, magnetic activity, granulation and/or convection may impact the noise budget on various timescales, and in particular at those associated with planetary transits (typically from a few hours to half a day). This may have consequences for transit detection and precise characterization for candidates orbiting slightly-active to active stars.

For example, this is a main concern for CoRoT exoplanet light curves showing that the majority of stars in the CoRoT field exhibit variability at a level near 1 mmag, *i.e.* higher than the Sun's variability (0.3 mmag at maximum activity; Debosscher et al. 2009, Aigrain et al. 2009). We know since activity monitoring studies at Mount Wilson 20 years ago that this is not the case for stars in the solar neighborhood: half of them present activity levels similar to the one of the Sun or smaller and close to 25% of them are very non-active. These fractions are also observed in the volume-limited subsample of the HARPS planet-search program. Part of the effect seen on CoRoT light curves could be attributed to some instrumental effect (*e.g.* hot pixels) but can also be related to the specific property of the field (younger stars, magnitude limited favouring thus earlier dwarfs). In the *Kepler* field, the very recent preliminary analysis of 1 month of observation shows that at least 25% of the stars are less active than the quiet Sun (Latham, in "Towards other Earths" (ESO-CUAP) held at Porto, Portugal October 2009). This is very encouraging for programs aiming at the detection of very low-mass planets from the ground (radial velocities) or from space (transits).

Anyway, in presence of a fair level of stellar activity, for transit detection, the disentangling between stellar variability and transits becomes difficult when the timescales and amplitudes of both phenomena start to overlap. We have learned from CoRoT that this is not a problem for short-time transits (*e.g.* Barge et al. 2008, Alonso et al. 2008), but it may be of importance for the longer-time transits to be expected from PLATO. Fourier and/or filter techniques (*e.g.* Bonomo et al. 2009) are able to handle such detections, so this is not a limitation for the planets to be discovered with PLATO.

For transit characterization, it is however important to derive how contaminated the planetary signal is by intrinsic variability. For CoRoT-2, *e.g.*, the strong and variable stellar spots preclude the search for transit timing variations due to possible additional rocky planets (Alonso et al. 2009). Methods have been developed to identify and adequately model microvariability in the CoRoT light curves (Degroote et al. 2009, Alapini & Aigrain 2009). Planetary transits leave a distinct pattern of equally spaced frequencies in the Fourier spectrum, originating from their typical non-sinusoidal shape. This is easily detected by computing the autocorrelation of the Fourier periodogram. However, oscillations or rotating star-spots may affect the light curve analysis after the planet detection, by causing departures from the expected transit shape that vary from transit to transit. This affects the precision of the planet parameters, as well as makes more complicated transit timing variation detections. Additionally, out-of-transit variations modify the local out-of-transit flux around each transit and impede the search for secondary eclipses and the phase modulation of light emitted or reflected by the planet. Iterative light curve analysis should be used to discriminate between signal at the period of the planet and other signals in the light curve (see *e.g.* Alapini & Aigrain 2009), up to the point where relative errors on the transit parameters due to residual microvariability are below the level of other sources of error.

When searching for longer and shallower transits, such as the ones expected from *Kepler* and PLATO, stellar variability, especially for active stars, cannot be filtered out so efficiently, as one needs to preserve longer duration signals. While this part of parameter space is presently “terra incognita”, and should not preclude transit detection, we have to be aware of the importance of selecting stars as quiet as possible as prime targets of the mission, in order to be able to characterize the planetary parameters at the required level of precision.

False positives. False positives are troublesome configurations that can lead to photometry signatures similar to the ones induced by planetary transits. Follow-up of the detected candidates (radial velocities, high angular resolution imaging, etc) is designed to discard the false positives (see Sect. 5) but any efficient diagnoses applicable directly on the light curves themselves will save important time for the follow-up.

For instance, if the eclipse is flat-bottomed one knows that the eclipsing object has completely entered the stellar disk, and a V-shaped eclipse curve may point towards a grazing incidence eclipsing binary instead (although depending on the primary's size it can also be a larger planet). Also, if we observe a transit with high enough signal/noise, and if we have 2 or more transits, the orbit is near circular and we can ignore limb darkening and find a unique solution to both planetary and stellar parameters (Seager & Mallén-Ornelas 2003). The stellar density can be roughly estimated from the light curve alone if we assume that we know the mass-radius relation. We can then immediately classify the star from colours and light curve alone, and thus obtain a first estimate of the planetary radius. The presence of background eclipsing binaries along the line of sight that can mimic the signature of a star-planet pair can be excluded. The period can actually be determined from the transit profile if one has a good determination of the spectral type. After the determination of all these parameters, one can make a decision on if one should continue with ground-based follow-up - particularly the very demanding radial velocity measurements that can provide a planetary mass.

Such method has been used very successfully in the CoRoT space mission flying since 2007. CoRoT, with its 27cm telescope, simultaneously monitors up to 11,800 stars with a precision equivalent to about $1.3 \cdot 10^{-4}$ per hr for a star with $m_V=11.5$ (Auvergne et al. 2009). In this program, the light curve analysis is used to prioritize candidates for follow-up. The follow-up procedure then determines the other parameters of the system including the planetary mass and together with the already known R_p one can determine ρ_p and thus classify the planet. This is especially important for small planets that can be ice-worlds of the type of the Saturn moon Titan or 'rocky' worlds like our own, depending on where in a system they formed and what kind of central star dominates the system.

2.4 Characterization of exoplanet host stars

2.4.1 Stellar radii from Gaia

Gaia data will have a major role to play in the characterization of PLATO exoplanet host stars.

In particular, stellar radii to within 2% will be necessary, both to measure the planet radii to the same kind of accuracy, and to place tight constraints of stellar interior structure models of the exoplanet host stars. In the absence of interstellar absorption, Gaia will deliver relative precisions on the luminosities of FGK main-sequence stars at distances less than 200 pc in the range [0.7,5.5]% (Lebreton 2008). These performances, coupled to measurements of effective temperature to within 1%, achievable through dedicated high resolution, high signal-to-noise spectroscopic observations obtained as part of the ground-based follow-up programme, will lead to stellar radii with a relative precision better than 2% for un-reddened stars such as most of the PLATO targets. As explained below, the Gaia radii coupled to the seismic observations of PLATO will lead to model-independent masses with a relative precision of 2%.

2.4.2 Determination of stellar masses and ages

One of the main goals of PLATO is to provide precise and reliable measurements of the planet host stars' characteristics, in particular their masses and ages. Classical methods used for the determination of masses and ages of stars rely on a comparison of the star's location in the HR diagram with theoretical evolutionary

tracks. Unfortunately this method has severe limitations, even if stellar evolution theory was fully understood the location in the HR diagram does not uniquely determine the properties of a star. There are many uncertainties in evolution theory, most importantly linked to uncertainties in the calculation of theoretical tracks, in particular due to poor knowledge of internal metal mixture of stars. Uncertainties on physical processes in stellar interiors (microscopic diffusion, rotational mixing, etc.), imply that the metallicity can be wrong by up to a factor 2 by using surface values for the abundances derived from high-resolution spectroscopy; this propagates into relative uncertainties of 20% for the stellar mass. Moreover, stellar ages on the main sequence remain essentially unconstrained. The characterization of planet host stars, and in particular the measurement of their masses and ages, must therefore be obtained with another, more accurate and more reliable method. Seismic analysis is this much-needed method.

Measurements of the oscillation frequencies of the PLATO targets will allow much tighter constraints to be placed on the fundamental stellar parameters of exoplanet host stars. This improvement arises because the individual oscillation frequencies can be estimated to exotic levels of precision not usually encountered in stellar observations. Below we describe the seismic potential of PLATO and the results we can expect from the mission with specific emphasis on the mass and age for various kinds of exoplanet host stars of different magnitudes.

2.4.3 Basic principles of asteroseismology

The oscillation frequencies of a star are determined by its structure; hence, from an observed set of frequencies, we can infer properties of the structure of the star. There are basically two approaches to such an analysis: one is *model independent* and seeks to infer the internal structure which best fits the observational data set; the second one is *model fitting* which compares an observed data set with frequency sets predicted from a grid of stellar models, computed under a range of assumptions about the physical processes that govern stellar evolution, to find which model best fits the data. The second case uses both the fundamental properties of the star (m_V , T_{eff} , $\log g$, $[\text{Fe}/\text{H}]$, $v \sin i$, . . .) and the oscillation frequencies.

The oscillation modes of solar-like stars are acoustic waves trapped inside the star, and are governed by the sound speed $c(r)$ and density $\rho(r)$ throughout the star. The eigenfrequencies $\nu_{n,\ell,m}$ are described by 3 “quantum numbers” (n, ℓ, m), where n is the radial order and ℓ, m the latitudinal degree and azimuthal order of the spherical harmonic $Y_{\ell,m}(\theta, \varphi)$ representation of the geometry of the mode. For a spherical star there is no dependence on the azimuthal order m ; this degeneracy is lifted by rotation (and/or magnetic fields). For slow rotation the frequencies $\nu_{n,\ell,m} = \nu_{n,\ell} + m \langle \Omega \rangle$, $m = -\ell, \ell$; where $\langle \Omega \rangle$ is a weighted average of the interior rotation which depends on the internal structure of the star and the particular eigenmode. This can be used to probe the internal angular velocity of a star. The eigenfrequencies for $m = 0$ can be represented as

$$2\pi T \nu_{n,\ell} = (n + \ell/2)\pi + \alpha_\ell(\nu_{n,\ell}) - \delta_\ell(\nu_{n,\ell}) \quad \text{where } T = \int_0^R \frac{dr}{c} \quad (2.4.1)$$

is the total acoustic radius of the star, and the inner δ_ℓ and outer α_ℓ phase shifts are determined respectively by the detailed structure of the inner and outer layers. The phase shifts α_ℓ, δ_ℓ are slowly varying functions of frequency, therefore we expect almost equal spacing between modes of same degree ℓ and successive orders n .

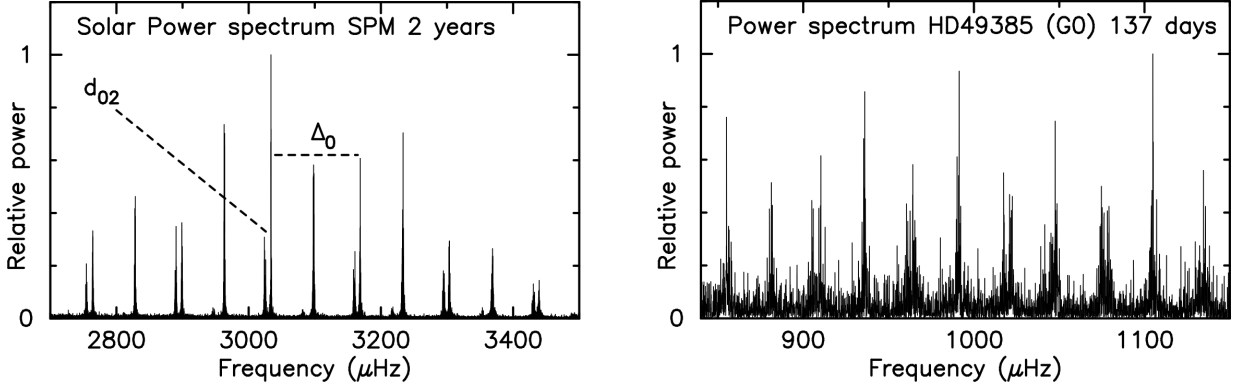


Figure 2.5: Left: Solar power spectrum from 2 years of SPM photometric data. The almost equally separated large peaks are modes of degree $\ell = 0, 1$ with successive n values, the prominent smaller peaks close to modes of degree $\ell = 0$ are $\ell = 2$ modes. Low amplitude modes of degree $\ell = 3$ close to modes of $\ell = 1$ can just be seen in this figure. Right: Power spectrum of HD 49385 from 137 days of observation with CoRoT. The large separation Δ_0 , and small separation d_{02} , provide information on the structure, mass and age of a star.

Measurements of modes with ℓ values up to 3 are expected for PLATO targets, for which the stellar disc cannot be resolved. The oscillation frequencies, including the rotational splitting, are determined by fitting the peaks in a power spectrum of the light curve with Lorentzian line profiles. Two examples are given in Fig. 2.5 – one from 2 years of photometric observation of the Sun with SPM on SoHO, the second from 137 days of observations with CoRoT of the G0 star HD 49385. Determining frequencies of modes with $\ell = 0, 1, 2, 3$ with the solar data is quite straightforward giving estimated errors $< 0.1\mu\text{Hz}$, while for the 137 day run on HD 49385, we can extract frequencies with errors $\sim 0.3\mu\text{Hz}$. The goal with the much longer monitoring to be performed with PLATO is to achieve accuracies $\sim 0.1\mu\text{Hz}$.

The power spectra exhibit an almost equal spacing between the large peaks; these are usually described in terms of separations such as the large separations $\Delta_\ell = \nu_{n,\ell} - \nu_{n-1,\ell}$ between modes of the same degree ℓ and adjacent n values and the small separations, e.g. $d_{02} = \nu_{n,0} - \nu_{n-1,2}$ between the narrowly separated peaks corresponding to modes $\ell = 0, 2$ (see Fig. 2.5). Additionally we have the small separations $d_{01} = \nu_{n,0} - (\nu_{n-1,1} + \nu_{n,1})/2$ which are particularly valuable when only modes of degree $\ell = 0, 1$ can be reliably determined. These separations provide diagnostic information on the star's structure. The large separations give an estimate of the star's acoustic radius which is related to the stellar mean density, while the small separations such as d_{01}, d_{02} give diagnostics of the interior structure. Periodic modulations in these separations give diagnostics of the location of the boundaries of convective cores and envelopes.

The diagnostic power of the frequencies and separations can be enhanced by techniques which model, or subtract off, the contribution of the outer layers of a star which are poorly understood (Kjeldsen et. al. 2008, Roxburgh and Vorontsov 2003a). This is possible since the sound speed $c(r)$ in these layers is small so their contribution to the frequencies (e.g. α_ℓ in Equation (2.1)) is almost independent of degree ℓ and can be subtracted off by a suitable combination of frequencies, such as the ratio of small to large separations $r_{02} = d_{02} / \Delta$. As shown by Roxburgh and Vorontsov (2003a) models with an identical interior structure but with substantially different outer layers had separations d_{02} and Δ varying by up to 20% but the same value of the ratios r_{02} . Such ratios can be used when comparing an observed frequency set with that of a stellar model (cf. Miglio and Montalbán 2005).

2.4.4 Model independent inversions for the stellar mass

The result that $\alpha_\ell(\nu)$ is almost independent of ℓ provides the basis of a *model independent* inversion procedure to determine the internal density profile inside a star from an observational set of frequencies. Equation (2.4.1) above can be re-written as

$$F(\nu, \ell) = 2\pi T \nu_{n,\ell} - (n + \ell/2)\pi + \delta_\ell(\nu_{n,\ell}) = \alpha_\ell(\nu_{n,\ell}) = \alpha(\nu_{n,\ell}) \quad (2.4.2)$$

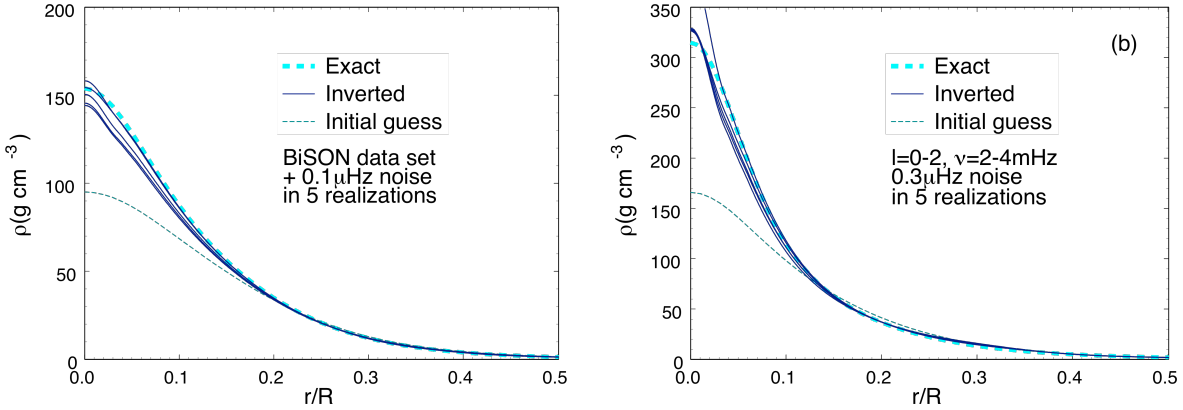


Figure 2.6: Inversion for the density distribution inside solar-like stars. Left: inversion for the Sun using BiSON frequency set with added noise, right: inversion for a model of a $0.8M_{\odot}$ star with only $\ell = 0, 1, 2$ modes and added noise of $0.3\mu\text{Hz}$. From the density distribution we get the mass of the star and by comparison with stellar models an estimate of its age.

with α a function only of ν . Given an observational set of frequencies $\nu_{n,\ell}^{obs}$ with estimated errors $\sigma_{n,\ell}^{obs}$, and a model of the stellar interior, we can calculate the internal phase shifts $\delta_{\ell} \nu_{n,\ell}^{obs}$ at say $r/R = 0.95$ using the observed frequency set. If the model is correct, $F(\nu_{n,\ell}^{obs})$ should collapse to a function of ν alone. The term $2\pi T\nu_{n,\ell}$, is itself a function of frequency alone and an adequate estimate of T can be obtained from $\Delta\theta$, to subtract off the major contribution from $(n + \ell/2)\pi$.

The unknown density profile $\rho(r)$ can be represented in terms of some basis functions $B_k(r)$, e.g. $\rho(r) = \sum C_k B_k(r)$. With an initial guess at $\rho(r)$ one calculates the mass distribution and hence pressure from hydrostatic support. To determine the sound speed $c(r) = \Gamma_1 P / \rho$ we need the adiabatic exponent Γ_1 ; since we only consider layers below the HeII ionisation zone this is very close to $5/3$ inside solar-like stars. The parameters C_k describing $\rho(r)$ are then iteratively corrected to find the optimal fit where $F(\nu_{n,\ell}^{obs})$ collapses to a function only of ν , and hence the internal density profile (Roxburgh & Vorontsov 2003b). The left panel of Fig. 2.6 shows the density profiles obtained using this procedure with the observed BiSON data set with added noise with standard deviation $0.1\mu\text{Hz}$, the right panel that obtained for a model of a $0.8 M_{\text{Sun}}$ using only $\ell = 0, 1, 2$ modes and added noise of $0.3\mu\text{Hz}$, both with different random realisations of the errors. The results are quite satisfactory.

Once we know the density profile, the total mass of the star is simply

$$M = \int_0^R 4\pi r^2 \rho(r) dr \quad (2.4.3)$$

Note that the regions where the density is not best constrained make only a small contribution to the total mass: in the centre the radius r is small and in the outer layers the density is small. The resulting density profiles can then be compared with those predicted by stellar evolution models to estimate the evolutionary age of the star (see Section 2.4.5 below). It should be stressed that the derivation of a model-independent mass requires that the radius R of the star is determined by other means; this is a necessary condition since the frequencies are invariant under a scaling of M and R that leaves M/R^3 invariant. As mentioned earlier, radii of the PLATO exoplanet host stars will be known to an accuracy better than 2% thanks to Gaia, which translates into **a well constrained model-independent exoplanet host star mass with a relative precision better than 2%**.

2.4.5 Model fitting to get masses and ages

In this approach, we compare the properties of set of observed frequencies with the predictions from a grid of evolutionary stellar models to find the model that best fits the observables (e.g. Brown et al. 1994, Miglio et al 2005, Metcalfe et al. 2009). The unknown effect of the surface layers can be overcome by scaling the difference between theory and observation for the Sun (Kjeldsen et al 2008), by comparing separation ratios as described in Section (2.4.3) above, or by the collapse of $F(\nu_{n,\ell})$ in Equation (2.4.2) to a function only of ν .

The best fit model then gives values for the mass, radius, age and internal structure of the stars.

We base the expectations on the nature and the quality of the seismic input data from PLATO on results of extensive hare-and-hounds exercises using artificial seismic data, which have been performed by the asteroFLAG consortium (Chaplin et al. 2008), and on direct experience of analysing seismic data from the photometric CoRoT observations (*e.g.* Appourchaux et al. 2008, see also Section 2.4.6). The results show that for PLATO we should be able to extract high-precision estimates of individual mode frequencies of main-sequence targets brighter than $m_V \approx 12$. For F, G and K main-sequence targets at $m_V = 11$ typical frequency uncertainties of individual modes in G and K stars will be about 1 part in 30,000, while in the hottest F stars the uncertainties may rise to about 1 part in 10,000.

Metcalf et al. (2009) estimated that with half a dozen surface-corrected frequencies available at each of $\ell = 0$ and $\ell = 1$, it becomes possible to constrain **the model-dependent masses to 3%, and the corresponding ages that the star has spent on the main sequence to 5%, if we assume the heavy-element abundances to be known to within a factor of two**. This result assumes that the model physics is correct. With the addition of more frequency estimates (*i.e.* of $\ell = 2$ modes, and of more overtones) further improvement of the parameter uncertainties will be possible. For a main-sequence target observed at $m_V = 11$, we would expect to be able to measure more than ten overtones of its $\ell = 0, 1$ and 2 frequencies. The largest source of observational uncertainty comes from the estimated heavy-element abundances. From the precision on the luminosity expected from Gaia, it would in principle be possible to constrain the abundances seismically, to a precision of about 10% (Metcalf et al. 2009), thus further improving the accuracy of the star's mass and age. The efficiency of model fitting to the observed frequencies depends on our ability to model stellar evolution, and the reliability of these models. Indeed, we stress that any technique that aims at determining the stellar age from observed properties of the star, be they classical observables, oscillation frequencies or quantities such as the small separation derived from such frequencies, depends on reliable modelling of the star. Thus the asteroseismic investigation of stellar structure and evolution is an essential part of the characterization of planet hosts. Some advance in our understanding of stellar modelling will come from investigations with data from CoRoT and Kepler but the superb PLATO data will provide a further dramatic improvement in the understanding of stellar evolution and hence in our ability to characterize the properties of the planet hosts.

The above techniques assume we have individual frequencies. However when the S/N ratios in the seismic data are insufficient to allow robust extraction of individual p-mode frequencies, it will still be possible to extract average estimates of the large and small separations $\langle \Delta_0 \rangle$, $\langle \Delta_1 \rangle$, $\langle d_{01} \rangle$, $\langle d_{02} \rangle$ and their ratios over one or more frequency ranges, owing to their regularity. These average values provide a complementary set of seismic data well suited to constraining the exoplanet host star parameters (*cf* Christensen-Dalsgaard, 1988). Coupled with classical observations of L , T_{eff} , $[Fe/H]$, $\log g$ delivered by Gaia (or even more precise by other means) this has considerably better diagnostic power than the classical observables alone. For very low signal to noise data the mean large separation $\langle \Delta \rangle$, some indication of its variation with frequency, and possibly an average value of the small separation d_{02} , can be determined from frequency windowed autocorrelation of the time series (Roxburgh & Vorontsov 2006, Roxburgh 2009b, Mosser & Appourchaux 2010). Measurement of the average large separation should allow the stellar density to be constrained to a precision of several percent from model fitting. In turn, because of the strong relationship between this separation and the stellar radius, the radius could also be estimated seismically to a similar precision.

2.4.6 Seismic achievements from CoRoT

The CoRoT satellite, launched in December 2006, has already observed several solar-type stars in its asteroseismic programme, and the results of these first analysis can be used to demonstrate the potential of this method to derive the stellar parameters. We take here the example of HD 49385, which is the coolest star observed so far in the asteroseismic programme of CoRoT and whose frequency spectrum was already shown in Fig. 2.5. HD 49385 is a G0V type star with an apparent magnitude $m_V = 7.4$. Taking into account the difference in collecting area between CoRoT and PLATO (in the PPLC concept), it would correspond to a star with $m_V \approx 10$. Importantly, the CoRoT data of HD 49385 are based on a 4.5 month monitoring, while PLATO will observe continuously for several years, yielding a far better quality, or equivalently, a similar quality for fainter stars. The effective temperature and luminosity of HD 49385 are estimated to be $T_{\text{eff}} =$

$6095 \pm 50 K$ and $\log L/L_{Sun} = 0.67 \pm 0.5$. Placing the star in the HR diagram results in a mass estimate of $1.36 \pm 0.15 M_{Sun}$ and age of $3.8 \pm 1.2 Gyr$, owing to the uncertainty on the details of the physics in the star's interior, and in particular on its initial core chemical composition. The star was observed by CoRoT during 136.9 days, with a duty cycle of 88.2%. Figure 2.7 shows the power spectrum in the 400-1600 μHz domain, smoothed with a 10 μHz boxcar. The comb-like structure, which can be seen in this figure, is typical of p mode oscillations. The large spacing can be easily measured at 56 μHz on this spectrum, allowing us to construct the échelle diagram also presented in Figure 2.4.3, folded with this value for the large spacing.

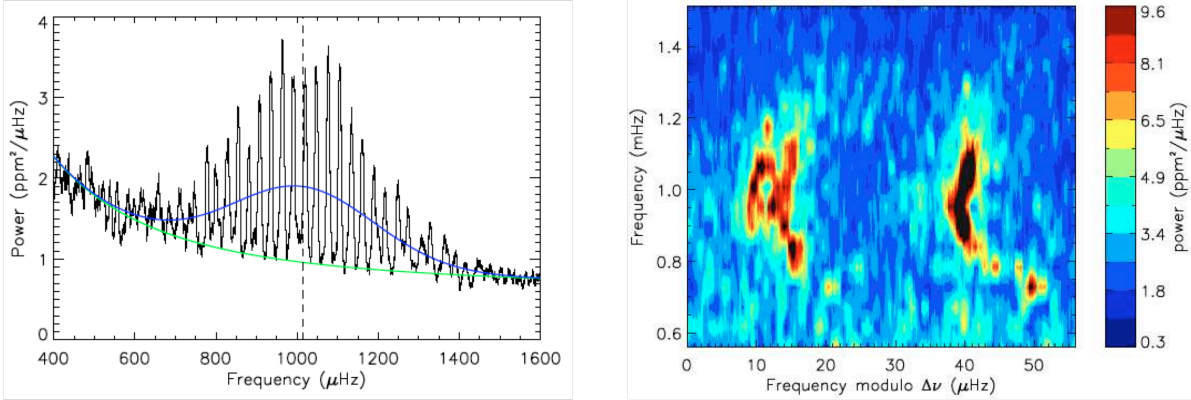


Figure 2.7: Left: Power spectrum of HD 49385 in the frequency range of the oscillations. The green curve represents the fitted background (granulation and white noise components). The blue curve corresponds to a Gaussian fit of the raw power spectrum giving $v_{max} = 1013\mu\text{Hz}$ (dashed line). Right: Echelle diagram of the same data computed with a large spacing of 56 μHz . From Deheuvels et al. (in preparation).

Three ridges appear clearly on the échelle diagram, with the ridge on the right corresponding to modes with $\ell = 1$, and the two ridges on the left to $\ell = 0, 2$. This identification allowed Deheuvels et al. (2009, submitted) to exploit about 30 oscillation modes present in this spectrum. A grid of models was computed, with different masses, ages, helium abundances, metallicities and overshooting distances. Deheuvels et al. then searched for the model offering the best fit with the fundamental parameters and the seismic parameters (large spacing, small spacings and their variations with frequencies). This preliminary modelling showed that we could expect a much better accuracy than with classical methods in the determination of the stellar mass, radius and age. At the present stage, using only a mean value of the large spacing and of the small spacing d_{01} , but working with fixed metallicity, we have $M/M_{Sun} = 1.36 \pm 0.04$ and age = $3.9 \pm 0.4 Gyr$, to be compared to the much larger uncertainties of determinations without asteroseismic observables. These early results from CoRoT demonstrate that indeed, masses, radii and ages of solar-type stars can be determined accurately via asteroseismology. Several other solar-type stars observed by CoRoT are being analyzed at present, including those of HD 52265, a $1 M_{Sun}$ star hosting a giant planet in a close-in orbit, with very encouraging results.

3 SCIENTIFIC REQUIREMENTS

3.1 Basic observation strategy

The main scientific objective of PLATO is to detect and thoroughly characterize a large number of exoplanetary systems. This will be achieved by monitoring the visible flux from a large number of bright stars during a long time (months, years) – and with a high cadence, thus obtaining a high quality light curve of each individual object. From these light curves one can detect the signatures of planets transiting in front of their parent stars, and using the same light curve to measure the micro variations of the same stars. The latter data will be used to perform a seismic analysis of the planet-host star from which one can derive the fundamental physical parameters of planet *and* star with ultra high precision. The long uninterrupted high precision photometric monitoring of large samples of stars will, combined with ground-based follow-up observations, such as high-resolution spectroscopy and interferometry, enable a full characterization of the

planetary systems. The primary targets of PLATO are therefore stars that are sufficiently bright for such characterization to be possible.

Because the transit depth is inversely proportional to the square of the star's radius, transiting planets will be preferentially searched around the small radii cool dwarf stars (and because our Sun is such a star). However, the stellar sample will be extended also to sub-giants, which have radii only slightly larger than dwarfs. The restriction to cool stars is also motivated by the need for subsequent radial velocity follow-up observations. Their spectra supply the large number of lines necessary to get very accurate radial velocity measurements and are thus eminently suited for the programme. Consequently, the core star sample for the PLATO mission will consist of cool dwarf and sub giant stars that are bright enough for the photometric precision required for the detection of small planets and for seismic analysis, namely 2.7×10^{-5} in 1 hr (see below) to be reached.

Each star with a detected transit will be followed up from the ground, including using high precision radial velocity measurements, in order to confirm that the detected event is indeed due to a planet, and also in order to measure the planet mass. These follow-up observations will be facilitated by the brightness of the PLATO targets, and will be most efficient for spectral types later than F5.

All exoplanetary transits will be investigated, leading to an extensive knowledge of exoplanet populations (mass function for exoplanets) and allowing us to relate the physical properties of the planet to the central star properties for an unbiased statistical sample. In particular, telluric exoplanets in the habitable zone will receive special attention. The mission design must be such that a statistically significant number of such planets can be studied.

Asteroseismic data from PLATO will be used to measure the stellar masses and ages, to confirm and improve the star's radius already known from the Gaia mission, as well as to study the internal structure and internal angular momentum of planet host stars.

Ground-based high resolution spectroscopy will be used to confirm or measure the stellar fundamental parameters (T_{eff} , $\log g$, chemical composition, rotation velocity, etc), as well as used to detect and measure radial velocity variations due to the orbiting planets and derive the planet/star mass ratio.

The knowledge of the planet orbital period, the planet/star radius ratio and the planet/star mass function, coupled to the measurement of the star's radius and mass, will allow us to derive all the planets fundamental physical parameters (mass, radius, orbit, age), assuming the stellar and planet ages to be equal. Additional ground- and space-based follow-up observations will also be obtained for the brightest targets, in particular in- and off-transit photometry (visible and IR) and high signal/noise spectroscopy providing information on the planet atmospheric composition and dynamics by differential observations.

In addition to the main goals focusing on the observation of the brightest stars of the sample, PLATO will also perform a more extensive survey of exoplanetary transits in front of a very large number of fainter stars. Also, in complement to the seismic analysis of planet host stars, asteroseismology of the many other types of stars present in the field of view will be used for a more complete study of stellar physics & evolution. Observations of stars of masses and ages, all across the HR diagram, including members of several open clusters and old population II stars, will be obtained for this purpose.

In order to maximize the surveyed sky area and the number of monitored stars at all magnitudes, the mission will comprise two long monitoring phases of two successive fields. A third step-and-stare phase at the end of the mission will be used to extend the sample of stars surveyed for short period planets and for stellar structure studies, as well as for revisiting targets of the first two pointings in an optimized way, to confirm longer period exoplanets.

3.2 Star counts

The choice of the stellar samples is a key issue in order to define the best pointing of the instrument and hence to maximize the science return, because the number of transiting systems scales linearly with the number of cool dwarfs and subgiants monitored. In the case of PLATO this is compounded by the need to focus on bright stars in order to guarantee an efficient follow-up of transiting candidates. This subject has been approached using either models of the Galaxy or star counts from available extensive photometric

catalogues. The star count approach has the advantage that it is based on real data, but generally only gives approximate stellar parameters of the population. The model approach, based on average stellar populations in the Galaxy, has the weakness that local fluctuations such as spiral arms are effectively removed. However, by definition, models give a complete knowledge of the (modeled) stellar population in terms of mass, temperature, luminosity class, radius, metallicity etc., allowing us to derive a precise characterization of the sample. Here we initially adopt a star count approach which we then validate using models.

The star count method is based on the Ofek (2008) catalogue, which contains 1,560,980 stars and is built from the cross-correlation between Tycho2 and 2MASS catalogs. In particular it includes Tycho stars with $B_T \leq 13$ and $V_T \leq 12$ with only one 2 MASS counterpart within 6 arcsec, which excludes stars with close objects that may contaminate the PLATO Point Spread Function. For each star in this catalogue, a fit to the Spectral Energy Distribution, using the Spectral Library of Pickles (1998), provides the spectral type and luminosity class. The simplified approach used by Ofek, ignoring interstellar reddening, has produced unphysically large numbers of K and M dwarfs in the solar neighbourhood. For a better identification of cool dwarfs and subgiants, an additional criterion on the J-H color was used: F5-M9 IV-V stars were counted only $0.10 \leq J-H \leq 0.65$. Moreover the Ofek catalog includes only 62% of the Tycho2 catalogue, and is therefore incomplete, presumably in the most crowded regions, so the derived numbers are likely lower limits to the true star counts.

Using the above method, cool dwarf and subgiant densities were estimated in a series of 550 deg² fields located in the continuous viewing zone of PLATO. The resulting maximum density of cool dwarfs and subgiants later than spectral type F5 is 12.27 stars per deg² for stars with $m_V \leq 11$. A fit to the cool dwarf and subgiant star counts gives a $\log(N)-m_V$ slope of 0.55, slightly lower than the 0.6 slope expected in spherical approximation, with absorption and scale effects as second order effects. These figures are very similar to those used for the payload studies, both in the industry and in the Payload Consortium, which were based on a preliminary estimate.

We have estimated the uncertainties of these numbers with different methods. First we critically analyzed Ofek's classification and made several small corrections (see Barbieri et al. 2009 in preparation, for details), evaluating the impact of the overestimates of K and M giants mentioned above. Finally the 2MASS catalogue was used for star counts at fainter magnitudes. Cool dwarfs and subgiants are taken as the stars with $0.11 \leq J-H \leq 0.62$ and $0.01 \leq H-K \leq 0.12$ and $1.45 \leq B-K \leq 2.9$, corresponding approximately to F5-K0 stars. These analyses show that the numbers derived with the Ofek catalog are uncertain within a factor 25%. Furthermore the 2MASS analysis allows to derive that the number of expected stars with $m_V \leq 13$ is ≈ 113 per deg²

We have further tested our results in an independent way using the Besançon model, bearing in mind the caveat stated earlier about the use of average densities in these modelling methods. Hence, we would expect the Besançon model to give lower star counts. This model is a synthesis of the stellar population in our Galaxy and includes dynamical and evolutionary aspects (Robin et al. 2003, Robin & Cr ez e, 1986). The Besançon model also includes some spatial structures such as the thin disc, thick disc, spheroid, and bulge. Each component has its own spatial distribution (scale height and density), IMF, evolutionary tracks and metallicity. The extinction is modelled by a diffuse thin disc. The model is reasonably complete but, of course, it predicts the average properties of the Galaxy and cannot account for local spatial fluctuations.

The output of the Besançon model is a catalogue of simulated stars, for which all the information is known: distance, mass, age, spectral type, luminosity class, metallicity, age, etc. Thanks to these capabilities it is possible to explore in detail the "average" properties of the stars in selected fields of view of PLATO. Note that the model accounts also for poissonian noise on stellar counts. We have simulated stars with visual magnitudes in the $m_V = 6-18$ range in a region in the $70^\circ \leq \text{longitude} \leq 130^\circ$ and $0^\circ \leq \text{latitude} \leq 60^\circ$ range, which is part of the visibility region of PLATO. We have used the Besançon model in its "grid" mode that allows us to take into account the variations of stellar density with the position in the Galaxy within the considered area, which is needed because of the large area that PLATO will observe.

As a further check we have used the Trilegal model (Girardi et al. 2005, <http://stev.oapd.inaf.it/cgi-bin/trilegal>). The counts from both models are within 25% of the counts derived from star count analysis.

All the star count tests performed during the assessment phase show that the numbers used so far are reasonably reliable, with some uncertainties on the actual number of cool dwarfs and subgiants. In the next

phase of the mission the precise final pointing(s) will have to be defined on the basis of a specifically designed observational campaign, likely based on medium-band photometry, including filters sensitive to temperature and gravity. Spectroscopy of a subsample will help in calibrating and testing the photometric classification. Based on the outcome, the best observational strategy will be defined. Finally early Gaia results (2015) will be used for the selection of individual targets within the selected field of view.

3.3 PLATO high level science requirements

3.3.1 Required noise levels and monitoring durations

The depth of a planetary transit is given by the ratio of the areas of the planet and its transited star, which is of the order of $\Delta F_{star} / F_{star} \approx 10^{-4}$ in the case of Sun-Earth analogs, while transit durations are typically of the order of 12 hours. In order to detect such transits at more than 4σ , a dimensioning requirement, we need to obtain a photometric noise level lower than about 2.5×10^{-5} in 12 hours, i.e. about 8×10^{-5} in one hour. This is the minimum requirement for the detection of an Earth-like planet in front of a solar-like star.

However, the measurement of several points across the transits will be necessary, implying lower levels of noise. In practice, a minimum of 8 to 9 points across the transit are necessary to characterize its shape, in particular the ingress and the egress parts. We therefore require a photometric noise level below 2.7×10^{-5} in one hour, for the highest priority star sample of the mission.

Recent results from CoRoT have shown that detecting, measuring and identifying oscillation modes in solar-type stars requires a noise level in amplitude Fourier space below about 1.6 ppm per $(\mu\text{Hz})^{1/2}$ (Michel et al. 2008, Deheuvels et al. 2009, Garcia et al. 2009), which is equivalent to 2.5 ppm in 5 days, or 1 ppm in 1 month, and which translates approximately into a noise level of 2.7×10^{-5} in 1 hr, i.e. similar to that for the detection and characterization of Earth-like transits.

The duration of the observations needs to be longer than 2 (goal 3) years, so that at least 2 (goal 3) consecutive transits for Sun-Earth analogs can be detected.

For the seismic analysis of the target stars, the total monitoring time must be sufficient to yield a relative precision of 10^{-4} for the measurement of individual mode frequencies, which is needed to perform the inversion of the oscillation spectra. For solar-type stars, this comes down to an absolute precision of 0.2 to 0.1 μHz , which translates into a minimum monitoring time of 5 months for a reasonable S/N of 10 in the power spectrum.

3.3.2 Basic measurement principle; PLATO products

R0a PLATO must provide long, high duty cycle, high precision photometric time series in visible light of a large number of bright stars. The basic PLATO data products are white-light curves with characteristics and of the stellar samples specified by the requirements below (see **R2** and **R5**).

R0b In addition, it is required that part of the payload (e.g. a small subset of the telescopes or individual detectors if a multi-telescope concept is chosen) provide photometric time series in at least two separate broad bands (see **R8**). These will be used in particular to constrain the identification of the detected oscillation modes in bright classical pulsators.

R0c PLATO must also provide relative astrometric measurements of the targets of the bright samples (defined in **R2** below). These astrometric measurements will allow us to search for giant planets through the detection of the associated star wobble, and will also be used to identify false positives, due for instance to background eclipsing binaries. Astrometric measurements may also be used to evaluate a posteriori instrument jitter properties.

3.3.3 Surveyed field

A preliminary examination of potential stellar fields for PLATO was performed, and resulted in the definition of two template fields. The first one, in the southern hemisphere, is centered at ecliptic coordinates (210°, -60°). The second field encompasses that of the *Kepler* mission, and is centered at ecliptic coordinates

(306°, +61°). During the step & stare phase, the instrument must be capable of accessing other fields at any position in the sky, at a proper time for these observations to be feasible.

R1 Two successive fields must be monitored, followed by a step & stare phase, during which additional fields will be surveyed. During the step & stare phase, the instrument may also have to come back to the two fields observed during the two long monitoring phases.

3.3.4 Stellar samples and photometric noise level

R2 Five complementary stellar samples were defined as targets of the PLATO mission, and are listed and justified below, by order of priority :

P1: Given the probability to detect planet transits, estimated to be about 0.1% (geometric probability x fraction of stars with planets), we estimate that at least 20,000 cool dwarfs and subgiants need to be surveyed for a sufficient amount of time to detect long period orbits, i.e. typically for 2 to 3 years. This number of surveyed stars implies an expected number of telluric planets in the habitable zone of the order of 20, which we consider as the objective for PLATO. This would represent a very significant improvement compared to *Kepler*, considering in addition that such exoplanetary systems detected by PLATO would also be fully characterized. Additionally we would expect to detect many transits of larger planets around these stars. Therefore, more than 20,000 dwarfs and subgiants later than spectral type F5, with a noise level below 2.7×10^{-5} in 1 hr, must be observed with the required duty cycle for more than 2 (goal 3) years. **This sample, with m_V typically between 8 and 11, is the backbone of the PLATO mission, and is considered as the highest priority objective.**

P2: Some of the targets can be observed at a noise level enabling the detection of small exoplanets, significantly below 8×10^{-5} in 1 hr (Earth-size). This strategy defines a second, more numerous, star sample, for which planet detection and seismic analysis can potentially be achieved in different phases of the mission.

This dual observation must be potentially performed on targets chosen among as large a sample as possible, with a goal of 80,000 dwarfs/subgiants later than spectral type F5 for this sample and with noise levels in between 2.7×10^{-5} /h and 8×10^{-5} /h. These objects will typically be between 11 and 13 in m_V .

P3: The search for planetary transits around very bright and nearby stars presents a specific interest, as these sources will become privileged targets for further ground- and space-based observations. We therefore request the monitoring of a large number of very bright stars with the goal of detecting a few telluric planets in their habitable zone. Hence, more than 1,000 dwarfs and subgiants later than spectral type F5 and brighter than $m_V=8$ must be monitored with a noise level below 2.7×10^{-5} in 1 hr, with the required duty cycle for more than 2 (goal 3) years.

P4: The detection of an even larger number of short period planets around such very bright stars will also be used as input for further instruments aimed at characterizing the planetary atmospheres. Hence, more than 3,000 dwarfs and subgiants later than spectral type F5 and brighter than $m_V=8$ must be monitored with a noise level below 2.7×10^{-5} in 1 hr, with the required duty cycle for more than 5 months.

P5: Finally, we need the observation of very large number of stars with the required precision to detect telluric planets around solar-type stars, i.e. 8×10^{-5} in 1 hr, but without seismic analysis. For these detections, we will rely on other, less precise and less reliable techniques to assess the mass and age of the host stars. These other methods, e.g. based on a correlation of stellar rotation with age, will likely be improved by a proper calibration using the seismological measurements of the P1 sample. The minimum number of such stars is 250,000, out of which we expect several hundred transits from telluric planets. As for the first sample we would also expect many more transiting larger planets. Hence, more than 250,000 dwarfs and subgiants later than spectral type F5, with a noise level below 8×10^{-5} in 1 hr, with m_V typically between 8 and 13-14, must be observed with the required duty cycle for more than 2 (goal 3) years.

The above noise levels are specified as corresponding to photon noise only. With the addition of requirement **R6b** below, ensuring that the measurements remain photon-noise limited, similar noise levels are expected when taking account all sources of noise.

3.3.5 Duration of monitoring

R3a & b: The total duration of the monitoring of the first and second fields must be longer than 2 (goal 3) years.

R3c: The step and stare phase at the end of the mission must have a duration of at least 1 (goal 2) year. During this phase, previously monitored fields, as well as additional fields, will be surveyed for at least 2 months and up to 5 months each. In addition, further visits of the previously surveyed fields will be organized in an optimized way to study long period exoplanets (several years), and will possibly occur at any time during the step and stare phase.

3.3.6 Time sampling

The duration Δt_{tr} of a transit of a planet with semi-major axis a and orbital period P in front of a star with radius R_{star} is given by $\Delta t_{tr} = P R_{star} / (a/\pi)$. For true Earth analogs $\Delta t_{tr} = 13$ hours. More generally, the duration of a transit around a single star may last from about two hours (a "hot giant" planet around a low-mass star) to over one day, for planets on Jupiter-like orbits (five AU distance). Planets in the habitable zone, however, will cause transits lasting between five hours (around M stars) and 15 hours (for F stars), for equatorial transits.

Because individual transits have durations longer than 2 hours, a time sampling of about 10 to 15 minutes is in principle sufficient to detect all types of transits, as well as to measure transit durations and periods. However, a higher time resolution is needed in order to accurately time ingress and egress of the planet transits for which the S/N in the light curve will be sufficient. The accurate timing will allow the detection of third bodies, which cause offsets in transit times of a few seconds to about a minute, and will allow to solve ambiguities among possible transit configurations through the determination of ingress and egress time of the planet. In practice, a time sampling of about 50 sec will be necessary to analyze in such detail the detected transits.

The needed time sampling for the asteroseismology objectives can be derived directly from the frequency interval we need to explore, which is from 0.02 to 10 mHz. In order to reach 10 mHz, the time sampling must correspond to at least twice this frequency, i.e. of the order of 50 sec.

R4a: The sampling time for intensity measurements of stellar samples P1, P3 and P4 must be shorter than 50 sec.

R4b & c: The sampling time for intensity measurements of stellar sample P2 & P5 must be shorter than 10 min, and shorter than 50 sec after a first transit detection, for a precise timing of further transits.

R4d: The sampling time for relative astrometric measurements of stellar samples P1, P3, P4, as well as of sample P2 during the step & stare phase, must be shorter than 10 min.

3.3.7 Photon noise versus non-photonic noise

R6a: the photon flux of the target stars must be sufficiently high to ensure that photon noise complies with the photometric noise requirements.

R6b: all other sources of noise must remain at least 3 times below that of the photon noise, at least for stars of sample P1, in the frequency range 0.02-10 mHz. Downward of 0.02 mHz, the non photonic noise level is allowed to rise gradually, to reach a maximum of 50 ppm per $(\mu\text{Hz})^{1/2}$ in Fourier amplitude space at a frequency of 3 μHz , for stars with $m_V = 11$.

3.3.8 Overall duty cycle

The probability that N transits of the same planet are observed is given by $p_N = d_f^N$, where d_f is the fractional duty cycle of the instrument. In order to achieve an 80% probability that all transits of a three-transit sequence are observed, a duty cycle of 93% is needed, ignoring gaps that are much shorter than individual transits. The requirement for planet-finding is therefore that gaps which are longer than a few tens of minutes do not occur over more than 7% of the time, with a loss by gaps as small as 5% being desirable.

A similar requirement is also imposed for seismology. Gaps in the data produce sidelobes in the power spectrum, which make mode identification ambiguous. Periodic gaps in the data must be minimized, as they will produce the most severe sidelobes in the power spectra. It can be shown that periodic outages representing 5% of the total time produce aliases with a power of about 1.5% of that of the real signal. Such sidelobes are just acceptable, as they will remain within the noise for most of the stars observed. It is therefore required that periodic data gaps are below 5%.

Non-periodic interruptions have a less catastrophic influence on the power spectrum, and can therefore be tolerated at a higher level, provided the time lost is compensated by a longer elapsed time for the observation. Random gaps in the data representing a total of 10% of the monitoring time yield sidelobes with a power lower than 1% of that of the real signal, which will be adequate for this mission. The requirement on random data gaps is therefore that they do not exceed 10% of the elapsed time.

R7a: Gaps longer than 10 minutes must represent less than 7% (goal 5%) of the total observing time per target, for the longest observation period (3 years).

R7b: Periodic gaps of any duration must represent less than 5% (goal 3%) of the total observing time, and less than 2% at any given frequency in Fourier space, over periods of 5 months.

R7c: The total amount of gaps, periodic or non periodic, of any duration, must represent less than 10% (goal 5%) of the total observing time over periods of 5 months.

3.3.9 Colour information

In addition to the measurement of oscillation frequencies, asteroseismology requires the identification (l, m) of the detected modes. Knowing the l identification for the dominant modes of each of the bright target stars of PLATO implies a significant reduction of the free parameter space of stellar models and is a requirement to guarantee successful seismic inference of their interior structure parameters and ages.

For oscillations in the asymptotic frequency regime, the derivation of frequency spacings suffices to identify the modes. For most main-sequence stars excited by the κ mechanism, when the modes do not follow particular frequency patterns, the identification of l can be achieved by exploiting the difference in amplitude and phase of the mode at different wavelengths.

Therefore, some degree of colour information must be present in the PLATO data.

R8: Part of the payload must provide photometric time series in at least two separate broad bands. (see **R0b**). If a multi-telescope concept is chosen, at least two of the telescopes, or a dedicated subset of individual detectors must provide photometric monitoring in at least two separate broad bands (one band per telescope). The photometric bands must be maximally separated, in such a way that the photon flux integrated in the common wavelength range represents less than 10% of the total photon flux. Less than 50% of the photons are allowed to be lost due to this broadband photometry.

3.3.10 The need to go to space

The science goals of PLATO require the detection and characterization of significant numbers of planetary transits, as well as the seismic analysis of their host stars. As argued earlier, photometric transits are needed to allow us to derive the planet radii and make sure that the orbit is seen edge-on, lifting a major uncertainty in the measurement of their masses. This in turn requires very high precision, very long duration and high duty cycle photometric monitoring, which cannot be done on the ground. The Earth's atmosphere indeed causes strong disturbances that limit the achievable performance to millimag accuracies, mostly through scintillation noise. The small amplitude of the photometric dips caused by terrestrial planets is therefore beyond the range of ground-based observations.

Alternative techniques can be used from the ground to achieve exoplanet detection, and has seen tremendous progress in recent years. The most efficient of these relies on radial velocity measurements, performed in high resolution spectroscopy. The most severe drawback of the radial velocity technique is that the resulting mass determination suffers from the $\sin i$ ambiguity, except in the rare cases where the inclination angle i can be estimated. Photometric transit techniques are the only ones that can overcome this difficulty. In addition, long, uninterrupted observations, that only space-based instruments can provide, are necessary to optimize

the probability of transit detection, as well as to avoid sidelobes in stellar oscillation power spectra. The duty cycle of ground-based observations can be improved by multi-site networks of telescopes equipped with appropriate spectrographs. The required duty cycle for reaching the science goals of PLATO would require a highly redundant network with at least 9 or 10 sites distributed in longitude. However, even if such an ambitious ground-based network can be set up in the future, the drift of sidereal time limits to only a couple of months the total time during which a high duty cycle can be obtained. An attractive alternative is to perform these observations from Antarctica, in high quality astronomical sites such as Dome C. However, even there, the total duration of high duty cycle observations would not exceed three months, well below the requirements. Space is therefore necessary on one hand because of its stability and the absence of photometric disturbances, and on the other hand because it offers the possibility to perform the long, uninterrupted observations that are needed to detect exoplanets and to perform seismic analysis of stars.

4 EXPECTED PERFORMANCES

As described in Sect. 8 below, three independent payload concepts have been studied. All three are basically compliant with the science requirements presented above. The corresponding designs are based on multi-telescope concepts with very wide fields of view.

The large size of the instrument field of view in all three concepts leads to very high performances for PLATO in terms of numbers of stars observable down to various magnitudes and various levels of photometric noise. These high performances are further enhanced by the adopted observation strategy, including two consecutive long pointings of several years, followed by a step-and-stare phase.

However, it is crucial to study all possible sources of photometric noise in order to correctly assess the level of noise expected for each target: photon noise, CCD readout noise, jitter noise, contamination by neighbouring sources, etc.

In order to properly study all these effects, and to estimate reliably the final expected performances of the mission, a full end-to-end simulator was developed in the framework of the PPLC payload study, which is described in the following section. This simulator was used extensively in the PPLC study, with results that are briefly summarized below and fully described in the PPLC study report. It is now being applied as well to the other two payload concepts proposed for PLATO, with the goal of verifying the conclusions of these studies in terms of final performances.

4.1 The PLATO end-to-end simulator

The PLATO end-to-end simulator is based on previous similar tool developed for *Eddington* (De Ridder et al. 2006). The tool developed for PLATO, dubbed "PLATOSim", allows us to perform a complete performance analysis of the instrument payload. It includes all characteristics of the star field, instrument, detectors, satellite jitter, and data treatment algorithms, in a realistic way, and therefore is very efficient and reliable as a performance estimator. The "PLATOSim" tool is fully described in a document produced by the PPLC, and will be soon published in the general literature (Zima et al., in preparation). We give here a brief overview of how the observations are simulated.

The modelling of a CCD image with PLATOSim is carried out in several steps. The first step is to define the field of view of the satellite. Important parameters here are the size of the CCD, the pixel-scale, and the input positions and magnitudes of the stars. The latter values were taken from a catalogue that has been compiled specifically for PLATO (see Sect. 3), and includes more than 10^7 stars in the PLATO field of view, down to $m_v=15$.

Each CCD pixel is represented by typically 32×32 sub-pixels, ensuring a realistic modelling of intra-pixel sensitivity variations and of the minuscule ACS jitter movement which is equivalent to a few sub-pixels. Only at the very end of the CCD modelling, the sub-pixels are re-binned to normal pixel scale. After this first step, a noise-free image is created, containing the locations and the fluxes of all stars in the field of view.

In a second step, the image is degraded by the optics, CCD readout modes are simulated, and we take into account photon noise, background, noise sources of the CCD, and finally satellite jitter. In the absence of a jitter model for the PLATO satellite at this early stage of the study, the jitter behaviour was derived from recorded time series in yaw, pitch and roll from the ISO and CoRoT satellites, rescaled to an overall rms of 0.2 arcsec, and resampled at 1 sec intervals to provide sufficient time resolution.

We model the global sensitivity variations (flat field) of the CCD by assuming a $1/f$ spatial power spectrum which resembles that of a typical CCD (De Ridder et al. 2006). Additionally, at sub-pixel level sensitivity variations that have white-noise characteristics are introduced. The lower sensitivity of the pixel-edges is also modelled at sub-pixel level. An example of such simulated images at sub-pixel level is shown in Fig. (4.1).

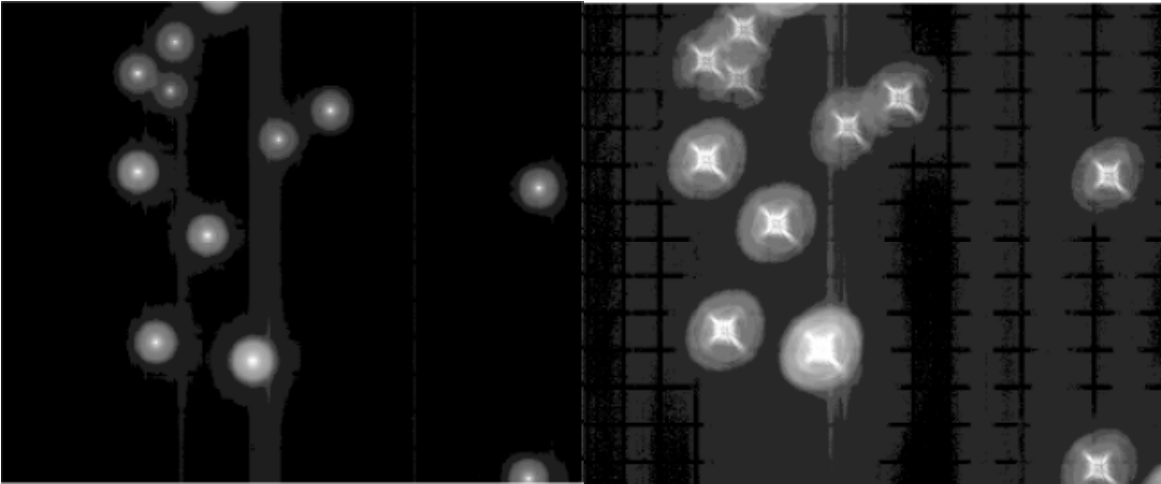


Figure 4.1: Simulated images at sub-pixel scale of a stellar field using PSFs at field center (left) and field edge (right). Note the grid-like structure at the image background which arises from the lower intra-pixel sensitivity. Image generated with PLATOSim, using all parameters of the PPLC design.

After series of images have been computed and stored, two photometric algorithms, simple aperture and weighted mask photometry, are fully simulated. A large number of simulations were made to test the impact of the various sources of noise and perturbations and to assess the expected performance of the photometric observations for different characteristics of the CCD and instrument, different positions in the sky, and different optical designs. These simulations are described in detail in the PPLC assessment study report and its appendices.

We give below the most important results obtained with PLATOSim.

4.2 Impact of confusion and contamination

In all three designs, the focal planes are populated with large format CCDs, with a large pixel size on the sky. For instance, concept C (see Sect. 8) has a pixel size of 15 arcsec, and a total optical PSF size of 30 arcsec (90% ensquared energy). All three studies were therefore concerned with potential decrease of performances due to confusion/contamination problems. Contamination by neighbouring faint sources has two main effects on the photometry :

- their relative position with respect to the photometric masks will change due to satellite jitter and produce photometric noise due to contaminating sources getting partly in and out of the photometric masks ;
- their presence in the photometric mask increases the level of photon noise, against which the brightness variations of the program star will need to be measured.

The PLATOSim tool was used to quantify both effects. We used the characteristics of the PPLC design for this assessment, but the conclusions would be very similar for the other concepts. We found that the first effect, due to jitter, is dominant, but can be corrected a posteriori on the ground, in a similar way as what is done for the CoRoT data. Details of how to perform this correction for the particular case of the PLATO data are given in the PPLC study report. It can be shown that, after correction, the impact of the jitter effect becomes negligible. The impact of contaminating sources is therefore limited to that of the second effect, which we examine in detail in the following.

We considered three cases for the stellar field, characteristic of the Carina star field, which was used as a template field for PLATO: a sparse field, a medium field and a dense field, roughly equally distributed in the full surveyed field.

Based on requirement R6b presented in Sect. 3, a target is considered as contaminated whenever the photon noise attached to its contaminating sources reaches one third of the photon noise of the target itself. Figure

4.2 quantifies these results, using both weighted mask and full aperture photometry for the sparse, medium, and dense fields. It demonstrates that for all three stellar field densities, stars with $m_V \leq 10$ are only marginally affected by pollution. For fainter stars, the dense field is more affected than the sparse and medium fields, as expected. For the two latter fields, pollution results in no serious degradation until magnitude 13, where more than 50% of the stars are not polluted. Even for the densest field, pollution affects less than 40% of the stars down to 11th magnitude, when using weighted mask photometry. The plots also reveal that in average less stars are affected by pollution when using weighted mask photometry, as expected.

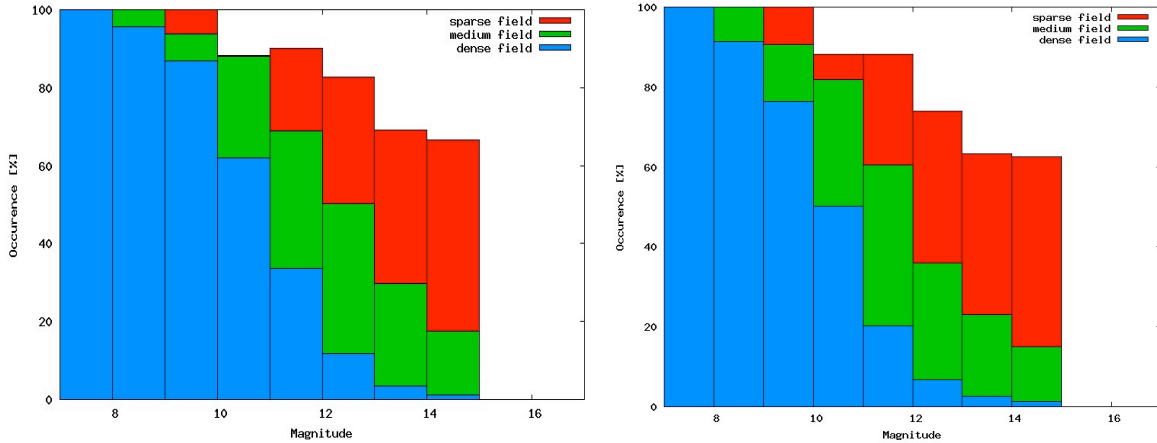


Figure 4.2: Percentage of stars that are NOT polluted by nearby sources as a function of the input magnitude in the sparse, medium, and dense field using the central PSF and weighted mask photometry (left) or full aperture photometry (right). A star is considered contaminated if the flux of polluting sources in the photometry mask contributes at least 1/3 of the source's photon noise.

Extensive simulations were also performed to test how pollution will degrade the seismic signals for 3-year runs. The main conclusion is that almost none of the PLATO stars up to $m_V=11$ with oscillation amplitudes above 10 ppm will be affected by confusion.

These results demonstrate that confusion, although non negligible, is definitely not a major concern at the magnitudes of the main targets of PLATO.

4.3 Expected noise level

The PLATOSim end-to-end simulator was also used to estimate the overall level of noise for all stars present in the simulated field, as well as to study in detail the various contributors to this noise. This analysis was performed for concept C, but similar analyses are in progress concerning the other two concepts. All details of these calculations can be found in the PPLC study report.

Fig. 4.3 presents these results for a representative fraction of the PLATO field, and shows that photon noise level is approached closely at magnitudes brighter than $m_V=10$, and that non photonic noise remains below 1/3 of the photon noise at least down to $m_V=11.5$. It also shows that a level of noise of $2.7 \cdot 10^{-5}$ in 1 hr is reached down to $m_V=11$, while a photometric noise of $8.0 \cdot 10^{-5}$ in 1 hr is obtained for stars with magnitudes around 12.5. At fainter magnitudes, the noise becomes significantly higher than pure photon noise, due to the contribution of contaminating sources in the photometric mask, as discussed in the previous section.

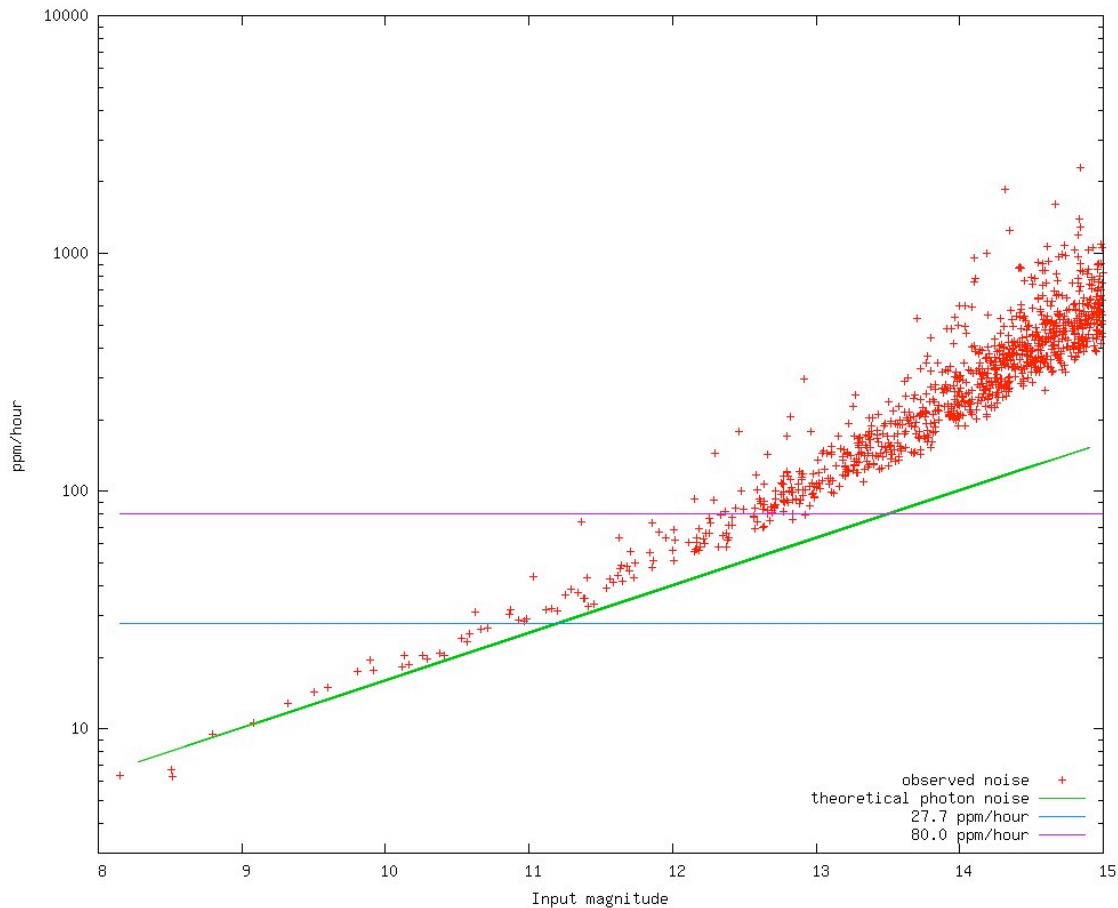


Figure 4.3: noise level measured in the PLATOsims simulation for stars in a representative subset of the PLATO field, using full aperture photometry. The full straight line represents the expected photon noise of the sources only.

4.4 Expected numbers of targets

The impact of PLATO on exoplanet science will be directly related to the number of exoplanets that can be detected and fully characterized, and to the coverage of the planet parameter space (orbit, radius, mass) achievable by the mission. The key asset of PLATO in this respect will be the brightness of its target stars, which will be bright enough for enabling an asteroseismic analysis to determine the star's mass and age, as well as for a fast and efficient radial velocity follow-up from the ground.

Table 4.1 shows the expected numbers of dwarfs and subgiants later than spectral type F5, observable with PLATO and *Kepler* at various levels of noise: 2.7×10^{-5} per hr, needed to measure transits of small terrestrial planets and to perform seismic analysis of their host stars; and 8.0×10^{-5} per hr, enabling the detection of telluric planets. These estimates are based on the star counts presented in Section 3.2 and on the various instrumental concepts studied for PLATO. The numbers quoted for *Kepler* are based on the same assumptions concerning the expected counts of cool dwarfs and subgiants, and take into account the actual instrument efficiency and field of view.

Table 4.1: Expected numbers of targets from PLATO and Kepler, at various photometric noise levels and various magnitude limits

Design & surveyed area	PLATO concept A 3600 deg ²		PLATO concept B 1250 deg ²		PLATO concept C 3600 deg ²		Kepler 100 deg ²	
noise level (10 ⁻⁵ /hr)	# cool dwarfs & subgiants	mag lim	# cool dwarfs & subgiants	mag lim	# cool dwarfs & subgiants	mag lim	# cool dwarfs & subgiants	mag lim
2.7	22,000	10.4	21,000	11.1	21,000	9.8-11.1	1,300	11.2
8.0	260,000	12.7	257,000	13.5	238,000	11.8-12.9	25,000	13.6
design & surveyed area	PLATO concept A 3600 deg ²		PLATO concept B 1250 deg ²		PLATO concept C 3600 deg ²		Kepler 100 deg ²	
magnitude	# cool dwarfs & subgiants		# cool dwarfs & subgiants		# cool dwarfs & subgiants		# cool dwarfs & subgiants	
6					90		0	
8	1,350		675		1,350		30	
9	3,800		1,320		3,800		100	
10	13,500		4,700		13,500		370	
11	48,300		16,800		48,300		1,300	

5 GROUND-BASED SUPPORT

The prime science product of PLATO consists in a sample of fully characterized planets of various masses, sizes, temperature, and ages, with a special emphasis on terrestrial planets in the habitable zone of their parent stars. To reach this ambitious goal, in addition to the space-based photometric transit detections and asteroseismic characterization, a ground-based support is absolutely required, mostly for candidate planetary system follow-up.

The role of the follow-up is multiple. We first need to discard false positive configurations leading to photometric signatures similar to the ones induced by planetary transits. Then, complementary observations provide information on the planet properties not available from the light curves, the most important among them being the planet mass derived from radial velocities. Taking advantage of the expertise gained with the successful ground-based transit search surveys, and with the CoRoT space mission (Léger et al. 2009), a battery of diagnostics have been developed to detect some of the most common false positive configurations directly from the photometric observations. Typical false positives include grazing eclipsing binaries, eclipsing binaries diluted by a physical or optical bright stellar companion, transits by planetary-size stars (e.g. late M dwarfs for giant planets, or white dwarfs for terrestrial planets). The most efficient surveys on the ground still have 5 to 6 times more false positives than real planets in their candidate list. From the CoRoT experience, we are furthermore learning that this ratio seems to get less favourable when going to lower-size planets (Almenara et al. 2009). **The final performance of the PLATO space-based transit search program is thus ultimately determined by the associated follow-up capabilities.** It is therefore particularly important to include these considerations in the planning of the mission.

For low-mass objects the radial velocity follow-up will require large telescopes and very high precision measurements (0.1 m/s). In addition, it will be time consuming since a large number of measurements will be necessary to average the intrinsic stellar noise over an entire orbital period as discussed in the next section.

5.1 Limitations to precise radial velocity follow-up measurements

The planet minimum mass estimated from Doppler measurements is directly proportional to the amplitude of the reflex motion of the primary star. The characterization of the lowest possible mass planets detected with PLATO will then be intimately linked to the ultimate long-term precision achieved on the radial velocity (RV) measurements of the star. Looking for the highest RV precision, several sources of uncertainty have to be considered. They can be classified into several broad categories: photon count, technical, and astrophysical. Each of these sources is essentially independent from the others and thus the actual precision eventually obtained on the measurements will be a quadratic combination of the different contributions.

Instrumental requirements: The exciting results obtained with the ESO HARPS spectrograph demonstrating sub-m/s long-term radial velocity precision (typically 80 cm/s for published planetary systems) have motivated new studies to push down the limits of Doppler spectroscopy to reach the few cm/s precision level with especially-designed spectrographs. From the instrumental perspective, reaching this precision level should be possible provided that a special care is put in some very important aspects (Pepe & Lovis 2008): spectrograph stability, high spectral resolution ($R > 150,000$) to resolve the spectral lines, adequate sampling, precise wavelength reference, efficient image scrambling, and precise guiding and centering. The ESO ESPRESSO/VLT and CODEX/E-ELT materialize the efforts in this direction. PLATO will provide secure Earth-like candidates to be followed with these new instruments.

Contamination effects: the contamination of the target spectrum by an external source is also a potential limitation for the precision of the RV measurements, especially if the contaminant contains spectral features. The most disturbing cases are:

- *Light from a close-by object:* the light of faint objects close to the science target may fall on the spectrograph fibre and contaminate the science target spectrum. This is in particular the case of transit false positive detection due to triple star blends. High-resolution, high-contrast preparatory or follow-up observations with instruments equipped with AO capabilities will be required to point out visible companion of any magnitude closer than typically 3 arcsec from the science target.

- *Moonlight:* In the same way, we have to avoid that direct or indirect sunlight reaches the detector with a contrast magnitude compared to the science target smaller than ~ 10 .

- *Atmospheric effects:* Since correction or modelling of atmospheric features is very difficult, the scientific data reduction must avoid spectral zones with atmospheric lines deeper than 1/10000 of the spectral lines of the observed science target.

Photon noise: The uncertainty on the RV's associated with photon noise roughly scales with the measurement signal-to-noise ratio (S/N) of the spectra, i.e. it scales with the square root of the flux, or also with the telescope diameter. With HARPS, we achieve 1 m/s on a V=7 K dwarf in a 1 minute exposure. This corresponds to an exposure time of close to 4 hours for a V=13 star. Assuming a similar spectral window (0.38-0.68 μ m), considering an expected efficiency about 4 times better for ESPRESSO (from phase A study), and taking into account the difference in collecting areas, we estimate that we will reach 10 cm/s in 15 min for a V=8 star, or in 4 hours for a V=11 star, with ESPRESSO on the VLT. These estimates demonstrate the need for bright stars when considering the radial velocity follow-up of very low-mass planet candidates.

Stellar jitter: Besides instrumental, environmental and photon-noise limitations, other phenomena intrinsic to stellar atmospheres, which we call "stellar noise" or "stellar jitter", have to be taken into account.

- *p-mode oscillations:* Stars having an outer convective envelope can stochastically excite p-mode oscillations at their surface through turbulent convection. These so-called solar-like oscillations have typical periods of a few minutes in solar-type stars and typical amplitudes per mode of a few tens of cm/s in radial velocity (e.g. Bouchy & Carrier 2001, Kjeldsen et al. 2005, Figure 5.1). The observed signal is the superposition of a large number of these modes, which may cause RV variations up to several m/s. Amplitudes of the RV variation become larger for early-type and evolved stars. Low mass, non-evolved solar-type stars are therefore easier targets for planet searches. However, even in the most favourable cases, it remains necessary to average out this signal if aiming at the highest RV precision. This can be done integrating over a few typical oscillation periods. Usually, an exposure time of 15 min is sufficient to decrease this source of noise well below 1 m/s for dwarf stars. Estimates based on asteroseismology models show that for the quietest stars, we easily get down below 10 cm/s in about 20-30 minutes (Eggenberger P., private comm).

- *Granulation and super-granulation:* Granulation is the photospheric signature of the large-scale convective motions in the outer layers of stars with convective envelopes. The granulation pattern is made of a large number of cells with upward and downward motions tracing hot matter coming from deeper layers and matter having cooled down at the surface. On the Sun, the typical velocities of these convective motions are 1-2 km/s in the vertical direction. However, the large number of granules on the visible stellar surface ($\sim 10^6$) efficiently averages out these velocity fields, leaving some remaining jitter at the m/s level for the Sun, probably less for K dwarfs (e.g. Palle et al. 1995, Dravins 1990). The typical timescale for granule evolution is about 10 minutes for the Sun. On timescales of a few hours to about one day, other similar phenomena occur, called meso- and super-granulation. These are suspected to be larger convective structures in the stellar photosphere that may induce additional stellar noise, similar in amplitude to granulation itself. Overall, granulation-related phenomena likely represent a significant noise source when aiming at sub-m/s RV precision, and observing strategies to minimize their impact must be envisaged (see next section, Fig. 5.1).

- *Magnetic activity:* Magnetic phenomena at the surface of solar-type stars induce radial velocity variations through the temporal and spatial evolution of spots, plages, and convective inhomogeneities (Saar & Donahue 1997; Saar et al. 1998). When the star-spot pattern is long-lived, variations in line asymmetry are modulated by the rotational period of the star and can mimic a planetary signal (e.g. Queloz et al. 2001; Bonfils et al. 2007). When the star is observed longer than the typical lifetime of starspots, the signal becomes incoherent and is detected as radial-velocity "noise", potentially inhibiting the detection of planetary signals of lower amplitude. In practice, radial-velocity perturbations related to stellar activity are referred to as "stellar jitter". Stellar jitter depends on effective temperature, stellar activity, and projected rotational velocity (e.g. Wright et al. 2004). Typical values of stellar jitter are below 1 m/s for slowly rotating, chromospherically quiet G-K dwarfs (Mayor et al. 2009b). To quantify the activity level of their targets, Doppler planet searches traditionally use the parameter R_{HK} which represents the fraction of a star's bolometric flux emitted by the chromospheres in the Ca II H and K lines (Noyes et al. 1984). Since this chromospheric emission is closely related to the surface magnetic flux, a high value of R_{HK} is an indication that a star may exhibit significant activity-related velocity variations.

The bottom level of the stellar-induced velocity jitter for the quietest stars is not known yet. An illustration of this is given by the distribution of the velocity rms in the HARPS high-precision programme which peaks at 1.4 m/s, despite it includes all possible sources of noise: instrument, photon noise, stellar jitter, as well as undetected planets.

5.2 Timescales of intrinsic variations and optimal observing strategy

Although stellar noise is a major limitation on very high precision Doppler measurements, adequate observing strategies might help us diminish its effect.

Solar-like oscillations are clearly detected with HARPS. The strategy adopted to minimize this oscillation noise consists in setting the exposure times to 10-15 minutes to average out the signal over a few oscillation periods. Although time consuming, this approach allows us to keep the residual noise below ~ 10 -20 cm/s for late G and K dwarfs. Following theoretical predictions we anticipate exposures of 20-30 minutes with ESPRESSO (or CODEX) to go down to a few cm/s. On intermediate and long time scales, Doppler measurements are affected by stellar granulation and stellar activity, respectively. A strategy aiming at statistically averaging the perturbing effects is possible with enough observations covering a span larger than the typical time scale of the effects (hours or stellar rotation period).

Simulations have been performed to quantify the amount of observations required to reach a given level of precision (Figs. 5.1-5.3; Dumusque et al. in prep). First, from publicly available HARPS asteroseismology radial velocity measurements for 6 stars (β Hyi, δ Eri, α Cen B, τ Ceti, μ Ara, and α Cen A), synthetic high-frequency observations were generated from models of the stellar noise in Fourier space. The rms of the synthetic velocities binned according to different observing strategies was then calculated for stars with different spectral types in our sample (Fig. 5.1).

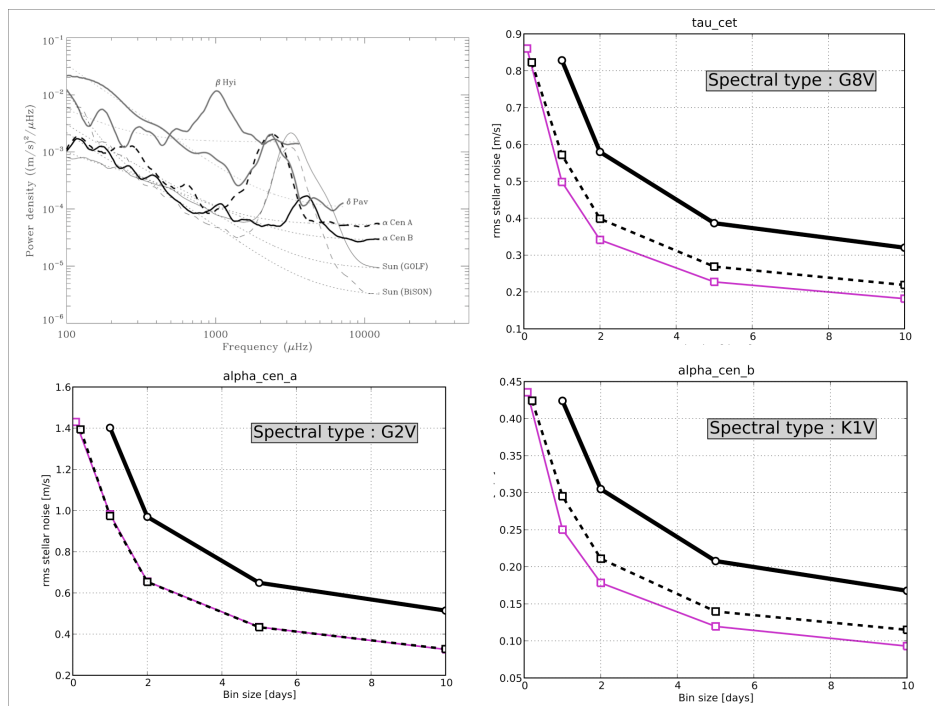


Figure 5.1: Top left: Frequency structure of the radial velocity jitter observed on several solar-type stars (from Kjeldsen et al. 2005). Envelopes of p -modes are prominent at the milli-hertz level whereas power due to granulation and activity-related effects is growing towards lower frequencies. Top right and Bottom: Radial velocity rms for different observing strategies and binning of synthetic observations carrying the same “noise” structure in Fourier space as a set of intensively observed stars with HARPS in asteroseismology campaigns spanning from 1 to 7 nights.

For stellar activity, present results indicate that well-selected quiet G-K dwarfs exhibit a jitter level well below 1 m/s (Pepe & Lovis 2008). The lowest level for quiet stars is not known, the minimum value observed with HARPS being at the level of the instrumental limitations. Moreover, binning the observations over time scales comparable to the rotational periods of the stars permits to significantly average out stellar noise. Proceeding in this way, a precision of 35 cm/s is already obtained on a few test cases as e.g. HD69830 (Lovis et al. 2006). Simulations are ongoing to better quantify the ultimate limitations imposed by stellar activity. Families of spots are generated in a realistic way and estimate of the radial velocity effect induced by the spots are derived. The spots appearance law, their number, the spots lifetime, and corresponding filling factors for different activity levels are calibrated from actual data of the Sun. The combined effect of the different stellar noises is presented in Fig. 5.2 for different activity levels and observing strategies. Although decreasing less rapidly than what is expected in the best cases (i.e. in a statistical way, with the square root of the number of measurements), the decrease of the measured rms is very encouraging and demonstrates the pertinence of the approach.

Finally, these simulations are allowing us to derive, through a Monte Carlo approach, the detection limits in the mass-separation plane expected for each of the considered strategies. Very interesting detection limits are obtained in the case of a realistic strategy (optimization of precision versus cost in observation time) consisting in three 10-minutes observations per night, individually separated by 2 hours. A binning over several days can then be applied when looking for longer period planets (Fig. 5.3). The interesting point to note here is that, for a given planet mass, the detection limit is weakly depending on the period. Indeed, for longer periods, the lower amplitude of the signal is compensated by the larger temporal bins considered for the average.

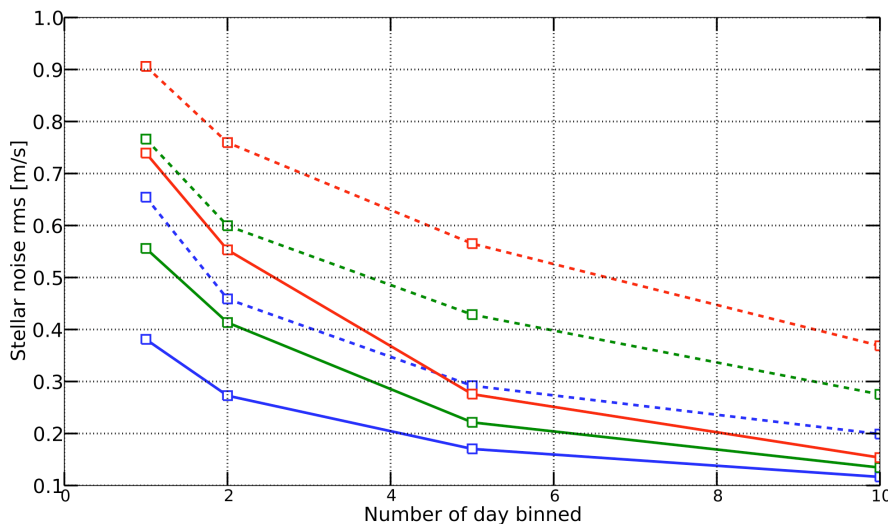


Figure 5.2: Results of stellar-noise impact simulations on Alpha Cen B (KIV). Curves represent the estimated rms of stellar noise in function of the binning of the measurements. The 2 line types correspond to different observing strategies: the dashed lines correspond to the actual strategy presently used for the HARPS-GTO high precision program (1 measure per night of 15 minutes, on 10 consecutive nights each month); the continuous lines correspond to a better strategy with 3 measures per night of 10 minutes each, 2 hours apart, every 3 nights. The different colours correspond to different stellar activity levels: blue for $\log(R'_{HK}) = -5.0$, green for $\log(R'_{HK}) = -4.9$, and red for $\log(R'_{HK}) = -4.8$.

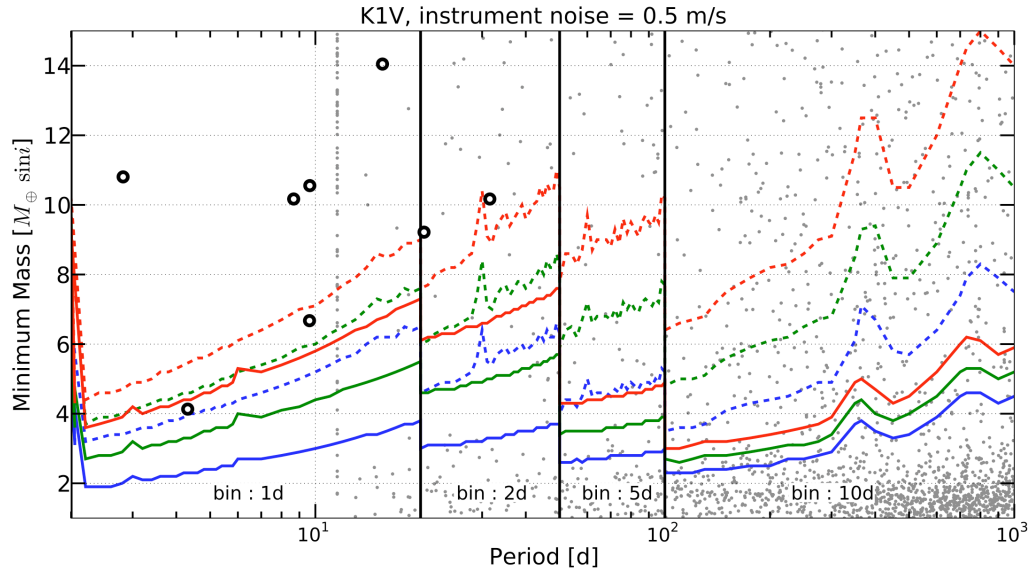


Figure 5.3: Limits of planet mass detection as a function of orbital period for Alpha Cen B (K1V) derived from the simulations. The open circles represent the smallest planets found with HARPS around G and K dwarfs, and the lighter dots correspond to the expected planets from the Bern population synthesis models (Mordasini et al. 2009). Line types and colours have the same meaning as in Fig. 5.2. The diagram is separated in 4 separation regimes, each one using a different binning, well adapted to the corresponding period range.

With the chosen strategy, for a quiet K V star like α Cen B, we would be able to detect planets with masses a few times the mass of Earth with an orbital period of 200-300 days, which corresponds to the habitable region of this type of stars. These estimates are still including HARPS instrumental limitations (with centring and guiding effects) and a contribution from photon noise. Improvements are then expected with more stable instruments as ESPRESSO and longer exposure times to better average the stellar oscillations. The estimated yield of the PLATO survey presented in the next section is using the results of these simulations to realistically take into account limitations set by stellar noise for the radial velocity follow-up.

Another promising approach to better characterize stellar noise will be to simultaneously monitor activity indicators at the same time as the velocity observations and then use correlation between the velocity and the indicator to correct the velocity from the stellar intrinsic contribution. Studies are being conducted in this direction using photometric, activity indicators, and line shape measurements.

5.3 Organization of the follow-up

The main aspect of the ground-based follow-up of PLATO transit candidates will reside in the basic planet characterization through radial velocity measurements. As seen above, the same level of precision cannot be reached for all stars due to various sources of stellar intrinsic limitations: spectral type, luminosity class, activity level, star brightness. In particular, photon-noise limitations and activity-related jitter require a large amount of telescope time in order to detect the lower-mass planets.

False positives related to stellar diluted blends will usually not display large radial velocity variations. Due to the PLATO large pixel size on the sky, the situation will appear often. It is thus important to point out these cases before spending expensive time on large telescopes. Many cases will be discarded from the light curve analysis (shape of the transit curve), from correlations between light curve and centroid curve from PLATO data alone, or from moderate-precision spectroscopic observations (variation of the shape of spectral lines through bisector measurements). For the remaining cases, it will be important to check that the low-depth transit is not due to a deeper eclipse of a fainter star very close to the primary target. This can be achieved at higher spatial resolution, checking for transits on the neighbouring stars. The radial velocity follow-up coupled with the high-angular confirmation that the transit is indeed taking place on the primary target should be sufficient to safely characterize the planet candidates.

Due to the number of expected PLATO candidates, a systematic observation of all detected transits with large telescopes will be unfeasible and an optimized follow-up scheme has to be organized. A very important amount of telescope time will be required as well, and at some point ESA or the PLATO Consortium will have to discuss and agree with the owner institutes of the observing facilities on a scheme for guaranteed/reserve time to observe the candidates. This has to be a global effort of the community, in the line of the open data property policy of ESA.

In practice for the characterization follow-up, a multi-step approach going from moderate- to high-precision instruments is already successfully used in most of the on-going surveys. It will also nicely apply to PLATO candidates. It is sketched in Fig. 5.4.

- 1) The candidate list has to be cleaned as much as possible from false positives by diagnoses applied directly on the high-precision PLATO light curves, as described above.
- 2) Small telescopes will be used for a first screening of the remaining transit candidates, rapidly discarding unrecognized binaries from the list. As PLATO prime targets consist in bright stars, instruments similar to FEROS on the ESO 2.2-m telescope or CORALIE on the 1.2m Swiss telescope at La Silla will be perfectly suited for this part of the follow-up. Moreover, such instruments will easily be able to fully characterize most of the giant planets.
- 3) Given that the host star's brightness and activity level will define the expected ultimately achievable radial velocity precision, this will dictate which telescope+spectrograph facility has to be used for the planet characterisation.
- 4) HARPS on the ESO 3.6-m telescope at La Silla (or similar instruments) will be the working horse for the most active part of the sample (anyway limited by stellar noise to a level comparable to the instrument precision) and/or for planets with masses down to the super-Earth regime not too far from their central stars.
- 5) Finally the most interesting and demanding lower-mass, longer-period planets will require the best possible radial velocity precision that should be available with ESPRESSO on the VLT and CODEX on the E-ELT. These facilities are planned to be available at the time of PLATO detections.

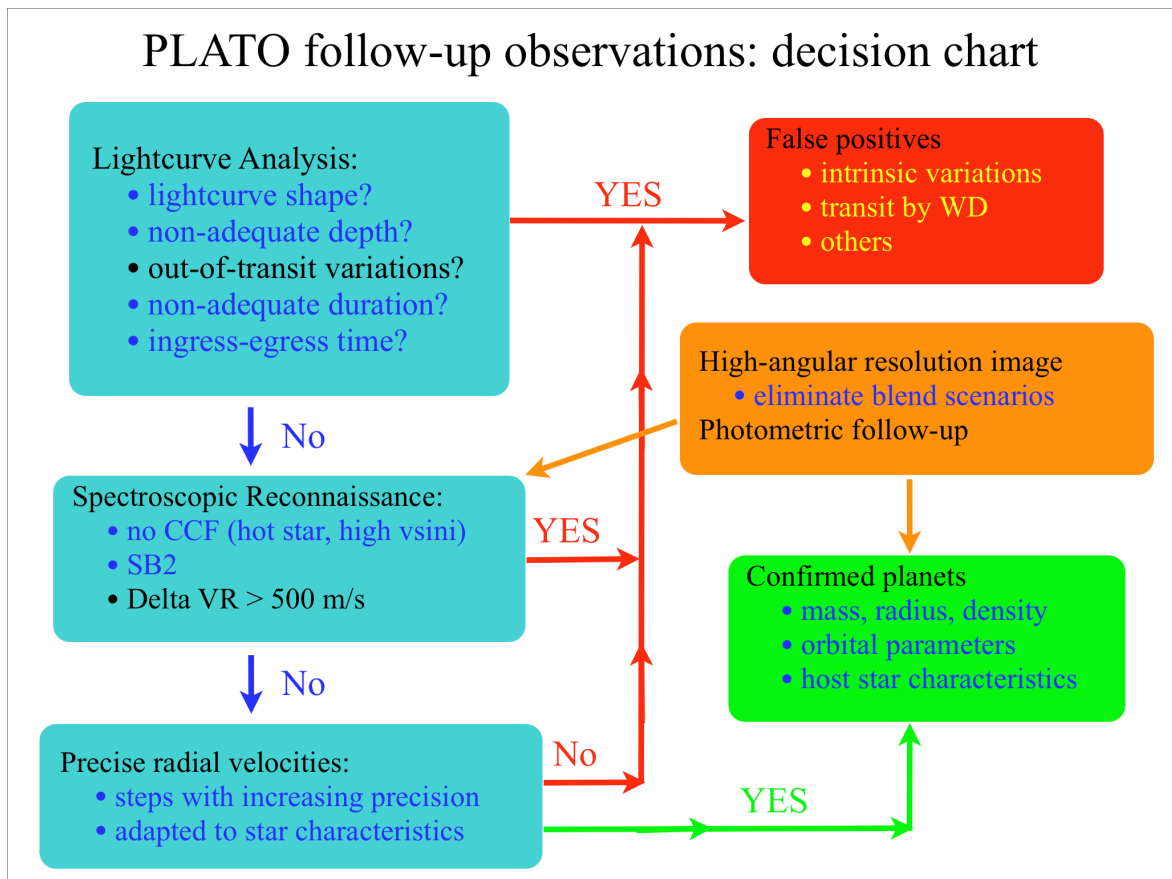


Figure 5.4: PLATO follow-up organization describing the different steps making use in an optimum way of the different observing facilities. WD is a white Dwarf, CCF is the Cross Correlation Function used in radial velocity observations of exo-planets, SB2 stands for a type of Spectroscopic Binary that can mimic an exo-planet and VR is Velocite Radial.

5.4 Preparatory observations

As previously mentioned (Sect. 2.4), Gaia results will be used to optimally prepare PLATO observations. In particular, Gaia early releases in the 2014 – 2016 time frame will easily provide estimates of the radii of PLATO targets to within 10-20%, allowing us to distinguish dwarfs from giants and optimize target selection, which at the end should improve the percentage of successful detections of small-size planets. Gaia data will also be extremely useful to precisely characterise the vicinity of each PLATO target, by identifying fainter neighbours and measuring their exact positions and magnitudes. This additional information will be used to finely tune on-board and on-ground data treatment, e.g. by optimizing photometric masks and jitter correction algorithms. Thanks to Gaia, the preparation work of PLATO will therefore be much easier than that of previous missions such as CoRoT and *Kepler*.

6 SCIENTIFIC IMPACT OF PLATO

PLATO will allow us to study planets as well as their host stars. PLATO host stars will be amongst the brightest (and closest) stars and hence the *easiest* to study. Given the difficulty of confirmatory observations for terrestrial-sized planets, this is especially important as current missions are struggling to achieve both the level of accuracy and quantity of the required follow-up observations.

By determining planetary and stellar parameters for its bright targets with a precision surpassing that of any previous mission, PLATO will provide a statistically significant sample of exoplanetary parameters that will usher in a new era of understanding. Planet parameters provided by PLATO are: a large sample of exoplanets around bright stars, spanning a wide range of orbits with precise and reliable orbital parameters, planet sizes and masses (in combination with radial velocity follow-up). In particular the bright host stars will be characterized by seismic observations with PLATO as well as spectroscopic ground-based support observations, allowing us to measure all their fundamental parameters, including mass, radius, age, temperature, chemical composition, rotation, etc. This sample will provide extremely well characterized planetary systems (planets and their hosts) in terms of their primary parameters. An additional very large sample of stars will be too faint for asteroseismology, but will nevertheless provide planet detections down to the size of the Earth, around stars that can still be characterized by standard methods. The precise age determination provided by the PLATO approach will allow us to place the detected planets on a time axis with high precision for the first time, and it will be possible to make the first investigations into the evolution of mature planetary systems - allowing comparisons with our own Solar System.

6.1 Samples of Exoplanets: from Giants down to Earths

A full statistical description of exoplanetary systems, down to masses and sizes of terrestrial planets, is a prerequisite for any decisive advancement in the field of planetary formation and evolution. However, although more than 400 planets in total are currently known, the number of terrestrial planets is still sparse (Figure 6.1). If we by terrestrial mean 'rocky' or actually planets similar in composition to Earth, Venus and Mercury in our Solar System, currently only one terrestrial exoplanet is known - CoRoT-7b. Although a number of other exoplanets are known with minimum mass in the range below 10 Earth masses, CoRoT-7b is the only low-mass exoplanet for which also a radius has been measured. PLATO will significantly extend the sample of terrestrial exoplanets beyond CoRoT (and *Kepler*) over a wide range of orbital and stellar parameters and for the first time allow us to determine the planetetary mass function for low-mass planets as a function of other parameters, like evolutionary status.

The investigation of the still mysterious connection between giant planets and the metallicity of their parent stars requires good statistical knowledge of planet and parent star properties, including stellar ages and metallicities, of the type PLATO will provide (Santos, Benz & Mayor 2005). The potential chemical composition difference between core and the convective envelope of a late-type star, that will be present if high metallicity hosts have ingested planetary material (Bazot & Vauclair 2004), can be investigated via asteroseismology. However, recent analysis of low-mass (Uranus-Neptune range) planets from radial velocity surveys have indicated that such planets may not display the same metallicity bias as found in gas giants (Udry et al. 2007). The combined analysis of planet hosts stars via asteroseismology and precise planet parameters makes PLATO ideally suited to provide a deeper understanding of the star-planet-metallicity relationship, in particular for small, terrestrial planets. Such an approach is beyond our capabilities for the planets that will be discovered by CoRoT and *Kepler*, which are orbiting stars that are too distant and too faint for such a detailed characterization, but is within reach of PLATO, which focuses on stars that are bright and nearby.

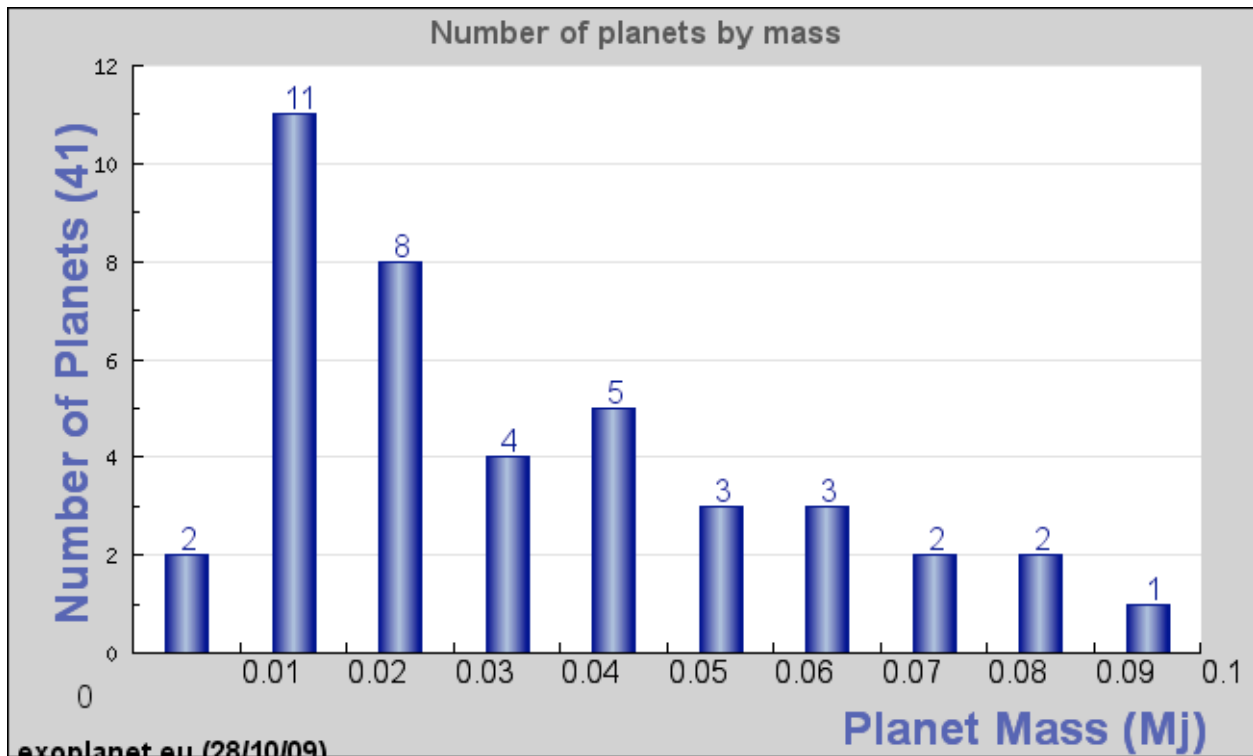


Figure 6.1: Masses of extrasolar planets in the range 0.001 - 0.1 Jupiter masses.

A question to address is the possible dependence of planet formation on stellar environment. For instance, it has been recently conjectured that stars formed in regions that are richer in molecular hydrogen, such as the galactic inner disk, may host more giant gaseous planets (Haywood 2009). The distribution of smaller planets may also depend on their location in the galaxy. In its long monitoring phase, PLATO will observe two vast regions of the galaxy, and will be able to investigate differences in the planet distribution between these two regions. The PLATO targets will also be significantly closer to the Sun than those of CoRoT and *Kepler*, giving us more insight into how planet formation may depend on location.

During its step-and-stare phase, PLATO will scan different regions in the sky (e.g. clusters) and detect more exoplanets in a reduced range of orbital periods. This phase will be even more ideally suited to address how planet formation depends on stellar environment. The young transiting planets are an example of such an investigation: all of the transiting planets known so far are orbiting normal mature main-sequence stars. There is only one transiting planet known around a star younger than 1 Gyr – CoRoT-2b (Alonso et al, 2008). To study planet formation and early evolution, young transiting planets need to be observed, e.g. by observing and monitoring young stellar clusters, with different ages from about 1-100 Myrs, with many stars in the PLATO field of view. Determining the planet radius from transits one can then study the contraction of planets with time. Observing very young transiting planets (Myrs), one could also study whether young planets form by growing due to accretion or by gravitational collapse.

6.2 Planet characterisation

Based on the presently known transiting giant exoplanets, we already know that these objects allow for a plethora of scientific studies, such as the detection of the planet atmosphere via transmission spectroscopy (Charbonneau et al. 2002) or measurement of their equilibrium temperature while they are occulted by their central stars during secondary transit (Charbonneau et al. 2005) and measurements of the stellar spin axis versus planetary orbit (Winn et al. 2005, Johnson et al. 2008) through the Rossiter-McLaughlin effect (Rossiter 1924, McLaughlin 1924). The results of PLATO will, of course, allow similar studies to be made. However, due to its bright target stars we can confidently expect that PLATO will significantly increase the

number of suitable targets for such follow-up investigations, and such analysis will be possible for planets of smaller size than accessible to this kind of investigation before.

The large number of known hot-Jupiters which transit their star (hence for which the planetary radius is known) has already motivated numerous theoretical studies of planetary evolution (simulating accretion, migration and loss) with age (e.g. Liu et al. 2008, Fortney et al. 2007, Lecavelier des Etangs et al. 2004). Such studies are critically constrained by uncertainties in planetary age, which PLATO will address. Other important uncertainties in the models include e.g. the rate of migration (e.g. Kirsh et al. 2009) and the mechanisms for escape (Lammer et al. 2003, Khodachenko et al. 2006). As the database of transiting hot-Jupiters as well as small sized planets expands, it will be informative to apply the evolution models to a wide range of scenarios. To succeed in this, the age of the system needs to be well constrained, *which can only be done through PLATO*.

The main focus of PLATO is, however, on small, terrestrial planets. Figure 6.2 shows a mass-radius diagram calculated for terrestrial planets with different assumptions on their interior. It is evident that the planetary radius is a strong constraining factor to place a given terrestrial planet into such model scenarios, much more than the planetary mass. Indeed, Valencia, Sasselov & O’Connell (2007) have shown that ~5% precision in planetary radius and ~10% in planetary mass are required to distinguish between bulk terrestrial planet properties, like ocean planets and dry rocky planets. Thus, radii with accuracies of just a few percent will be needed to fully understand planetary compositions. Again, the stellar samples of PLATO containing bright stars will be prime targets to provide accurate planet parameters around well characterized central stars. **The data expected from PLATO, therefore, will allow us to derive high-precision mean planet densities and to constrain models of planet interiors, even for very small, terrestrial planets.**

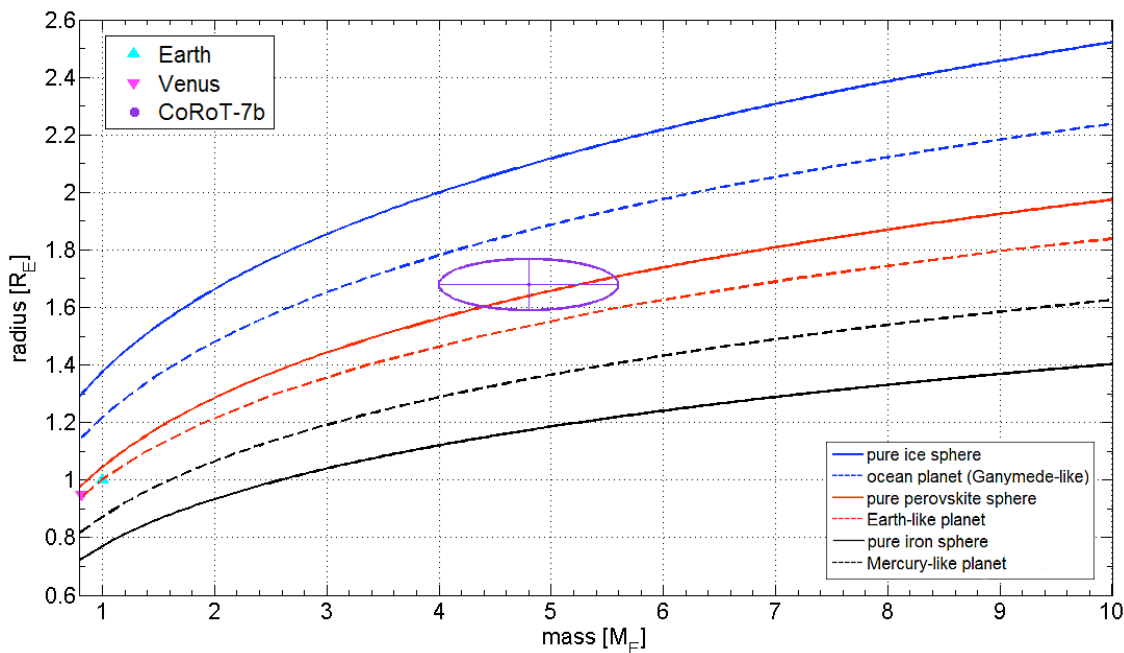


Figure 6.2: Calculated mass-radius relationships for terrestrial planets with different internal composition (Wagner et al. 2009a,b). The positions of CoRoT-7b (cross) and the Earth and Venus are marked (data from Leger et al. 2009, Queloz et al 2009).

Lessons from our Solar System imply that the factors determining habitability are many and varied - a complex interplay between e.g. geochemical, biological and physical factors. The terrestrial planets, Venus-Mars-Earth, are/were habitable but at different geological ages. One can only understand the evolution of planetary atmospheres and their water inventories if the evolution of the radiation and particle environment of the host stars is known. Observations of young solar proxies indicate that the early Sun was a much more active source of energetic particles and electromagnetic radiation in the X-ray and EUV spectral range ($\lambda < 100$ nm) (e.g. Zahnle & Walker 1982, Micela, 2002, Ribas et al. 2005). The short wavelength radiation is of particular interest because it can ionize and dissociate atmospheric species, thereby initiating photochemistry that can change atmospheric composition. The soft X-rays and EUV radiation is absorbed in a planetary

thermosphere, whereby it can heat and expand it significantly (e.g. Kulikov et al. 2006, 2007, Lammer et al. 2008, 2009, Tian et al. 2008). This results in high atmospheric escape rates from primitive atmospheres. For numerical studies of atmospheric loss processes, it is therefore crucial to know the parameters of the whole system as well as a good estimate of the system age.

Small terrestrial planets detected by PLATO together with an improved determination of system age and stellar evolution models as well as models of potential planet atmospheres/habitability conditions will lead to a candidate list of potentially-habitable systems for future study. Many of its detected giant planets, and also some favourable super-Earth planets, will be target for future spectroscopic follow-up.

6.3 Expected number of planet transit detections

The impact of PLATO on exoplanet science will be directly related to the number of exoplanets that can be detected and fully characterized, and to the coverage of the planet parameter space (orbit, radius, mass) achievable by the mission. The key asset of PLATO in this respect will be the brightness of its target stars, which will be bright enough to enable an asteroseismic analysis to determine the star's mass and age, as well as for a fast and efficient radial velocity follow-up from the ground.

In this respect, we note that PLATO will provide a far better coverage of planet parameter space than *Kepler*, thanks to its extended surveyed area and to the brightness of its targets. *Kepler* will monitor up to 100,000 stars down to $m_v = 14.5$, for at least 3.5 years, in a field of about 100 deg^2 . Many transit candidates should be discovered, including a few Earth-sized planets. However, most of these transit candidates will be in front of faint stars with $m_v = 13.5-14.5$, which represent the majority of the surveyed sample. The radial velocity follow-up of these transit candidates will be very difficult to perform, even impossible in most cases. Similarly, seismic analysis will be possible on only a handful of the host stars of the detected planets, although a substantial asteroseismic programme exists on *Kepler*.

While radial velocity follow-up of giant planets detected by *Kepler* can be performed with available facilities, such as the HIRES spectrograph on the Keck telescope, for small planet candidates, *Kepler* will have to rely on HARPS-North, which will not be on the sky before 2011, and even then, will provide radial velocity follow-up capabilities for small planets only for the few brightest stars in the *Kepler* sample.

On the contrary, PLATO thanks to its extended surveyed area (3600 deg^2 in the PPLC concept), is concentrating on bright stars ($m_v < 11$), and therefore will not suffer from the same limitations. It will also benefit from improved radial velocity performances of instruments in the Southern hemisphere, such as ESPRESSO on the VLT, and later CODEX on the E-ELT.

Table 4.1, which shows the expected numbers of stars observable at various noise levels and various limiting magnitudes, outlines these enhanced capabilities of PLATO. Figure 6.4 illustrates the comparison of PLATO versus *Kepler* performances, by showing a simulation of the total number of *detectable planets* as a function of their mass and orbital semi-major axis for both missions. The numbers indicated are those of the expected detectable planets by PLATO, while the sizes of the coloured regions show the respective discovery potential of both missions (blue: PLATO and green: *Kepler*). Note that there is no underlying planet formation model. The simulation simply takes as starting point the star sample observable by each one of the missions (Table 4.1, PPLC concept assumed here for PLATO), and assumes that each star has one (and one only) planet in the considered box in the (mass, semi-major axis) parameter space. The planet is then considered detectable if it can be seen in transit by the satellite and confirmed by follow-up radial velocity measurements with a reasonable amount of telescope time. Such a scheme could consist of a 1h observation each night for ten nights, repeating this sequence every month for the visibility period of the star during a couple of orbital revolutions.

The expected results depicted in Fig. 6.4 have been obtained as realistically as possible, taking into account all sources of noise for the radial velocity follow-up (oscillation, granulation, activity level), and limiting the required observing time to reasonable values. The estimate can even be considered as conservative, as for especially interesting cases more observing time can be dedicated to the follow-up. Future developments in our understanding of the interplay between activity level and induced radial velocity jitter might help correct for the spurious effect and further improve our characterization ability.

As can be seen in Fig. 6.4, we expect a significantly increased number of planet detections with PLATO, and in particular a significant number of detections in the lower mass range, where *Kepler* is not expected to produce confirmable planets. The main reason for the vast increase in sensitivity to small planets arises in the much larger field of view of PLATO, potential observational follow-up instrumentation and, in particular, the brightness of the candidates. The main conclusion of this analysis is that, although *Kepler*, will bring considerable progress in the area of exoplanet research, it is very unlikely that it can detect unambiguously small mass planets in far-away orbits around their stars, mainly due to the faintness and the limited number of its targets.

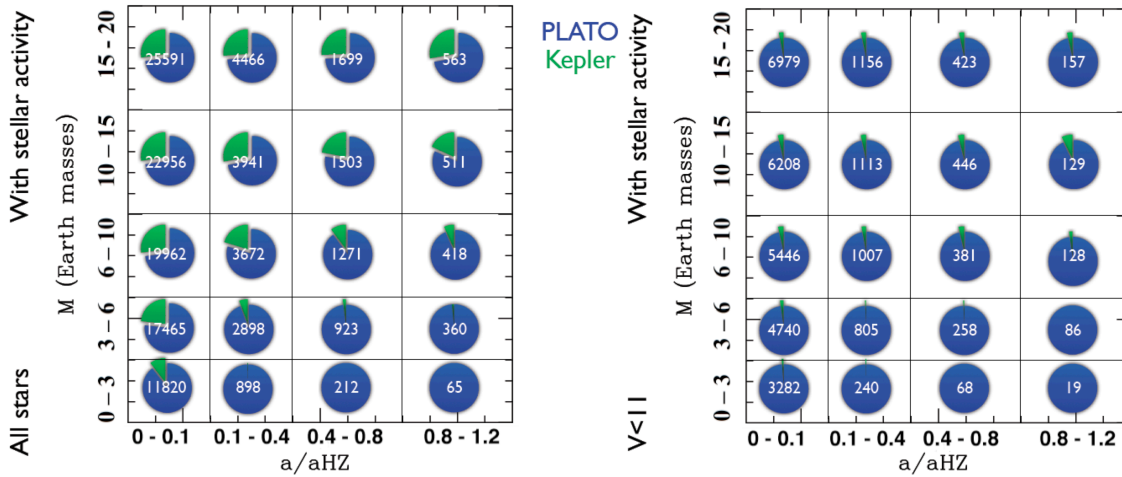


Figure 6.4: Estimated total numbers of detected transiting planets, which can be confirmed by ground-based radial velocity observations, for PLATO (in the PPLC concept) and Kepler (see text for details). Note that a large fraction of the (orbit, mass) plane, not covered by Kepler, can be explored by PLATO. The numbers indicated correspond to PLATO observations only, assuming that each observed star has one (and only one) planet. Left panel: all stars; Right panel: stars down to $m_V = 11$ only, indicating the number of systems for which the host star can be characterised seismically. The x-axis is the orbit semi-major axis, expressed in units of the middle of the habitable zone for the stars considered. Stellar limitations (mainly p-mode oscillations and activity) have been taken into account in the production of this figure.

Only PLATO with its extended surveyed area and its main focus on bright cool dwarfs, will allow us to reach real Earth analogue systems and extend the search for exoplanets to small terrestrial planets in the habitable zone of their stars.

6.4 Additional Exoplanet Investigations

6.4.1 Reflected stellar light

The high-precision photometry of PLATO will allow detecting non-transiting planets by the modulation of the flux in the lightcurve. The fraction of reflected stellar light by a close-in giant exoplanet along its orbit, which depends linearly on its albedo A , is typically $F_p/F_* \sim 9.1 \times 10^{-5} A$ for a Jupiter size planet orbiting at 0.05 AU from its host star. Because the monitoring of such targets will cover several hundred planetary orbital periods, such a modulation will be detectable by PLATO down to $m_V = 9-10$ for albedos as small as $A = 0.3$. High precision photometric monitoring will therefore allow us to detect giant exoplanets in close-in orbits around stars down to $m_V = 9-10$, even for large inclination angles, where transits are not visible. For *nearby stars* this could be an important discovery technique as it is mostly free from the geometric constraints required for transit occurrence and will produce important targets for direct observation with the ELT etc. We note that reflected light from the 1.49 R_J exoplanet CoRoT-1b, which is orbiting a $m_V = 13.6$ star, was recently detected (Snellen et al. 2009, see Fig. 6.5) at a level of about 1.26×10^{-4} , using CoRoT data having a noise level of 200 ppm/hr (Barge et al. 2008). This pioneering result demonstrates that PLATO, reaching a noise level below 30 ppm/hr on stars down to $m_V = 11$, will be able to detect on its main targets

reflected light signals at least 7 times weaker, which could correspond to planets 2.5 times smaller in radius or 2.5 times further out, assuming a similar albedo.

Very bright stars, typically with $m_V = 6$, will be observed with a noise level of approximately 10 ppm/hr. Such a low noise level will enable the detection of stellar reflected light on planets with 0.15 R_J radii. *We will therefore be able to detect super-Earths in close-in orbits, without suffering from geometrical probability, and identify a large fraction of nearby stars hosting close-in planets, that will become privileged targets for further observations, including searching for smaller and further out planets.*

In addition, the exquisite noise level in the light curves of these very bright targets will give the possibility to study details of the atmospheres of giant planets in close-in orbits, such as global weather patterns. This kind of ultra-precise studies on very bright stars constitutes a unique possibility of PLATO such targets being out of reach of earlier missions like CoRoT and *Kepler*.

6.4.2 Astrometric detection of planets

The stellar reflex motion induced by a planets revolution creates an astrometric wobble, which can be

expressed as $w = 3 \frac{a}{d} \frac{m_{pl}}{M_{star}}$ where w is the amplitude of the astrometric wobble in μas , a is the semi-major

axis of the exoplanet orbit in AU, m_{pl} and M_* the mass of the planet and its star (expressed in m_{Earth} and M_{Sun} respectively), and d the distance to the exoplanetary system in pc. Thus a 1 M_J exoplanet, orbiting a 1 M_{Sun} star at 1 AU, placed at 15 pc, so that the star has $m_V = \sim 6$, would induce a 60 μas wobble.

PLATO will measure the astrometric position of each star in the surveyed field relative to all other stars in the field, which will provide a very precise reference frame. Preliminary simulations have shown that indeed relative centroid measurements are photon noise limited with negligible residual jitter noise. In this case, precisions of about 10 μas will be achieved down to $m_V = 6$ after one month of integration. This will be sufficient to detect all giant exoplanets with orbits near 1 AU, orbiting nearby bright stars, irrespective of the inclination angle of the orbital plane with respect to the line of sight.

These astrometric measurements, coupled with measurements of reflected stellar light described earlier, will constitute a powerful tool for identifying exoplanetary systems around nearby stars, out to distances of 15-20 pc, and therefore can help select targets for further follow-up observations, for instance in interferometry and coronagraphy.

6.4.3 Secondary transits

For transiting planets it will also be possible to measure the secondary transit (the occultation of the planet by the star). This will provide valuable information about the heat redistribution in the atmosphere of the planet and the eccentricity of its orbit. CoRoT data has been used to demonstrate the feasibility of this, with the measurement of the secondary transit for CoRoT-1b (Alonso et al. 2009a; see also Fig. 6.5), and for CoRoT-2b (Alonso et al. 2009b). In the case of CoRoT-2b, the measured depth of the secondary transit is only 0.006%, while the star has $m_V = 12.6$, and the planet has a radius of 1.49 R_J . The noise level in the light curve used for this study is of the order of 130 ppm/hr. Recently Borucki et al (2009) have published results of the measurement of the secondary eclipse of HAT-P-7b showing a rms residual of 60 ppm on a $m_V \sim 10$ star. The expected performance for PLATO (30 ppm down to $m_V \sim 11$) is at least 4 times better than CoRoT and at least 2 times better than Kepler, allowing the detection of weaker signals around the majority of the targets.

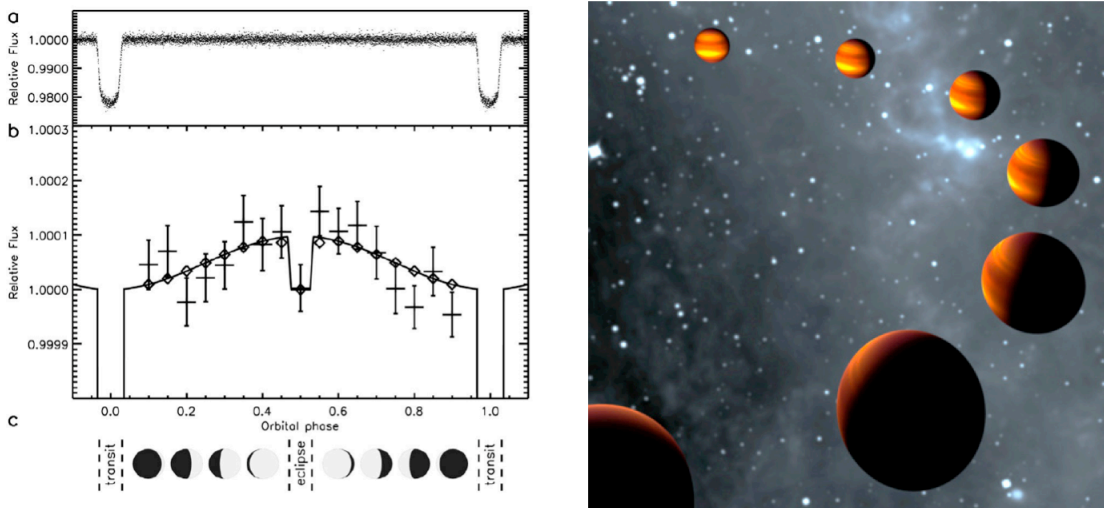


Figure 6.5: Phase effects in the light curve of CoRoT-Ib (Snellen et al. 2009). Non-transiting planets are also detectable with this method.

6.4.4 Rings and moons

Planetary rings and large moons can also be detected by their modification on the shape and duration of the transit lightcurve. For example, for a Saturn-analogue at 1 AU from the parent star, the ingress and egress take one hour for the planet and two hours for the ring. In addition, the planet ingress (egress) starts (ends) steeper for the planet than for the ring. Finally, the projected inclination of the ring with respect to the planet's orbital plane and the ring optical depth can be derived from the transit shape, which provides valuable information for the formation and evolution studies of the system. Furthermore, we may expect discoveries of planet configurations not found in our own Solar System, like e.g. binary planets.

6.4.5 Transit timing variations

Planetary transits can be studied further to search for variations in the mid-transit times caused by gravitational distortions due to additional planets in the system or moons around the planet ("transit timing variation" analysis). It is particularly interesting to search for the presence of Trojan planets (planets in 1:1 resonance), which can be stable up to the mass range of the Super-Earths within the orbit of a Jupiter planet. The photometric precision of PLATO will allow detecting perturbations with an amplitude of a few seconds, which is a performance at least two times better than *Kepler* and four times better than CoRoT.

6.5 PLATO objects as targets for atmospheric studies

The host stars of PLATO planets will be amongst the brightest (and hence closest) known. **Consequently they will be the natural targets for atmospheric studies (either through transmission or reflection spectroscopic studies) and indeed prime targets to search for bio-markers.** While these observations may prove difficult, the value of these targets would remain as suitable instrumentation was developed (indeed their existence would help drive development forward).

6.5.1 Follow-up with complementary space facilities

The Hubble Space Telescope (HST) and the Spitzer Space Telescope have been highly successful in the characterization of extrasolar planets atmospheres, through high-contrast measurements during primary and secondary transit. Several major results have been published with Spitzer concerning the attempts of understanding atmospheric circulation, in particular the temperature difference between the day and the night side, since Hot Jupiters are expected to be tidally locked, presenting continuously the same face to the host star. Spitzer has shown that it is possible to have planets with extreme differences between a very hot dayside and excessively cold side (ν And), as well as an efficiently redistribution of the stellar absorbed flux

from the dayside to the night side (HD189733b). Other remarkable discoveries made by Spitzer are the temperature inversion on the dayside of HD209458b (Burrows et al. 2007, Knutson et al. 2008), and detection of water vapor (Tinetti et al. 2007) and methane (Swain et al. 2008).

The James Webb Space Telescope (JWST) with its large mirror size and high thermal stability will continue Spitzer's legacy, enabling studies for a wide range of star brightness of smaller exoplanets, potentially habitable ones, as well as moons transiting giant planets. JWST will be able to detect hot Jupiters thermal emission at a SNR=25 for stars at ~ 150 pc. Low-resolution spectra of NIRSpec will enable detections of various molecules, H₂O, CO, CH₄, and CO₂ of transiting Jupiter-like planets orbiting out to 1 AU host stars with $m_V = 13.4$. PLATO's star magnitude range is $m_V = 5-13$, therefore, JWST will be able to fully characterize the hot Jupiters found by the PLATO mission.

6.5.2 Imaging and spectroscopy with the E-ELT

In the next decade ESO is likely to construct the largest telescope - the 42 m E-ELT. Phase-A studies of the likely first generation suite of instruments are currently underway. This includes the Exo-Planet Imaging Camera and Spectrograph (EPICS), which will be optimized for visible and near-IR photometric, spectroscopic and polarimetric observations. Using extreme adaptive optics and novel data analysis techniques contrast ratios of 10^{-9} will be achievable around bright stars.

Using the Benz et al population synthesis models and the instrument simulation software we have produced Monte-Carlo simulations that allow us to probe the detectability of planets in a sample of cool stars (F5V - M0V) in the magnitude range $8.5 < m_V < 13.5$. As one may expect planets are easiest to detect around the nearest and lowest luminosity stars. For planets with $P \sim 1$ year, then we may expect that EPICS will be able to image some rocky planets found by PLATO *in the habitable zone* of late G, K and M dwarfs. Thus the atmospheres of these objects could also be directly studied.

Further into the future it is not unreasonable to expect a second generation coronagraphic instrument optimized for planet observations to further improve on the contrast detectability and hence, be capable of imaging lower mass planets and/or planets around solar type stars.

6.6 Planet dynamics

The orbit of planets obviously plays a crucial role for their habitability. Large eccentricities ($e > 0.3$) significantly affect the mean isolation received by a planet for a given semi-major axis (Williams & Pollard 2003). This means than a twin planet of the Earth around a Sun like star at 1 AU and with an eccentricity of e.g. $e=0.3$ would have a mean temperature averaged over its orbit of 23°C (compared to the value of 15°C for the Earth). But the seasonal variation of the mean temperature is significantly more pronounced than on a circular orbit and can have important consequences for life, therefore modifying the standard definition of the habitable zone.

It is evident that a crucial orbital parameter for a habitable planet, besides the semi-major axis, is the eccentricity. High precision measurements with PLATO will significantly improve the determination of orbital parameters as a basis to further address conditions for their habitability. The full knowledge of the properties of planets, their orbits and their parent stars, in particular their ages, will therefore allow us to better understand the mechanisms controlling orbital eccentricities and planet migration (Namouni 2005).

Another point of interest for extrasolar system research is how large is the percentage of planets in double stars. There are in principle two different types of such orbits, one is of the so-called P-type orbiting both primary bodies, the other one is the S-type, orbiting only one primary. A body on an S-type orbit could possibly be detected, because it is relatively close to the hosting star, which enlarges the detection possibility via transit observations. Stable P-type planets need to have a semi-major axis at least 2.5 times bigger than that of the binary, which makes the detection by transit extremely difficult due to the low geometric probability and the large period. However, companions of planetary mass around low mass close binaries can be detected through transit timing variations analysis (using the Light-Time Effect, Irwin 1952). The long-duration observations of PLATO together with its high-precision timing measurements will allow us to address the question of planets in binary star systems.

7 ADDITIONAL SCIENCE

Besides the core program, PLATO will allow a broad range of studies involving photometric variability. It will provide us with a unique database of stellar variability, with precisions of the order of a few 10^{-5} per hr, and on all time scales between 1 minute and a couple of years. These exquisite properties will be used to address many different scientific questions, mainly (but not exclusively) in the area of stellar physics. Some of these additional science programs are briefly mentioned below.

The high signal to noise, the long time coverage and the very large field of view, will make possible the study of variability on several time scales on statistically significant stellar samples. It will be possible also to study very small and short term variations easily distinguishable from instrumental noise thanks to the large number independent telescopes. We here discuss the major advance in our understanding of stellar evolution that will come from using the PLATO data and some of the additional science cases in which PLATO will have significant impact on stellar astrophysics in general. The following list is non-exhaustive and is mainly for illustrative purposes of what kind of science can and will also be covered by PLATO as free important by-products.

7.1 Asteroseismology and stellar evolution

The discussion of asteroseismology in Section 2.4 concentrated on the exoplanet host stars, which are low-mass main-sequence stars. However the mission will provide data that far exceed, in terms of extent and quality, any previous dataset for the study of stellar interiors. In this way PLATO will greatly strengthen our understanding of stellar structure and evolution which remains a basic, yet at the moment somewhat shaky, foundation for a large part of astrophysics. An improved understanding of stellar modelling is essential for estimating the ages of the host stars of planetary systems.

Our understanding of the physical processes controlling stellar structure and evolution is subject to major uncertainties. Convection, convective overshooting and various other mixing and transport processes are poorly understood and yet play a major rôle in stellar evolution, determining evolutionary time scales, and must be taken into account for measuring stellar ages. One of the consequences of this unsatisfactory modelling is that the ages of the oldest globular clusters are still very uncertain and, for some values of the parameters in the models, can be higher than the estimated age of the Universe (van den Bergh 1995, Clementini & Gratton 2002, and Krauss & Chaboyer 2003).

The large range of values for parameters modelling core overshooting needed to fit data on young open clusters (Mermilliod & Maeder 1986), on eclipsing binaries (Claret 2007), and on the oscillation frequencies of a few massive stars (Aerts 2008), prevents the reliable determination of stellar ages for stars with convective cores. This clearly points out that our current knowledge of convective and rotational mixing processes inside massive stars is very incomplete, resulting in huge uncertainties in masses, ages, internal composition and structure of supernova progenitors, and hence in the modelling of the explosion and the resulting nucleo-synthesis yields. Uncertainties in convective overshooting can lead to uncertainties in the ages of open clusters up to a factor of two (Perryman et al. 1998). In view of these difficulties, it is clear that the age ladder of the Universe, which rests on stellar age estimates, is still highly unreliable. Moreover, the ages of field stars are even more uncertain than those of cluster stars. This has serious consequences for the use of results from Gaia to investigate the evolution of the Galaxy.

Solar modelling has evolved considerably with the advent of helioseismology, which has provided precise insight into the properties of the solar interior (Christensen-Dalsgaard 2002). Based on this very positive experience, it is clear that asteroseismic investigations of a large number of stars of various masses and ages constitute the only and necessary tool to constrain efficiently our modeling of stellar interiors, and improve our understanding of stellar evolution. Some progress should be achieved using data on the few dozen bright stars observed by CoRoT and any bright stars included in the limited asteroseismic programme of Kepler, but a thorough investigation into stellar evolution requires a large number of bright stars sampling all stellar parameters (mass, age, rotation, chemical composition), including main-sequence members of open clusters, and old Population II stars. The PLATO mission will provide the necessary data to reach this goal since the

data will allow us to study the oscillations of a large fraction of the target stars (with or without planets), and to investigate the seismic properties of various classes of stars.

Asteroseismic investigations of stellar interiors will compare the density structure obtained as described in Section 2.4 with the results of stellar modeling; in fact, the inferred density profile may provide direct evidence for the extent of the central mixed region in stars with convective cores. Also, the model fitting discussed in Section 2.4 will undoubtedly result in highly significant residuals, as evidence that the parameterized representation of the model physics is inadequate at the accuracy of the PLATO data; the challenge will then be to determine how the physical description must be improved. This will, for example, allow detailed investigations of the uncertain mixing processes associated with convective cores in main-sequence stars, of great importance to their subsequent evolution.

Moreover sharp features in the stellar interior produce a quasi-periodic modulation of the oscillation frequencies (cf. Vorontsov 1988, Gough 1990). For PLATO stars with sufficient precision in the measurement of the frequencies this will allow us to probe the properties of the boundaries of convective cores using both solar-like pressure (p) modes (cf Roxburgh and Vorontsov 1994a, 2001) and the gravity (g) modes that are excited in more massive stars (Miglio et al 2008), and hence place tight constraints on the overshooting of convective motions into the layers above. This can provide a more accurate calibration of the ages of the affected stars. Sharp features in the outer layers give information on the depth or radius of convective envelopes, overshooting below the envelope and on the He abundance (Monteiro et al, 1994, 2000, Roxburgh & Vorontsov, 1994b, Roxburgh 2009).

Members of *open clusters* present targets of specific interest. Their uniform initial chemical composition and age, and nearly common distance, provide very stringent constraints on the modelling, increasing the information obtained from the oscillation frequencies. In young clusters, we may in particular observe the β Cephei stars as well as slowly pulsating B stars, and bring important constraints on the evolution of massive stars. In the older clusters, oscillations in sub-giants (similar to those observed in η Bootis, Carrier et al. 2005) can be studied. Therefore, the asteroseismic analysis of members of open clusters chosen to sample an age sequence, will allow us to constrain severely stellar evolution modelling. It is foreseen that the step & stare phase at the end of the mission can be used to optimize this open cluster coverage, by monitoring several fields for a few months each.

As mentioned in section 2.4 the rotation of a star induces a splitting of the oscillation frequencies producing multiplets of $2\ell + 1$ components for each mode of degree ℓ . To first order in the rotational frequency, the frequency splitting is given by

$$v_{n,\ell,m} = v_{n,\ell} + m \int_0^R K_{n,\ell,m}(r,\theta) \Omega(r,\theta) r dr d\theta \quad (7.1.1)$$

where $\Omega(r, \theta)$ is the angular velocity and the rotational kernel $K_{n,\ell,m}(r, \theta)$ depends on the mode and on the equilibrium structure of the star (e.g. Aerts et al. 2009). As in the solar case, rotational frequency splitting will provide information on the rotation of stellar interiors, and help us investigate the poorly understood evolution of stellar rotation as angular momentum is lost in stellar winds and redistributed in the stellar interiors, causing mixing by mild turbulence. Present asteroseismic can, at best, only yield an average value of the interior rotation, but PLATO will deliver the seismic data to probe the detailed variation of angular velocity inside stars in different evolutionary stages, among which may be some exoplanet host stars.

The detailed asteroseismic observations made by PLATO will be complemented by extensive stellar modelling. An important aspect will be the use of increasingly realistic hydrodynamical simulations to provide physical insight into the dynamical processes (e.g. convection) which surely play a major rôle in stellar evolution, yet which are so far treated crudely. For example, modelling of near-surface convection and its effect on the oscillations will likely have reached a stage where many aspects of the near-surface effects on the frequencies (cf. Section 2.4) can be modelled. The interplay between the exquisite PLATO data for a large variety of stars and the sophisticated models will further improve our understanding of these processes,

under conditions that are very different from those of the well-studied solar case.

The progress in stellar evolution modelling from PLATO data will result, in particular, in a much better measurement of stellar ages, both through direct asteroseismic age determination for a large number of stars, and by strengthening the use of stellar models to provide less direct age determinations. The properties of the metal-poor stars (Pop. II stars) are of great interest; these are expected to be amongst the oldest in the Galaxy, often similar to the stars that are used for age determinations of globular clusters, and may provide important limits on the age of the Galaxy and, by implication, the Universe.

Hence, PLATO will contribute the time dimension to the study of Galactic evolution which is a central goal of Gaia.

7.2 General Astrophysics

PLATO will also address a number of scientific issues in stellar and planetary physics in topics ranging from our own Solar System to star formation. Transneptunian objects – the so-called Kuiper Belt objects – are the residual of the protoplanetary disc beyond Neptune, and are therefore a key element in order to reconstruct the history of the Solar System. PLATO will detect these small objects through serendipitous stellar occultations (Roques & Moncuquet, 2000), measuring their size. At the same time, an important by-product of the transit search will be the possible detection of exo-comets.

Other areas where PLATO is going to make an impact are:

- Stellar ages: The measurement of rotation rates for a vast sample of stars, as well as the measurement of their ages via asteroseismology, will allow a full calibration of the rotation period-age relationship. In particular PLATO will give access to the very long periods associated with very small photometric variations expected for old stars.
- Stellar parameter determination with eclipsing binaries: The PLATO contribution in this area is particularly relevant for the study of eclipsing binaries with pulsating components. At present we lack a good sample of pulsating EBs to which seismic and orbital modelling can be applied. PLATO will deliver seismic data for sufficiently bright targets that can be monitored easily from ground spectroscopy, in contrast to the EBs discovered by CoRoT and Kepler.
- Pre-main-sequence stars: High precision photometric monitoring of the PMS T Tauri and Herbig_Ae/Be stars will provide valuable information on periodic phenomena, such as rotational modulation due to hot/cold spots on the stellar surface, or non-periodic phenomena, like accretion events and flares, in a variety of young stars on their way to the core hydrogen burning stage. The PLATO light curves will be used to identify previously unknown PMS stars.
- Stellar rotation: The brightness variations on time scales of days to months will allow us to detect small solar-like spots and derive their size, surface distribution, and evolution, which are fundamental to test the available hydromagnetic dynamo models.
- Flares: The variations on short time scales will allow statistical studies of the flare frequency and energetics in a broad range of stellar types. A unique PLATO contribution is the possibility to study microflares, and therefore to explore the origin of chromospheric heating in active stars.
- Understanding common-envelope evolution through subdwarfs: Common-envelope phase is a key stage of the evolution of subdwarf B stars (sdBs) in binary systems. They are extreme horizontal branch stars burning helium in their core and are responsible for the UV upturn of elliptical galaxies. Seismic estimates of the core mass and the mass of their external thin hydrogen layer allow to retrace their binary formation history (Hu et al. 2008).
- Disk accretion phenomena in compact binaries: High precision photometric monitoring of cataclismic variables can be used to discriminate among the two possible channels of accretion in CVs: via disk or directly towards the magnetic poles.

8 PAYLOAD

The purpose of this section is to provide an overview over the three potential baseline Design Concepts of the PLATO payload (mission design and Service Module designs are covered in chapter 9). It covers the telescopes and the focal plane instruments, including related electronics and data handling sub-systems. These components have been the subject of conceptual design activities, performed by two industrial companies and the PLATO Payload Consortium (PPLC) on the basis of input received from the PLATO Study Science Team (PSST).

The presentation provided in this chapter focuses on the description of alternative technical concepts compatible with launch dates within the Cosmic Vision M-class boundaries. Depending on the level of involvement of National Agencies in the payload procurement, a range of programmatic scenarios exists.

A tabulated overview over the three payload studies is given below in **Table 8.1**.

Table 8.1: Tabulated comparison of three different payload concepts.

	Design Concept A	Design Concept B	Design Concept C
Optical system:			
Number of telescopes	12 (4 groups of 3)	54 (48 normal, 6 fast)	42 (40 normal, 2 fast)
Number of lenses or mirrors	2 mirrors	6 lenses (all spherical)	6 lenses (2 aspheric)
Entrance pupil diameter [mm]	169	83	120
Collecting area per telescope [m ²]	0.02243	0.0054	0.0113
Total collecting area [m ²]	2×0.15	0.29	0.48
Instantaneous Field of View [deg ²]	2×900	625	1806
Detectors:			
Number of CCDs	176 (168 normal, 8 frame transfer CCDs)	120 (96 normal, 24 frame transfer CCDs)	168 (4 per telescope)
CCD size [pixel]	2080×2574	3000×6000	3584×3584, 2 fast in FT mode
Pixel size [micron]	27	18	18
Plate scale [arcsec/pixel]	12.5	17	15
Full well capacity [Me-]	1.8	1	1
Readout frequency [MHz]	1.8	1.8	4
Nodes per CCD	2	4	2

8.1 Industrial studies – Design Concept A

The PLATO P/L **Design Concept A** consists of 12 catoptric telescopes based on a 2-mirror optical design with two simultaneously observed "half fields of view" (FoV). These half FoVs are $\sim 900\text{deg}^2$ each, resulting in a total instantaneous FoV of $\sim 1800\text{deg}^2$. The entrance pupil diameter of each telescope is 169mm, leading to a collecting area of $\sim 0.15\text{m}^2$ per half field and a total collecting area of $\sim 0.3\text{m}^2$. A controlled level of defocus is introduced. The optical system is optimised for a good response between 450-1000nm.

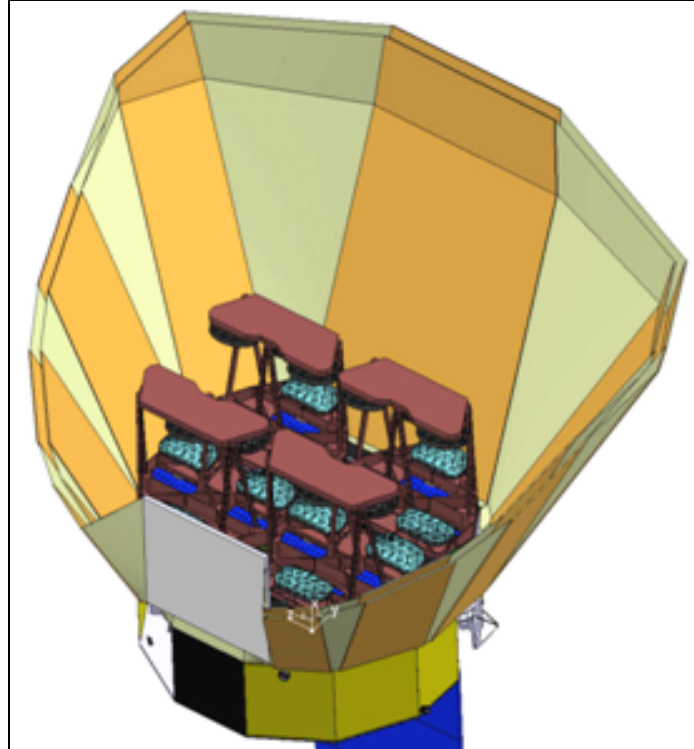


Figure 8.1: 4 groups of 3 telescopes (brown) mounted on an angled optical bench. The deployable sunshield is shown in yellow/orange

The spacecraft is rotated every 6 months along the Line of Sight (LoS) to point the solar arrays to the Sun.

The focal plane of each telescope is covered by 14 "normal" CCDs. Four focal planes are fitted with 2 "fast" CCDs. The latter are dedicated to the observation of bright stars in colour, operating in frame transfer mode (FT; see section 8.1.2). This results in a total of 176 CCDs used in this concept. The plate scale of the optical system is 12.5 arcsec / pixel across the whole FoV.

Three telescopes are grouped together to form four Telescope Assemblies (TA). Each three telescopes share a common structure and thus mass is saved and AIV processes simplified because each TA can be assembled and tested independently. The telescope modules are mounted to an optical bench.

A deployable sunshield is attached to the Service Module (SVM) and surrounding the telescopes in order to minimize vignetting effects (see **Figure 8.1**). The all-Silicon Carbide (SiC) telescope design also contributes to minimising optics mass and ensures very low thermal sensitivity.

8.1.1 Optical reference design

Each telescope consists of 2 mirrors; M1 and M2 (see **Figure 8.2**). The M1 mirror is rectangular with rounded corners to offer additional FoV for bright stars of sample P3 (see section 3.3.4). The dimensions of M1 are 342.5×615mm. The M2 mirror is elliptical (480×540mm). The entrance pupil diameter is 169mm and the collecting area per telescope is 0.02243m^2 . Both mirror surfaces are aspheric and will therefore require special tools and equipment for manufacturing.

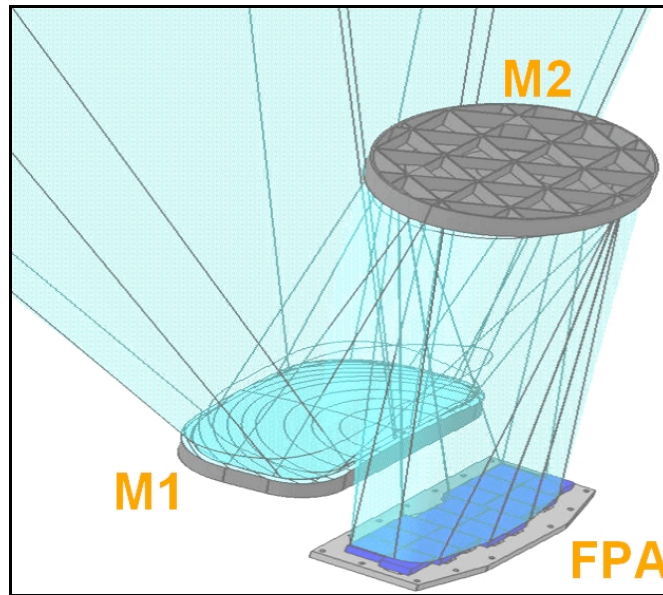


Figure 8.2: Telescope optical layout showing rectangular mirror M1, elliptical mirror M2 and the Focal Plane Array (FPA).

A preliminary stray light analysis showed that stray light from stars in direct view of the focal planes has a negligible impact on the radiometric performance, thus it is not necessary to baffle the focal planes. Baffling was considered for radiation shielding of the Focal Plane Assembly (FPA) but a different mitigation strategy is preferred (see radiation environment section 8.1.8).

Thermal analysis shows that annual thermal variations are lower than 7°C which is not critical for global alignment and defocus. Therefore no active thermal control is needed.

Figure 8.3 shows the Point Spread Functions (PSF) across the FoV. The PSFs at different locations on the focal plane have very diverse shapes. However, 99% of the encircled energy is always within 10-14 pixels.

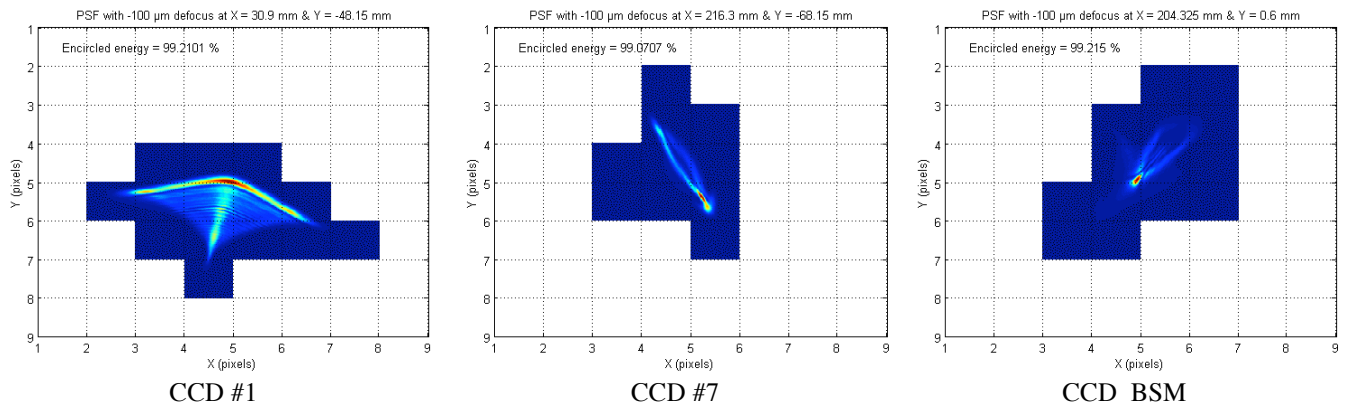


Figure 8.3: PSF shapes and sizes across the FoV. Locations of the different CCDs on the FP are shown in Figure 8.5.

The area density of the mirror elements is assumed to be 35kg/m² with a maturity margin of 5%. The unit masses are shown in

Table 8.2.

Table 8.2: Telescope mass budget for each telescope and Telescope Assembly (TA).

	Telescope	TA (3 telescopes)	PLM (4 TA)
M1	9.8kg	29.4kg	117.6kg
M2	6.4kg	19.2kg	76.8kg
Protective silica plate	2.5kg	7.5kg	30.0kg

		Total	124.4 kg
--	--	--------------	-----------------

8.1.2 Focal plane instrument

Figure 8.4 shows the upper and lower half of the FoV, each observed by 6 telescopes. Each FoV is obstructed on the bottom by the interaction of optical beams between M2 and the focal plane with M1. On the top/outer corners the optical performance degrades rapidly doubling the PSF diameter to ~ 50 arcsec. The resulting FoV, and therefore the shape of M1, is nearly rectangular, with only a circular gap at the bottom around the M2 mirror. The full performance FoV, where the PSF is smallest (< 43 arcsec), is defined as having more than 90% of the en-squared energy within 2×2 pixels. It has a total area of $\sim 900 \text{deg}^2$. The full-performance area of the FoV is covered by 14 "normal" CCDs and 2 "fast" CCDs on the FPA; the latter for only four focal planes. For the bright sample 3 stars the PSF size does not need to be very small and therefore the areas with enlarged PSFs, outside the "full performance" FoV, are used for these observations. The Bright Star Mode (BSM) CCDs in those corners are equipped with red or blue filters. This results in an additional FoV area of $\sim 130 \text{deg}^2$ per corner. The arrangement of half of these CCDs is shown in **Figure 8.5** on the right side. The coverage of the FoV by CCDs is shown in the same figure on the left side.

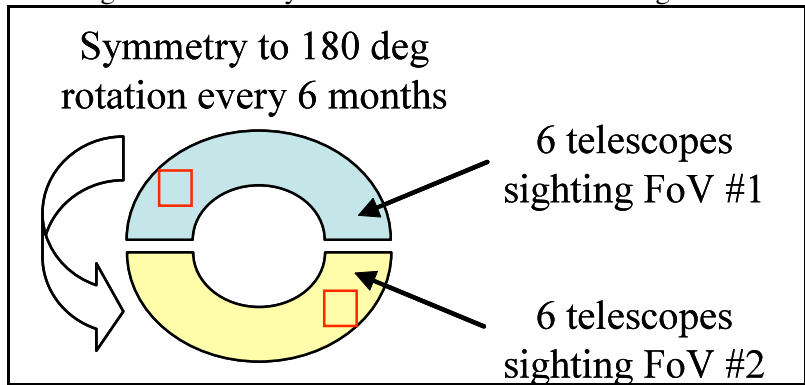


Figure 8.4: Symmetry of rotation of FoV every 6 months by 180 degrees. The red squares mark the positions of the red filter bright stars CCDs. The blue filter CCDs are located in the opposite corners

All 176 CCDs have 2080 columns and 2574 rows of pixels, with a pixel size of $27 \mu\text{m}$. This pixel size is valid for the baseline telescopes of pupil diameter 169mm. Each CCD has two read-out nodes connected to two video chains capable of reading out up to 2 Mpixel/s.

The budgets of the packaged CCD array are summarised in **Table 8.4**. These figures do not account for the SiC plate supporting all the arrays of each focal plane.

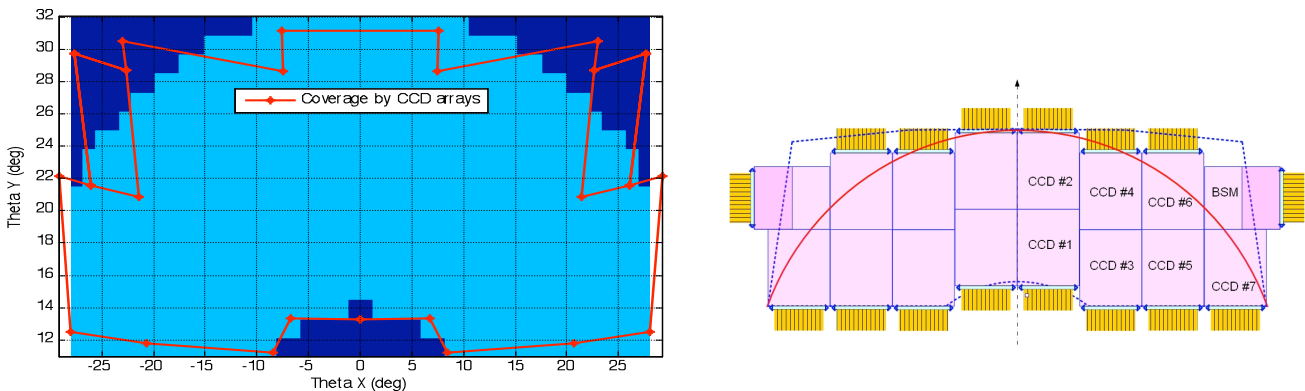


Figure 8.5: Left: Light blue: Full performance FoV with PSF size $< 43 \text{arcsec}$. Dark blue: PSF size $> 43 \text{arcsec}$. Right: Position of the CCDs on the FPA. Only labels for 7 "normal" CCDs and the BSM CCD are shown.

Table 8.4: CCD main budgets.

CCD main budgets				
Height	15 mm		Mass	131 g
Width	78 mm		Power dissipation	0.071 W
Length	62 mm		Density	1.8 kg/l
Volume	71.8 cm ³		Power density	1.0 W/l

8.1.3 Front end electronics

The CCDs are connected to the front-end electronics (FEE), which are located in close proximity to the FPA to avoid inducing noise in the signal. An initial data reduction is performed at FEE level so that only pixel data from the target windows are sent to the Data Processing Unit (DPU). This reduces the data flow between FEE and DPU to a fraction of the total data read-out from the CCDs. With two readout stages and two video chains per CCD, the AD conversion rate is 1.8 Mpix/sec using two 8-bit ADCs. If a faster 16-bit ADC is available at the time of the FEE design phase, the trade-off should be re-opened to simplify the video chain design.

A modular detection architecture to reduce the number of data links between the Payload Module (PLM) and Service Module (SVM) is foreseen. It consists of one FEE for each CCD and one Interface & Interconnection Module (I2M) per focal plane (see also section 8.1.4). The individual I2Ms feed signal to the Payload Data Processing Unit (PDPU).

The data link between I2M/DPU can be a SpaceWire link if the data rate, including 40% margin for the protocol, is less than 100 Mbits/s. This will be decided in a later phase of the study. Currently LEON FT telescope pre-processors are foreseen.

Power and mass budgets are estimated based on existing examples of controller and processor boards (mainly GAIA), without margin and they are presented in **Table 8.5**. The FEE is composed of two boards whose width is equal to the CCD width. In **Table 8.5**, also the I2M budgets are presented. The I2M is composed of three boards and their dimensions are equal to the focal plane dimensions.

8.1.4 Data handling

The signal from the CCDs is digitized in the Front End Electronics (FEE) unit and is then sent to the Data Processing Units (DPUs) which processes the data. Each DPU processes data from three telescopes. At DPU level initial correction calculations are performed such as calculating offset and smearing. The brightness of each target is calculated as well as the centroids for the four first stellar samples (see section 3.3.4). Functions such as compressing and packaging are also performed in the de-centralized DPU. The data is then sent to the mass memory where it is stored before being down linked

The following concept was taken as baseline for the electrical architecture: All CCDs of one Focal Plane Assembly (FPA) are connected to one FEE. An intermediate unit is implemented between the FEEs and the DPU: the Interfaces and Interconnection Unit (I2M). All FEEs of one FPA are connected to the I2M. The I2Ms are connected via SpaceWire to the DPUs. This is the split between PLM and SVM. A schematic of this data processing architecture is shown in **Figure 8.6**.

Physically, the FEE and I2M are located on the PLM and the DPUs etc are located on the SVM.

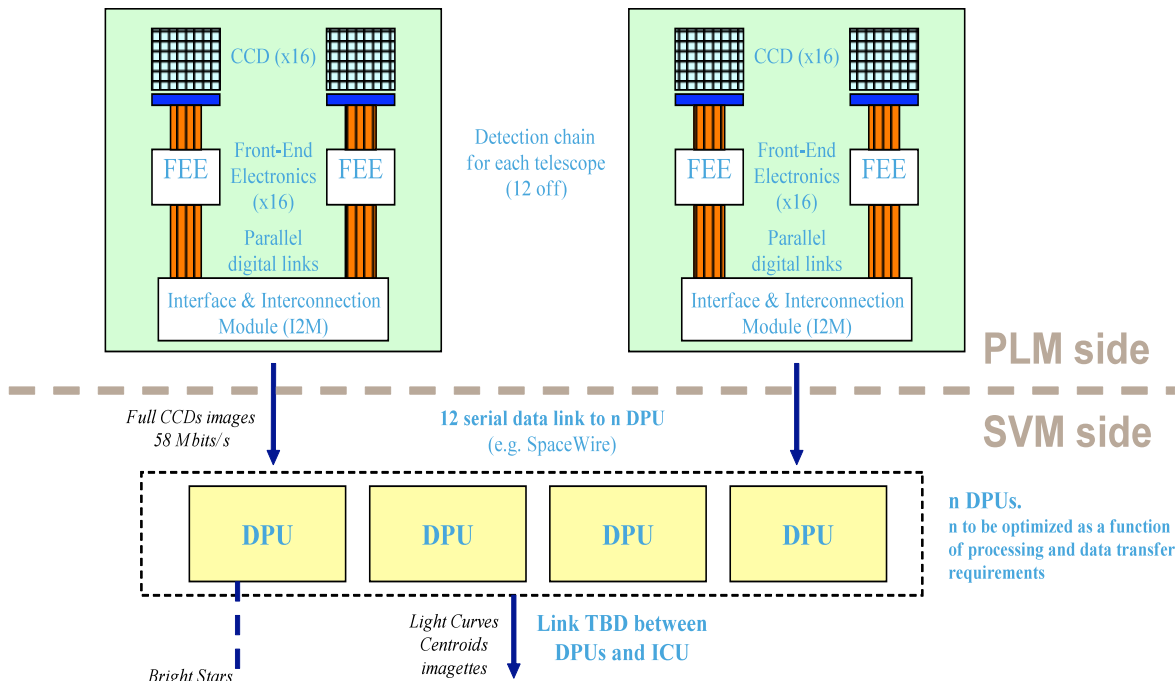


Figure 8.6: Schematic of the data processing architecture for Concept A.

The advantages of this electrical architecture are a minimization of the number of wires, simple payload interfaces and that dissipative DC/DC converters are not located close to the CCDs. One drawback is the need for one additional physical unit, the I2M. The power distribution is performed by several DC/DC converters inside the I2M. Each FEE has a dedicated converter. Having the DPUs located in the SVM also means additional harness and cabling mass.

The following **sequencing architecture** was adopted as baseline: The CCD pixels are readout during a time slot of 1.5s, leaving 28.5s for the acquisition. As the number of CCD pixels is equal to 5.4 Mpixels, and the CCD has two output registers, the maximum pixel readout frequency is up to 2 Mpixel/s.

8.1.5 Structures

A trade-off between single and integrated telescope modules was performed and the single telescope version was ruled out. No working solution was found trying to adapt standard Korsch or Cassegrain combinations. The number of telescope modules was optimized taking the spacecraft mass and volume into account.

To have a high dimensional stability and a low sensitivity to thermal variations, an all-SiC telescope design is proposed for the structure, mirrors, and the focal plane. The design is based on GAIA and Sentinel-2. From the trade-off performed in the beginning of the study, a structure common to three telescopes was chosen to minimise volume and mass, which are both critical for PLATO. A Telescope Assembly (TA) is composed of the following SiC structure components (see **Figure 8.7**):

- The TA base-plate, which is fixed by three ISM (Iso-Static Mount) on the PIP (Payload Interface Plate).
- 3 primary mirrors (M1), each isostatically fixed on the SiC base-plate by three *invar* bipods
- An isostatic structure composed of 6 struts supporting the TA upper plate
- 3 secondary mirrors (M2), each isostatically fixed on the upper plate by three *invar* bipods
- 3 CCD support structures, rigidly fixed on the base-plate (as on GAIA)

The focal plane proximity electronics (FEE and I2M), which are functionally part of the Telescope Assembly (TA), are fixed on the Payload Interface Plate (PIP) to allow good thermal decoupling with the cold focal plane. Each CCD array is connected to its FEE through a low conductance flexprint. During AIV operations,

the FEE modules are fixed on the TA base plate. The 16 FEE modules of one focal plane are thermally linked to the I2M module, so the I2M module is carried by the same structure as the FEE module.

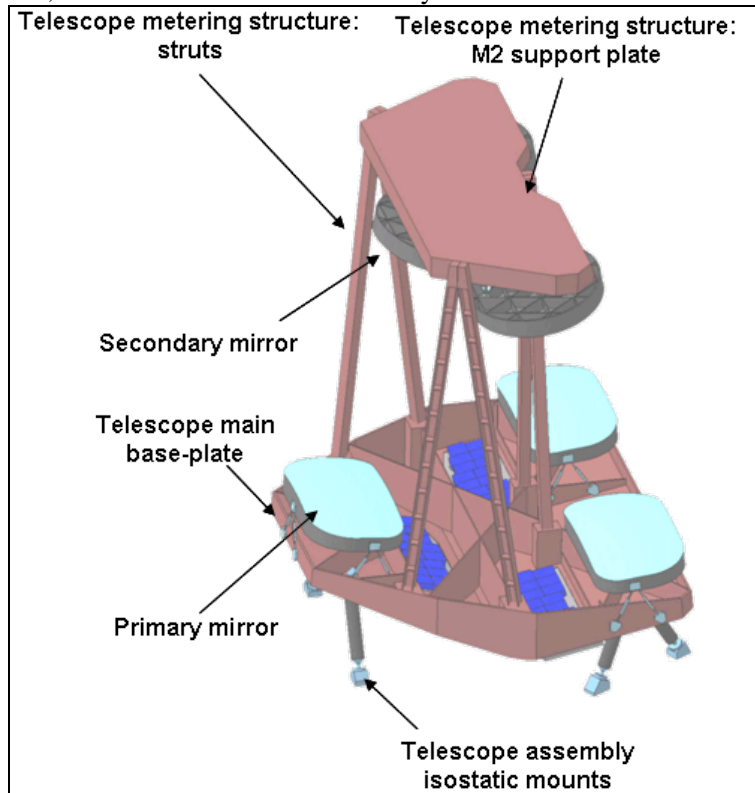


Figure 8.7: One module of 3 combined telescopes.

Each of the 4 TAs is isostatically fixed on the Payload Interface Plate (PIP). This structure is made of Carbon Fibre Reinforced Polymer (CFRP) honeycomb because of its large dimension (diameter = 3500 mm) and because inter-TA stability requirements are relaxed. The PIP provides the interface with the SVM through a set of 6 bipods attached to 6 hard points.

The Deployable Sunshield Array is attached to the SVM. No cover of the PLATO payload is foreseen in this design.

Table 8.5 shows the structural elements of the PLM and the corresponding mass in kg. Note that the mass of all elements is given with 5% margin.

Table 8.5: Mass of P/L structure elements.

Item	Mass [kg] incl. margin
M1 supporting plate	171.2
M2 supporting plate	62.7
Struts	39.2
Interfaces fixation devices	10.5
Secondary structures and baffles	2.1
Fixation H/W (bolts, nuts, washers,...)	6.3
Interface base plate	104.7
Isostatic I/F with SVM	20.0
Total	416.7

8.1.6 Thermal sub-system

The CCD arrays are implemented on a SiC base plate conductively coupled to the M1 base plate to allow passive CCD cooling to 150K through the cold SiC telescope structure. Proximity electronics are thermally

decoupled from the focal plane and controlled at 40°C by coupling with loop heat pipes with a lateral radiator.

The optics and the Focal Plane Assembly (FPA) will operate around 170 K. While the optics does not require a specific absolute temperature, the dark current is reduced in the CCD detectors at colder temperatures. So instead of complex thermal de-coupling, both elements will operate at that cold temperature. Since the electronics in the FEE units operate at ~320 K, it is important to have a well-designed thermal control system that de-couples the FEE from the FPA and optics and also efficiently removes dissipated heat. The FEE and FPA are thermally separated with the help of thermal shields. The power dissipation from the CCDs is achieved through the FPA coupling to the telescope base plate which acts as a radiator. The much larger heat dissipation from the FEE units is transported via heat pipes to a lateral radiator on the cold side of the spacecraft. The DPUs and Instrument Control Unit are physically located in the SVM where all the units operate at room temperature, and thus the Thermal Control System (TCS) is simplified with no thermal coupling among the units.

8.1.7 Operating Modes

The *instrument* operating modes are described here below.

Configuration Mode: At the start of a new pointing it is necessary to define the star apertures for all targets and the exact locations of the star centroids. The star positions will be known to a high precision from GAIA data.

Exposure Mode: Data for sample P1 (see section 3.3.4) are collected every 30s. Sample #5 data are collected at a 600s cadence. Sample #5 data is collected every 30sec and added up to an integration time of 600sec.

In exposure mode, a set of bright stars will be tracked in a manner similar to a star tracker. This data is then made available to the AOCS.

Manoeuvre Mode: The AOCS is based on cold gas thrusters. System design suggests it will be necessary to suffer pointing disruption once every 6 months to rotate the S/C. Data collection must be suspended for a number of days to allow for transients to disappear and allow for new definition of star apertures.

Calibration Mode: A number of calibration activities will have to be considered at occasional points during the mission. Note that this design does not foresee a payload cover and certain calibration measurements, like flat fields or dark fields calibration, will have to be obtained differently. This is TBD. In most cases one can assume that the FPAs are read out in normal sequences, and that data acquisition and selection is the main difference between calibration science data acquisition.

It is expected that the instruments are powered down in Safe Mode.

8.1.8 Interface requirements

The **mechanical interfaces** between the SVM and PLM are as follows:

Each of the 4 TAs is isostatically fixed on the CFRP honeycomb PIP which has a diameter of 3500 mm. The PIP provides the interface with the SVM through a set of 6 bipods attached to 6 hard points on the 2500 mm diameter SVM thrust cone. The sunshield is connected to the SVM. It protects the payload from stray light and thermal variations.

Radiation environment

The radiation levels for PLATO are calculated to be 10 times higher than for GAIA. A proper radiation analysis is needed in a possible future phase in order to better characterise and estimate the radiation effects.

A possible mitigation action against radiation damage would be to add a protective silica plate on top of each focal plane. Assuming 10mm thickness for this plate, the mass impact is an additional 30kg.

8.2 Industrial studies – Design Concept B

The PLATO P/L **Design Concept B** consists of 54 identical, wide-field optical telescopes with a useful FoV of $\sim 625 \text{ deg}^2$. Each telescope has a pupil diameter of 83 mm and a collecting area of $\sim 0.0054 \text{ m}^2$ resulting in a total collecting area of $\sim 0.29 \text{ m}^2$. Each telescope has a CCD array that en-squares the whole FoV. The plate scale of the optical system is 17 arcsec / pixel. A certain amount of de-focusing will be applied to enlarge the PSF to make it more resistant to satellite jitter. To ensure a common field coverage, the telescopes are co-aligned to the same direction within better than $\sim 2 \text{ arcmin}$. The optical system is optimised for a good response (reflectivity/Quantum Efficiency) in the 450-1000nm band. The total number of telescopes has been limited taking into account the maximum number of CCDs that can be procured on the timescale of the M-class mission programmatic constraints, targeting a launch in 2017 as well as mass budget restrictions. **Figure 8.8** shows the payload design along with the sunshield.

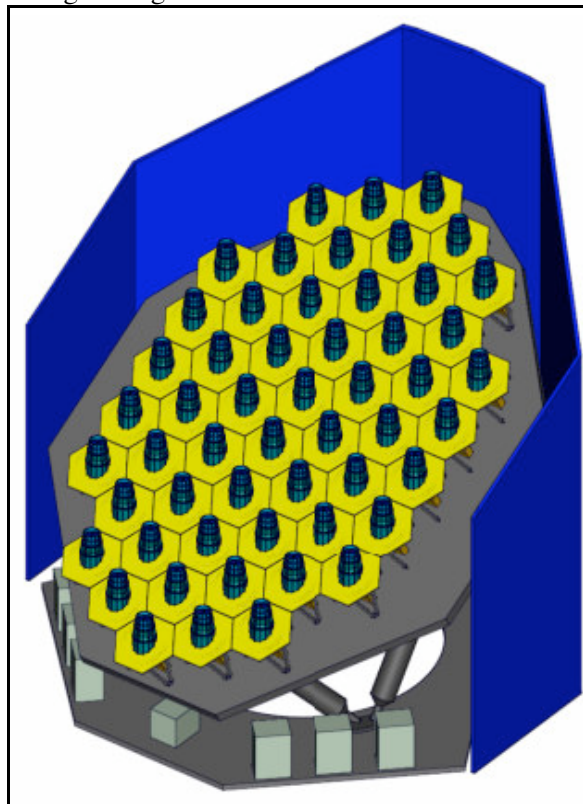


Figure 8.8: 54 telescopes mounted on the tilted base plate. The sun shield is shown in blue. FEE boxes are visible at the bottom. Each telescope has a hexagonal radiator attached to the barrel segment which is shown in yellow.

This design is based on a monthly 30° rotation of the spacecraft around the payload Line of Sight (LoS) in order to keep the sunshield and the solar arrays aligned towards the sun. As the FoV is circular, any degree of rotation around the line-of-sight is possible without interruption of the continuous observation of the stars. As a consequence of the monthly rotation, the other S/C manoeuvres are smaller and less propellant is used for orbit control. Note that the FoV is ultimately square because the CCDs are placed in a square configuration on the FPA. However, this has no influence on the rotation along the LoS.

8.2.1 Optical reference design

The telescopes are based on a design with 6 spherical lenses. Each telescope is individually mounted on a base plate that is tilted in order to avoid vignetting by the sunshield (see **Figure 8.8**). Due to the optical quality of the refractive design the diameter of the PSFs along the edge are still small enough to be valid for star samples 1 and 5, which means that almost the entire FoV can be used for observation.

48 of the 54 telescopes are dedicated to observing stars with magnitudes fainter than $\sim 6.5m_v$ and they are referred to as "normal" telescopes. Each normal telescope projects on 4 CCDs of 3000×3000 pixels of $18\mu m$ size. There are 8 video outputs per Focal Plane Assembly (FPA) and thus 2 outputs per CCD.

6 of the 54 telescopes are dedicated to the observation of brighter stars and are called "fast" telescopes. This refers to their faster readout time which is required to avoid saturation of the pixels due to the brightness of the target stars. Each of these telescopes projects on 4 CCDs which operate in frame-transfer mode. They also have 8 video outputs per FPA and 2 outputs per CCD.

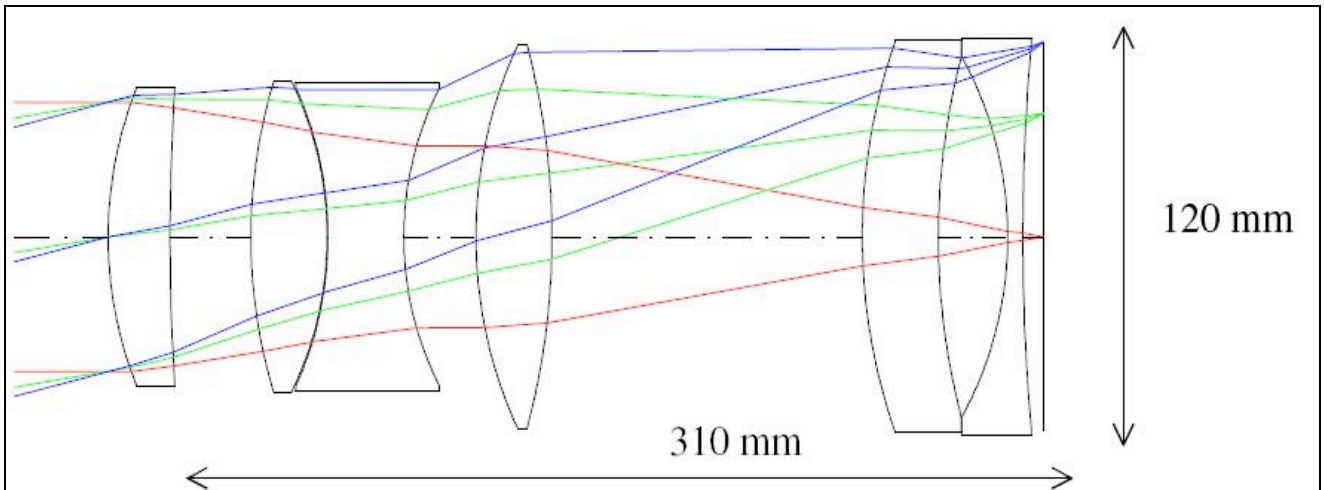


Figure 8.9: Optical layout: lens positions, sizes, and dimensions.

Two of the 6 fast telescopes provide colour information on a minimum of 300 stars (see section 3.3.4) of Main Sequence stars of all spectral types. They are optimized for a good response in blue and red wavelengths, respectively, using red and blue filters. They should preferably stare a complementary field in order to increase samples 3 and sample 4 performances. Then they would yield an additional ~ 160 cool dwarfs ($m_v < 6.1$).

All lenses are spherical with a maximum diameter of 120mm. This optical design is based on the COROT optical design.

Figure 8.9 shows the optical layout of the Design Concept B baseline design. The design drivers were to maximise the FoV, maximise the effective collection area, obtain a uniform surface brightness of the Point Spread Function (PSF), and to minimize the mass per telescope.

The size and shape of the PSF is affected by manufacturing and alignment of the optical elements as well as the operational environment. All these factors can enlarge the theoretical PSF calculated by optical model. The shape of the PSF of this optical design (see Figure 8.10) is circular in the centre of the FoV and becomes more irregular towards the edge of the FoV of each telescope.

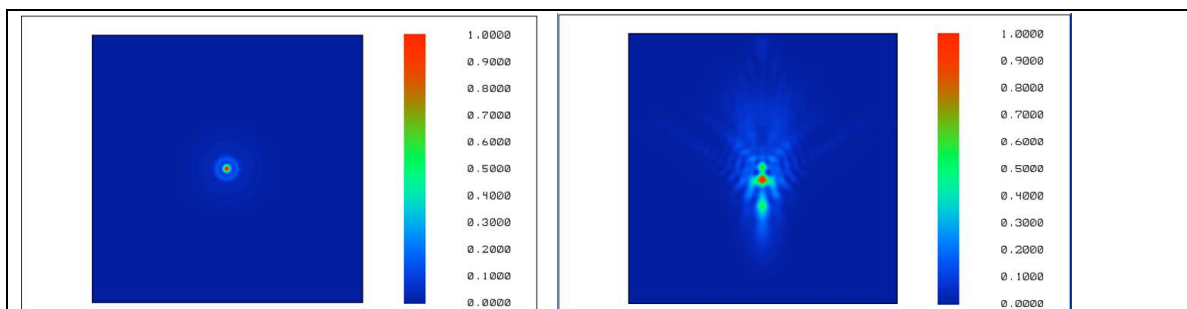


Figure 8.10: Polychromatic PSF at the centre (left) and at the edge (right) of the FoV. Scale: one blue image side is $\sim 65\mu m$ wide.

The PSF size is calculated to be $40\mu\text{m}$ containing 80% of the encircled energy and $45\mu\text{m}$ containing 90% of the en-squared energy. This results in an angular size of <34 arcsec for the PSF and it will span two pixels on the CCD. The probable end-of-life PSF inside the FoV would be between 30 arcsec and 40 arcsec.

The average transmittance over the whole spectral range is taken from COROT and was not calculated for PLATO. In the COROT case it is around 90% and it is assumed to be similar on Plato at beginning-of-life. This is based on the fact that the same number of lenses and the same materials are used as on COROT.

Concerning aging, the losses measured on COROT after more than 2 years in orbit (800 km altitude) are around 2% per year. This includes transmittance losses, detector losses and electronic ageing. It is assumed that the situation would be better for PLATO because the radiation environment is more benign than for COROT. A global loss of efficiency on Plato of $< 1.5\%$ per year is expected. However, the transmittance and the radiation effects are open issues in this design (see open issues section below).

The design of the sunshield allows avoiding a dedicated, complex, bulky and heavy baffle to be located on each telescope entrance.

All lenses are spherical and do not require specific tools and equipment for manufacturing. Details of the optical design can be found in **Table 8.6**.

Table 8.6: Details of optical design of Design Concept B and telescope budget.

Description	Value
Number of lenses	6
Glasses	SFPL51, SLAL9, SBSL7
Pupil size	83 mm
Total FOV	$28^\circ \times 28^\circ$
Working F-number	2.9
Max. lens dimensions	120 mm
Functional temperature	-120°C (TBC)

The proposed design is largely inspired by the COROT design and uses the same number of lenses and the same materials. It is foreseen to use mechanical interfaces to precisely align the lenses without optical assistance. This is to minimise cost and schedule of the payload development. A statistical analysis has been performed by using the Monte-Carlo method to derive the PSF enlargement sensitivity to the mechanical misalignment.

8.2.2 Focal plane instrument

The current baseline for this design is to use 3000×6000 pixel CCDs for all telescopes. The FoV for each telescope is covered by four CCDs per FPA. Each CCD has read-out nodes connected to video chains capable of handling the read-out of the pixels fast enough to avoid excessive smearing effects. The FPA is integrated at the bottom of the telescope barrel with some distance to the last lens to minimize thermal coupling.

a. Normal CCDs

The 48 "normal" telescopes each use two 3000×6000 pixel CCDs with a pixel size of $18\mu\text{m}$ and 4 outputs each (**Figure 8.11**). This number of outputs was chosen to stay compliant with the state-of-art in the domain of 16-bit ADC frequencies and to decrease the impact of smearing of $\sim 11\%$ with 2 outputs. The pixel full well capacity is currently assumed to be 10^6 electrons.

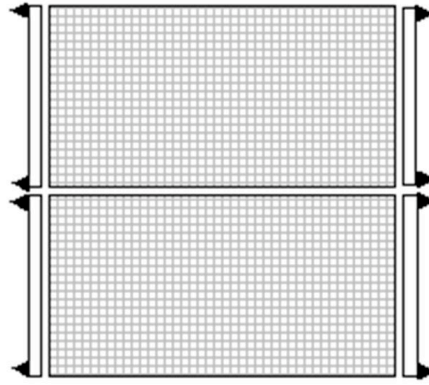


Figure 8.11: Normal telescope CCD architecture: baseline is $3k \times 6k - 2$ CCDs per FPA.

The sampling time of these telescopes is 25s divided into 22.5s integration time and 2.5s readout time. This prevents saturation while observing stars up to a magnitude between 6 and 7. The minimum number of flight model CCDs to be provided would be 96.

b. Fast CCDs

The 6 "fast" telescopes also use 3000×6000 pixel CCDs with a pixel size of $18\mu\text{m}$ but they are operated in frame transfer mode (Figure 8.12). Only an area of 3000×3000 pixels is photosensitive and the other half is covered and used for data storage. Each CCD has 2 outputs. The full-well capacity (FWC) currently assumed is also 10^6 electrons.

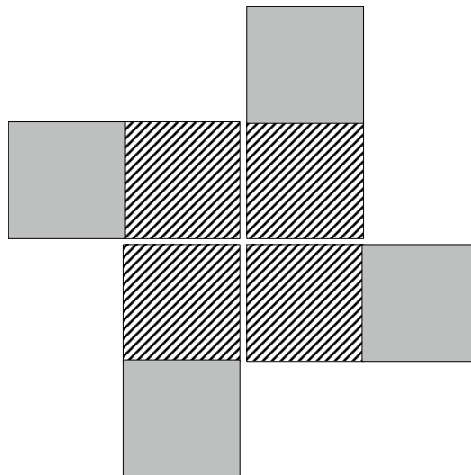


Figure 8.12: Fast telescope CCD architecture for one telescope Focal Plane Array. The striped areas are photo sensitive and the grey areas are the storage area.

The sampling time of these fast telescopes is 2.5s divided into 2.25s integration time and 0.25s readout time. Vertical transfer prevents saturation for stars with a magnitude up to 4. The number of flight model CCDs is 24.

The following estimates (Table 8.7) for power dissipation were made based on exiting heritage.

Table 8.7: CCD power estimates.

	NORMAL TELESCOPE	FAST TELESCOPE
CCD static consumption [W]	0.34	1
CCD dynamic consumption [W]	0.85	2

8.2.3 Front end electronics

The Front-end Electronic Units (FEEU) are attached directly to the optical bench and connected to the close-by FPA at the bottom of the telescope structures. It covers the following functions: video signal processing; generation of all clocks necessary for the CCDs, internal FEEU circuits and data transfer between FEEU and DPU; CCD phase driving; command/control interface; digital video interface; FEEU power supply; CCD biasing. There are dedicated "normal" and "fast" FEEUs for the normal and fast CCDs. One FEEU module is located behind each normal telescope. It will be able to drive frequencies up to 1.8MHz.

An ASIC with LEON2FT is baselined for the Central Processing Unit (CPU), utilizing heritage from e.g. GOCE. This is currently under qualification.

Considering the high data rate point-to-point links implemented by SpaceWire (SpW) are foreseen for distribution of instrument data. Due to the high number of SpW links from the instruments a dedicate SpW router is foreseen. This is available off the shelf.

The normal FEEU, with the successive sequence timing, dissipates 6.2W during the integration period of 22.5s and 8.2W during the readout period of 2.5s. The consumption has been minimized due to the timing. The allocation for the fast_FEEU consumption is currently 20W, as it includes supplementary functions.

Mass budgets (*Table 8.8*) are estimated based on existing examples of controller and processor boards.

Table 8.8: Mass budget for FEE.

Items	Unitary mass [kg]	Number	Total mass [kg]	Margin [%]	Max. mass [%]
Cabling video FEEU DPU	n/a	n/a	70.0	20.0	84.0
Power supplies	8.4	3	25.2	20.0	30.2
DPU	2.8	12	33.0	20.0	39.6
Payload Interface Unit	6.0	1	6.0	20.0	7.2
Total electronics mass			134.2		160.0

Power dissipation of the centralized Power Supply Unit (PSU): **887 W** average and **952 W** peak (no margin).

8.2.4 Data handling

The data is transmitted to the DPUs where each DPU processes data from 6 telescopes. As in Design Concept A, the DPUs perform most of the data processing. However, the compression and packaging functions are centralized in an Instrument Control Unit (ICU). The data is stored between two consecutive ground contacts during which data is down-linked. This design utilizes differential intensity measurements to calculate brightness and other science parameters in order to reduce the data rate. This allows retaining information from all individual telescopes when performing post-processing on-ground. Individual light-curves from each telescope make it easier to remove single-event effects. A large deviation in one telescope compared to the others signals means that this telescope's data should not be used in calculating the average flux for that particular sampling period. The main design driver is the payload output data rate, for which the allocation is 910 kbps.

The baseline data architecture can be summarized as follows: Each telescope is linked to one Front End Electronics Unit (FEEU); every 18 telescopes are grouped in 3 modules; each module consists of 18 FEEUs and 4 DPUs (3 normal + 1 redundant); every 6 telescopes/FEEUs share one DPU; 3 of 4 DPUs are active, one is redundant. In total there are 12 DPUs, 9 are nominal and 3 are redundant. The DPUs feed information into the Instrument Control Unit (ICU), of which there is one active and one redundant.

8.2.5 Structures

Each camera consists of:

- 6 lenses, each within its own barrel and assembled together to form a self standing dioptric objective,

- A focal plane holding 4 CCDs directly fixed on the last lens barrel.

Note that each barrel has an integrated hexagonal space radiator made of the same material to cool down the focal plane. Each **telescope structure** (see *Figure 8.13*) consists of four barrels and a FPA support. The lenses are glued to titanium rings, which are then mounted to a telescope barrel element using special glue. The four barrel elements are then attached to each other and the FPA support with a high level of alignment accuracy. The **telescope barrel** including the radiator as well as the focal plane support will use Carbon-fibre reinforced Silicon Carbide (CeSic). The bipod structure supporting each individual telescope is made of Glass Fibre Reinforced Polymer (GFRP) and is connected to the base plate via titanium end fittings. The **base plate** is made of Carbon Fibre Reinforced Polymer (CFRP).

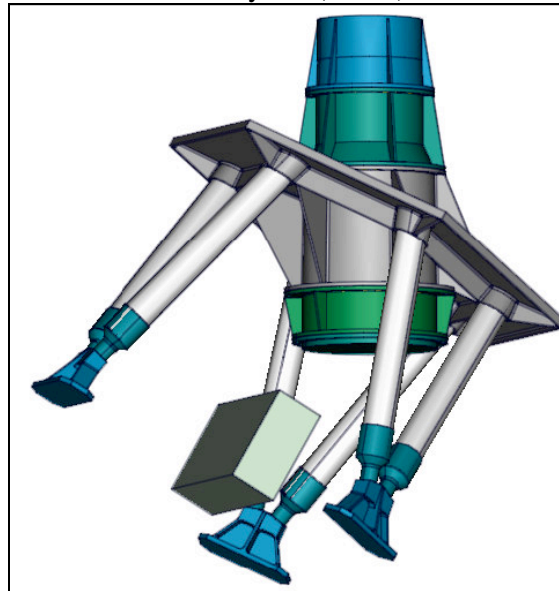


Figure 8.13: Self standing 83mm telescope objective holding 2 CCDs including GFRP struts and the FEEU (light green box).

Each telescope can be assembled aligned and tested separately, with an identification of the line of sight compared to the mechanical interface. Each camera is fixed to the payload base plate by 3 GFRP bipods holding it rigidly to the payload panel but decoupling it thermally. Shimming can be used for a proper relative alignment of cameras on the base plate.

The base plate is a CFRP sandwich panel with 1.6mm CFRP skins and 140mm aluminium honeycomb. This base plate is reinforced by 3 CFRP sandwich stiffeners located on the bottom face. The base plate is tilted by 30° in order to place all the PLM inside the shadow of the sun shield and to maximise the radiative surface for the FPA cooling. The sunshield (see *Figure 8.8*) is attached to the SVM. No cover of the payload is needed in this design. A detailed mass breakdown is shown in *Table 8.9*.

Table 8.9: Main elements of the telescope design.

Items	Unitary mass [kg]	Number	Total mass [kg]	Margin [%]	Max. mass [kg]
Telescope units					
Lenses	3.75	54	202.6	5.0	212.7
Sockets	0.41	54	22.0	20.0	26.3
Barrels+ integrated radiator	2.13	54	115.0	20.0	138.1
Camera support struts	1.40	54	75.5	20.0	90.7
Focal plane equipped	0.46	54	24.9	20.0	29.9
Payload I/F Base plate					
Base plate	93.3	1	93.3	20.0	112.0
Stiffeners of P/L panel	1.2	3	3.5	20.0	4.2
PL interface panel	9.7	1.0	9.7	10.0	10.7

8.2.6 Thermal sub-system

Since the operating temperature of the FPA was one of the input parameters for the study, the proposed design is also tailored to an operating temperature of the FPA and optics at $\sim 170\text{K}$. This design is lens-based and therefore it is sensitive to thermal gradients within each individual telescope. Excessive thermal gradients give rise to defocusing effects as well as alignment (e.g. tilt) effects. However, since each telescope is a closed structure the thermal stability can be modelled and controlled very accurately. The power dissipation from the FPA is done through conductive links to the individual telescope structure which has an integrated, tilted radiator attached to it. The power dissipation from the FEE units, with an operating temperature of $\sim 300\text{K}$, is done through the tilted base plate to which they are physically attached and thermally linked. The rest of the payload data-processing units (DPUs and ICU) are attached to the PLM bottom panel at the edges, meaning that the units can dissipate heat directly out to cold space. They are operating at room temperature.

8.2.7 Operating Modes

The operating modes which are most relevant for the payload described here below:

Configuration: At the start of a new pointing it is necessary to define the star apertures for all targets and the exact locations of the star centroids. The star positions will be known to a high precision from GAIA data.

Calibration: A number of calibration activities will have to be considered at occasional points during the mission. Note that this design does not foresee a cover and certain calibration measurements, like flat field or dark field calibration, will have to be obtained differently. In most cases one can assume that the FPAs are read out in normal sequences, and that data taking and selection is the main difference between calibration science data acquisition.

In the **Observation Mode** the following tasks are performed: a) the payload telescopes are operational; b) AOCS operates to provide fine pointing and stability; c) the power is generated by SA; d) transmitter and receiver are both on. Data for sample #1 are collected every 25 seconds. Sample #2 data are collected 2.5 sec cadence.

Manoeuvre: The Observation Mode is interrupted every 30 days for S/C sun reorientation and station-keeping manoeuvres. Data collection must be suspended for this period.

Transition to **Safe Mode** may occur in reaction to several events. In particular, a failure in power supply or in attitude control may cause the system to switch to Safe Mode. However, transition could also be commanded from ground.

8.2.8 Interface requirements

The **mechanical interface** between the P/L platform and the SVM thrust cone consists of six rods, which form three bipods between these two elements.

The FEEU interface with one telescope in order to acquire and process data from 4 CCDs. It will also deliver clock drivers for detector operating.

Radiation environment

The electronic units, CCD sensors, optics and lenses need to be designed to withstand the space radiation environment during PLATO's 6 years lifetime. For the outer most lens of each telescope it is foreseen to use radiation hardened glass. Additionally, a metal (e.g. Al) rim all along the PLM base plate of TBD dimensions is considered which shall shield the focal plane arrays against radiation damage.

8.3 Design Concept C

The PLATO P/L **Design Concept C** consists of 42 refractive telescopes based on a 6-lens optical design, including two a-spherical lenses. The telescopes are divided into four separate groups which observe partly overlapped sky fields (see **Figure 8.14**). The total instantaneous FoV is $\sim 1800\text{deg}^2$. Each telescope has a pupil diameter of 120mm, a collecting area of $\sim 0.01131\text{m}^2$ resulting in a total collecting area of $\sim 0.475\text{m}^2$. The plate scale of the optical system is 15 arcsec / pixel across the whole FoV.

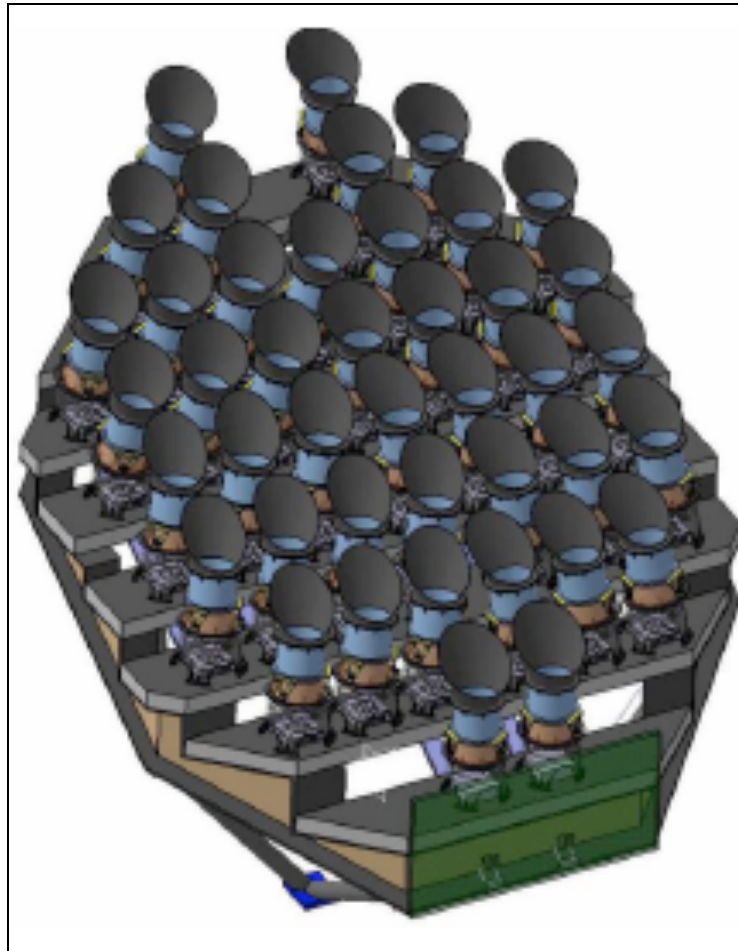


Figure 8.14: telescopes mounted in groups on a staircase shaped optical bench.

This design is based on a 3-monthly 90° rotation around the LoS. This is required to keep the solar arrays aligned towards the sun and to avoid stray-light from the Sun, Earth and Moon and is made possible due to the circular FoV. There are 10 telescopes arranged in 4 groups and these groups are off-set with respect to each other. Two telescopes are dedicated to the brighter samples of stars and also have colour filters to obtain colour information on sample P3 (see section 3.3.4). These coloured telescopes can be seen in the front see in **Figure 8.14**, close to the 1m^2 radiator (green panel).

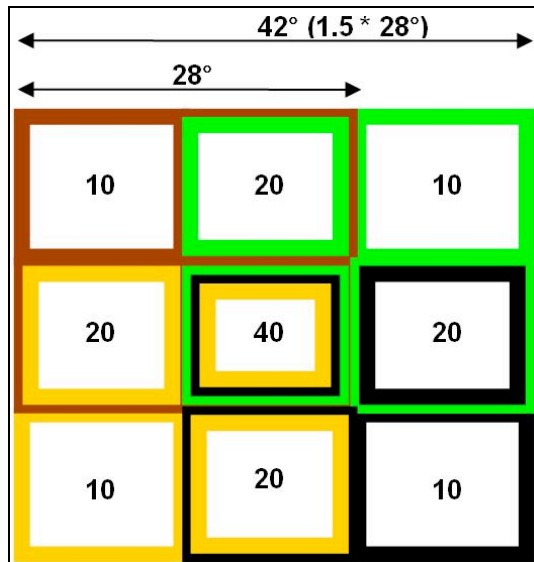


Figure 8.15: Schematic figure of the overlapping FoV for the 4 groups of telescopes. The number in each of the nine sub-squares shows the number of telescopes that observe that area.

The four groups of telescopes produce three zones with different collecting areas and FoV (**Figure 8.15**). Each of the 9 sub-squares has a FoV of $(42/3)^2 \sim 200\text{deg}^2$ resulting in $\sim 800\text{deg}^2$ observed with 10 telescopes; another $\sim 800\text{deg}^2$ observed with 20 telescopes and a centre area of $\sim 200\text{deg}^2$ which is seen by 40 telescopes. Since the central square is seen by all telescopes, it allows to re-observe interesting targets during the step-and-stare phase with a higher collecting area and thus with higher photonic accuracy. The result is 9 squares with different collecting areas depending on the number of telescopes observing that particular part of the sky. The numbers in the boxes of **Figure 8.15** represent how many telescopes are observing that particular sky field square.

The total FoV is therefore $\sim 1800\text{deg}^2$. This Design Concept as well as Design Concept A favour brighter stars and have a large FoV and smaller collecting area per field. The optical system is optimised for a good response (reflectivity/Quantum Efficiency) in the 450-1000nm band.

8.3.1 Optical reference design

The telescopes are based on a 6-lens optical design (see **Figure .-16**), including two a-spherical lenses which will require specific tools and equipment for manufacturing. Those lenses are marked as L1 and L2 in Figure 5-17. Note that the physical diameter of L1 is 200mm. The entrance pupil diameter is 120 mm.

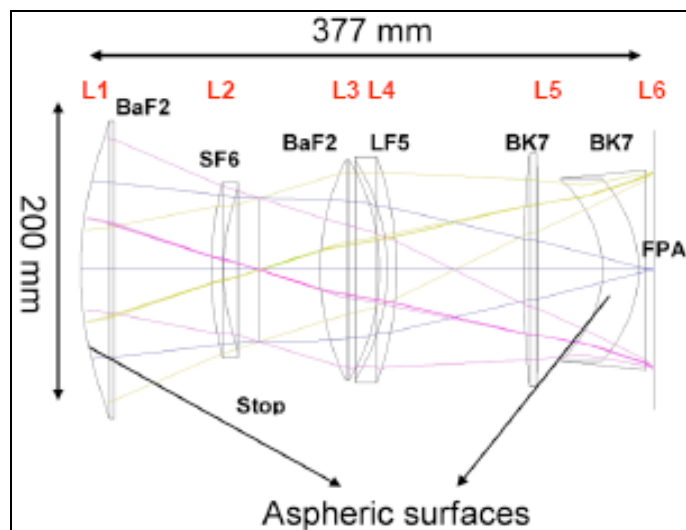


Figure .-16: View of the 6 lenses of Design Concept C.

All lenses are mounted in a barrel-shaped mechanical structure. Due to the refractive solution the FoV is circular. The lens materials are radiation hardened or resistant glasses. It needs to be confirmed that they are available off the shelf. Each telescope is equipped with a baffle which is designed to act as a radiator to remove heat from the detectors as well as minimize the stray-light entering the telescope. The presence of baffles for the telescopes also requires shielding from the mutual scattering of the telescopes inside. The shape of the PSF of this optical design (see Figure 8.17) is circular in the centre of the FoV and degrades towards the edge of the FoV. A minimum of 90% of the PSF photo-electrons are considered effectively used in the photometry mask. The size of the PSF on the sky is typically 30-35 arcsec and it will always be within 9 pixels on the CCD.

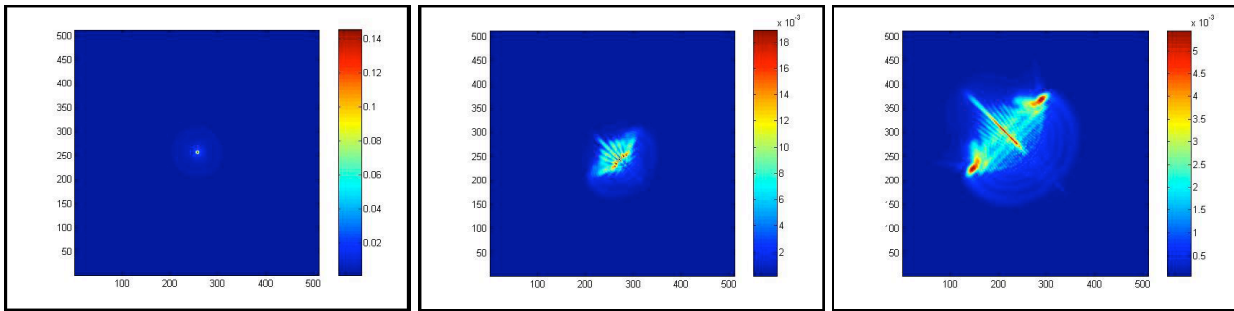


Figure 8.17: PSFs at centre, middle, and edge of FoV.

The present nominal mass of each telescope optical unit is ~ 10.7 kg. A breakdown of the telescope mass is shown in **Table 8.10**.

Table 8.10: Telescope mass budget including FPA and thermal equipment.

Item	kg per unit	Quantity	Total mass [kg] (without margins)
Structure	4.1	42	172.2
Optics glass	6.1	42	256.2
Baffle	0.5	42	21.0
total optical unit	10.7		
Thermal equipment	0.2	42	8.4
FPA	1.3	42	54.6
Total	12.2		512.4

8.3.2 Focal plane instrument

Table 8.12: Main CCD properties.

Parameter	Nominal value
Pixel size	18 μm (square)
Pixel format	3584 x 3584
CCD dimensions (image area)	64.5 x 64.5 mm ²
CCD flatness	better than 20 μm peak to peak
Mechanical mounting in the FPA	4 CCDs included in a 131.5 mm side square
Readout frequency	4 MHz
Number of read outputs	2 per CCD
Readout noise	<15 electrons r.m.s.
Full well capacity	1 Me-
Full frame readout time	< 2 s
CCD exposure duration	> 23 s
Fraction signal smeared	$\sim 9\%$
Mass per CCD	< 80g
Mass per FPA (CCDs, support plate, straps, ...)	1320g (incl. 20% margin)

The FPA for each telescope consists of 4 identical CCDs of 3584x3584 pixels with 18µm pixel size (see **Table 8.12**). The CCDs of the bright star telescopes (sample 3 and sample 4) have the same size but operate in frame transfer mode, where one half of the device is coated with Aluminium and serves as the storage area. In total, 168 CCDs are used for this design. Since for the "bright" telescopes only half the active area is used to collect charges in the CCDs, their FoV is also halved.

The **power** which is used per focal plane array (FPA) is 278 mW incl. 20% margin for the normal FPAs and 1374 mW incl. 20% margin for the fast FPAs. Power dissipation inside the FPAs is a main concern and to reduce the power the CCD nodes are power-cycled. Each node is powered on 2s before its readout commences, to allow stabilisation. When readout is finished, it is powered down for the remaining 21s of the period so that output stage average dissipation is reduced by 84%.

8.3.3 Front end electronics

Each telescope has its dedicated Front End Electronics (FEE) that only digitizes the data from the CCDs and sends it to the Data Processing Units (DPUs) where target windows are extracted and corrective data functions are performed as for the design concepts described in the earlier sections. From the DPUs, the data is sent to the Instrument Control Unit (ICU) where it is collected in packages and compressed before being sent to the mass memory and down-linked to ground. A key component for the normal telescopes is the 16-bit ADC. The need of readout of 13 Mpx in 2s through 2 channels gives a pixel rate of 4.0 Mpx/s. The fast FEE comprises 8 ADCs feeding directly into the fast DPU. This is co-located with the FEE to reduce the distance for high-volume data transmission which also reduces the power consumption.

Each FEE includes a high performance SpaceWire bidirectional serial interface to transfer the digitized CCD raw data to the digital electronics, to receive low level commands from the digital electronics, and to transfer digital housekeeping to the Instrument Control Unit (ICU) via the DPU assembly boxes.

The power budget (see **Table 8.13**) is based on a DC-DC converter efficiency of 0.7 for analogue voltages, and DC-DC converter efficiency of 0.8 for digital voltages. This budget presents the effective dissipated power in each sub-system box.

Table 8.13: Power consumption of electrical architecture.

Item	W per unit	Quantity	Total
Telescope thermal	2.0	42	84.0
FPA	0.5	40	20.0
FEE	3.5	40	140.0
Fast FPA	2.5	2	5.0
Fast FEE	7.3	2	14.6
AEU	16.0	5	80.0
CLK	5.0	1	5.0
MEU (5 DPU)	32.3	8	258.4
Fast DPU	10.3	2	20.6
ICU	21.2	2	42.4
Total [W]			670.0 (Without margin)

8.3.4 Data handling

The PLATO payload data processing system consists of several DPUs connected to two ICUs working in cold redundancy through a SpaceWire network. The ICUs are connected to the SVM through SpaceWire links. Each telescope has its own **DPU**. There are 40 normal telescope DPUs. Each normal telescope DPU is

responsible for processing the data (of samples 1, 2, 3, 4, 5) of one normal telescope. The sampling time for normal DPUs is 25s. There are 2 fast telescope DPUs. Each fast telescope DPU is responsible for processing the (sample 3 and 4) data of one fast telescope. The sampling time for fast DPUs is 2.5s. In observation mode, the role of **ICU** is to detect and remove outliers by comparing the measurements from the telescopes sharing the same LoS. It also stacks the flux and centroids for each telescope of selected data. Furthermore it computes for each telescope the mean and the standard deviation of the stacked flux and centroids measurements at a cadence depending of the sample category of either 50 sec. or 600 sec.. It then compresses the data before transmitting them to SVM.

The role of the ICU in configuration mode is mainly to provide to the DPUs certain configuration parameters like e.g. catalogue, to schedule the DPU tasks, to manage the data flow, and to perform cross checking operations between data from telescopes of the same LoS.

The power consumption of each element is shown in **Table 8.13**.

8.3.5 Structures

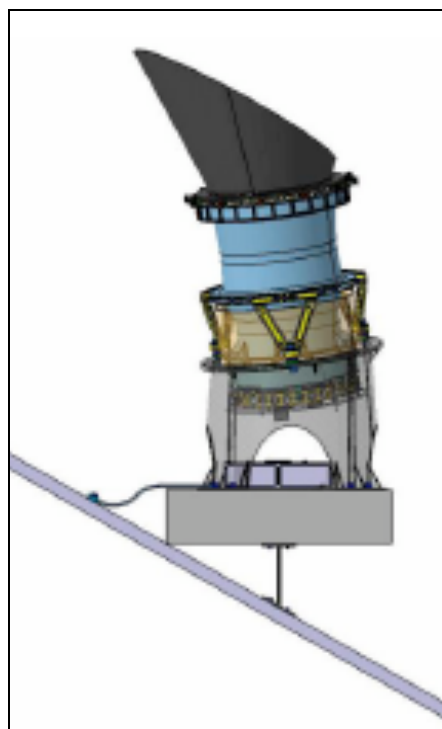


Figure 8.18: Top to bottom: telescope in blue with its three legs (in yellow), skew spacer, optical bench and thermal bus, supported by the optical bench through a hanging blade. On the left, the thermal braid connecting the FEE to the thermal bus.

The mechanical structure of the instrument has the followings **constraints**:

- **Mechanical constraints:** support the 42 telescopes separated in 5 sub-groups (4×10 normal and 1×2 fast), ensure a non-vignetted FoV for all telescopes, provide the common orientation of each telescope in a sub-group and its required stability, provide the adequate orientation of each telescope sub-set, and its needed stability.
- **Stray-light constraints:** the upper edge of the sunshield is illuminated by the Sun, and therefore must not be seen by the inside of the individual baffles.
- **AIV constraints:** access for sub-assembly mounting, electrical and thermal connections..., telescopes alignment verification.
- **Thermal constraints:** support of the cooling system for the analogue electronics boxes, take into account the thermal needs of the two fast telescopes, which are higher than those of the normal telescopes.

The telescopes are mounted on a stair-shaped optical bench in order to avoid vignetting of the telescopes close to the sunshield (see *Figure 8.18*).

The selected concept is based on an octagonal frame, supporting the optical bench (OB) in 8 separate steps. Each step supports from 2 to 7 telescopes. Several struts interface with the SVM and support the PLM frame. They also ensure a thermal decoupling between the payload and the SVM. Their number is not yet fixed because it depends on the interface with the SVM. Some preliminary studies were made based on different scenarios for an evaluation of their mass.

The power dissipation is provided by thermal buses under the optical bench, with heat-pipes increasing the efficiency of these thermal buses. These buses are thermally connected to the radiator panel located on the shadow side of the instrument, thanks to thermal braids and will transport the heat away from the electronic units. The frame is an "I-beam" in CFRP, while the OB is aluminium honeycomb with CFRP composite skins. In this Design Concept study, the **sunshield** and a possible **sunshield cover** were not studied as this depends on the design of the Service Module. However, the sunshield that was designed during ESA's CDF study ("Review of the optical design of the PLATO payload", ESA, Ref.: TEC-MMO/2009/52, version 1.1, July 2009) was considered during the stray light analysis. It was found that the upper edge of the sunshield is illuminated by the Sun, and therefore should not be observable from the inside of the individual telescope baffles. Also, the radiator panel is considered structurally included in the sunshield, but thermally isolated from it. The telescopes are mounted on the optical bench with skew spacers. The associated electronic boxes, mounted on the optical bench, and thermally connected to the PLM radiators. Each telescope is mounted on its skew spacer by way of three legs. The skew spacer gives the tilt angle of 10° in the appropriate direction according to the overlapping concept. The FEE box, connected to its telescope by the flex cables, is placed inside the spacer. Both are screwed on the OB, and a thermal braid provides the thermal connection of the FEE to the thermal bus running under the OB. The thermal bus is supported by the OB thanks to flexible hanging blades. The axis-symmetrical design was chosen because it is easier to align than an off-axis mirror design. The correct alignment of the telescopes and its stability will be verified by photogrammetry on the entire instrument.

Table 8.14 shows the structural elements of the PLM and the corresponding mass in kg.

Table 8.14: Mass of structural elements.

Item	kg per unit	Quantity	Total mass [kg] (without margins)
Frame	70.0	1	70
Optical bench	70.0	1	70
Skew spacers (prelim. design)		40+2	45.8
I/F struts	45.0	1	45
Thermal equipment	35.0	1	35
Total structure			265.8

8.3.6 Thermal sub-system

The FPA is set to operate at ~190K. To achieve this, the FPA is thermally linked to the telescope optical unit, which consists of a barrel and lenses. An active heating control has been implemented to manage the correct de-focus of the optics and to avoid very sharp PSFs which would increase the susceptibility to jitter effects and pixel saturation. The FEEs are attached to the optical bench and thermal links to the FPA and telescope are minimized.

8.3.7 Operating Modes

At the **payload data processing** level, four main modes can be distinguished:

Standby Mode: In this mode, some maintenance operations can be done, like software upload, etc.

Calibration Mode: In this mode, imagerettes and full-frame images can be acquired for calibration and test purpose. A number of additional calibration activities will have to be considered at occasional points during the mission. Note that this design does not foresee a cover and certain calibration measurements, like flat fields or dark fields, will have to be obtained differently. This is TBD. In most cases one can assume that the FPAs are read out in normal sequences, and that data taking and selection is the main difference between calibration science data acquisition.

Configuration Mode: During this mode, background and PSF are measured and the photometric masks are computed. The configuration mode will be effective at the start of every new pointing and each time the line of sight was temporarily lost.

Observation Mode: This is the normal mode of operation during which the data are acquired and transformed into light curves, to be down linked to the ground. There are two distinct data flows: one from the "normal" telescopes and one from the "fast" telescopes. The observation mode can be started as soon as the windows and the photometric masks are attributed. The main tasks performed in this mode are: a) calculating intensities and centroids; b) acquiring imagerettes; c) providing angle error measurements to SVM AOCs at a 2.5s cadence. Data for sample #1 are collected every 50s. Sample #2 data are collected at a 600s cadence.

As this design covers only the P/L part of a potential PLATO S/C, no information on **manoeuvres** is available.

8.3.8 Interface requirements

For the electrical architecture standard interfaces (e.g. SpaceWire) are used as much as possible.

Radiation does calculations depend strongly on the exact mission design. As this study focussed on the payload design only, exact radiation doses are not available. However, it is recognized that radiation damage mitigation measures need to be taken. They include e.g. radiation hardened glasses and latch-up protection circuitry for ADCs. A more detailed radiation analysis will be performed in a possible future phase.

8.4 Instrument Performance Model, Performance Prediction and Compliance

8.4.1 Instrument Performance

Each study has produced an instrument performance model (IPM) in order to evaluate the science results in terms of number of stars with the correct photonic accuracy. These IPMs take non-photonic noise sources such as satellite jitter, ageing effects and saturation of CCD pixels etc into account. The satellite jitter gives rise to "jitter-confusion effects". Due to minute, unwanted satellite movement (jitter), the PSF of the target stars will slightly move on the FPA. This gives rise to three effects:

- 1) When the PSF moves across the pixels in the target aperture mask, the output signal will change due to pixel response non-uniformity (PRNU) effects
- 2) If the PSF moves outside the aperture mask, the total signal will drop since the flux outside the mask will not be counted when the signal from the mask is read-out
- 3) Due to the jitter, background stars just outside the edges of the mask could come into view and give rise to extra, parasitic flux.

On top of these effects, there are also stars which will be lost due to static confusion in which there is a background star very close to the target star and the fluxes from these two sources cannot be separated (see section 2.3.4.). This makes it impossible to reach the required photometric accuracy for the target star and this is therefore lost. Taking into account all of these effects, the designs need to be able to observe more stars than the science requirements state since a certain percentage of the stars will be lost due to confusion,

which is relevant for fainter stars, and saturation, which is relevant for brighter stars. These effects are strongest when binary mask photometry is used. In these masks, the entire signal is collected from the pixels within the mask, and no signal is collected of pixels outside the mask. The use of weighted mask photometry would alleviate some of the issues related to confusion since pixels at the edges of the mask, or pixels that contain a parasitic background star, could be given less weight and thus the photometric accuracy could be achieved in a target that would otherwise be lost to confusion effects.

The results of these IPMs show that all designs are compliant with the science requirements of the most important sample 1 and mostly compliant with the requirements of the other star samples. In **Table 8.15** all sample 1 stars which can be observed with the respective concepts are listed. These numbers are results of the respective Instrument Performance Models.

Table 8.15: Observable sample 1 stars for each concept.

Concept	Observed sample 1 stars	Expected valid stars
A	23 900	22 010
B	23 200	20 800
C	23 000	21 000

8.4.2 Compliance Matrix

The following table demonstrates the compliance.

Table 8.14: Compliance matrix for the three designs.

Requirement	Compliance (Y/N)	Rationale and/or Comments	Value achieved by design A	Value achieved by design B	Value achieved by design C
Mission Requirements					
To stay below the maximum launch mass for the Soyuz Fregat 2B. In the PLATO case it is 2140 kg incl. all margins an adapter.			2140 kg (incl. all margins)	2093 kg (incl. all margins)	1098 kg (996 kg allowed)
To comply with the payload power requirement			969 W (incl. all margins)	887 W average 952 W peak (incl. all margins)	670 W (incl. all margins)
PLM output data rate (...telemetry rate...)	Y/Y/Y	All designs meet the minimum requirements	OK	OK	OK
Science requirements					
Sample 1: To observe a minimum of 20 000 dwarf stars later than spectral type F5 with the photonic noise level below $2.7 \cdot 10^{-5}$ in one hour for longer than 2 years.	Y/Y/Y	These are the numbers of stars which can be observed with the required accuracy.	23 900 ($m_v \leq 10.3 \text{ mag}$)	23 200	23 000
• The sampling time for intensity measurements must be shorter than 50 sec.	Y/Y/Y	sampling time (integration time/readout time)	30 s (28.5/1.5)	25 s (22.5/2.5)	25 s (23.0/2.0)
• The sampling time for relative astrometric measurements must be shorter than 600 seconds.	Y/Y/Y				
Sample 2: To observe a minimum of 80 000 dwarf stars later than spectral type F5 with the photonic noise level below $8 \cdot 10^{-5}$ in one hour for longer than 2 years.	Y/Y/Y		374 000 ($m_v \leq 11.6 \text{ mag}$)	400 000	316 000
• The sampling time for intensity measurements of stellar sample 2 must be shorter than 600 sec.	Y/Y/Y				
• The sampling time for relative astrometric measurements of stellar sample 2 must be shorter than 600 seconds.	Y/Y/Y				
Sample 3a: To observe a minimum 1000	N/N/Y		1000 ($m_v \leq 8.4 \text{ mag}$)	1000 ($m_v \leq 8.5 \text{ mag}$)	1350 ($m_v \leq 8 \text{ mag}$)

Sample 3a: To observe a minimum 1000 dwarf stars later than spectral type F5 with a photonic noise level below $2.7 \cdot 10^{-5}$ in one hour for longer than 2 years. The dynamic range of stellar sample 3 shall be $m_v \leq 8$.	N/N/Y		1000 ($m_v \leq 8.4 \text{mag}$)	1000 ($m_v \leq 8.5 \text{mag}$)	1350 ($m_v \leq 8 \text{mag}$)
Sample 3b: To observe a minimum 300 dwarf stars later than spectral type F5 with a photonic noise level below $2.7 \cdot 10^{-5}$ in one hour for longer than 2 years in colour . The dynamic range of stellar sample 3 shall be $m_v \leq 8$.			305 ($m_v \leq 7.7 \text{mag}$)		
<ul style="list-style-type: none"> The sampling time for intensity measurements must be shorter than 50 sec. 	Y/Y/Y	sampling time (integration time/readout time)	6 s	2.5 s (2.25 s/0.25 s)	2.5s (2.3 s/0.2 s)
<ul style="list-style-type: none"> The sampling time for relative astrometric measurements must be shorter than 600 seconds. 	Y/Y/Y				
Sample 4: To observe a minimum 3000 dwarf stars later than spectral type F5 for longer than 5 months with the photonic noise level below $2.7 \cdot 10^{-5}$ in one hour.	Y/Y/Y		11 900 ($m_v \leq 9.24 \text{mag}$)	3515	2700/5000 (one/two year step & stare)
<ul style="list-style-type: none"> The sampling time for intensity measurements must be shorter than 50 sec. 	Y/Y/Y				
<ul style="list-style-type: none"> The sampling time for relative astrometric measurements must be shorter than 600 seconds. 	Y/Y/Y				
Sample 5: To observe a minimum 250 000 dwarf stars later than spectral type F5 for longer than 2 years.	Y/Y/Y		374 200 ($m_v \leq 12.6 \text{mag}$)	379 700	316 000
<ul style="list-style-type: none"> The initial sampling time of stellar sample 5 must be shorter than 600 seconds. 	Y/Y/Y				
<ul style="list-style-type: none"> The sampling time of targets in stellar sample 5 after a first transit detection 	Y/Y/Y				

9 MISSION DESIGN

9.1 Maximising Observed Number of Stars

The PLATO mission has been designed to achieve the maximum scientific output (further described in section 3.3) while trying to minimize the technical complexity in order to reduce risk and cost, as well as complying with Cosmic Vision 2015-2025 M-class boundaries [for Cosmic Vision description see http://www.esa.int/esaSC/SEMA7J2IU7E_index_0.html]. The different spacecraft design concepts used requirements set up in the PLATO Mission Requirements Document and the PLATO Science Requirements Document to define the design constrictions. Each overall design is presented in this section on a global level in general and the satellite platform (Service Module) in particular. For details on the payload of each design concept, please refer to chapter 7.2.

Since the detection of exoplanets is of a statistical nature due to the fact that the percentage of stars with exoplanets is unknown, PLATO will need to observe as many stars of the necessary accuracy and type, as possible. This can be achieved via three main methods:

- 1) *As large FoV as possible* – as the observed sky field increases, more stars can be observed in the field-of-view
- 2) *As large collecting area as possible* – a large collecting area results in observing more faint stars with the required accuracy.
- 3) *Long mission lifetime* – a long mission lifetime allows for several sky fields to be observed during several years.

While the third driver is related to cost issues and increased risk (degradation of components), the first two points are difficult to combine. During the ESA internal pre-assessment study [CDF REPORT CDF-70(B)], the best observation strategy was determined to be the “staring” concept as opposed to a GAIA-like spinning concept [for information on GAIA see http://www.esa.int/esaSC/120377_index_0_m.html]. Using this concept, the observations are conducted using several individual telescopes of smaller size in order to comply with the demanding requirements on large FoV and large collecting area. Using a higher number of sub-apertures gives several advantages compared to using one large aperture; it allows meeting the stringent requirements in terms of signal-to-noise and the large sky field size required to observe enough stellar targets. It also achieves a higher level of redundancy since the loss of a telescope will reduce the signal-to-noise ratio, but will not cause the mission to fail.

9.2 Mission Profile

The current mission scenario is to launch PLATO using a Soyuz 2-1b launcher, which will inject the spacecraft in a direct transfer orbit around the Sun-Earth second Lagrange point, L2, with a transfer orbit inclination of 5.3 degrees. The orbit, selected for maximising spacecraft mass (less delta-v required and hence less propellant) is a large amplitude libration orbit with 500.000 km and 400.000 km axes. An example of such an orbit is seen in Figure 9.1. For this type of orbit, the launcher has a capability of ~ 2140 kg (Mellado and Hechler, 2007, ESA working paper 503) L2 was chosen for its stable ambient environment in terms of temperature, radiation, possibility to have eclipse-free orbits and un-obstructed view of large parts of the sky (Sun, Earth, moon are all located in a relatively small solid angle).

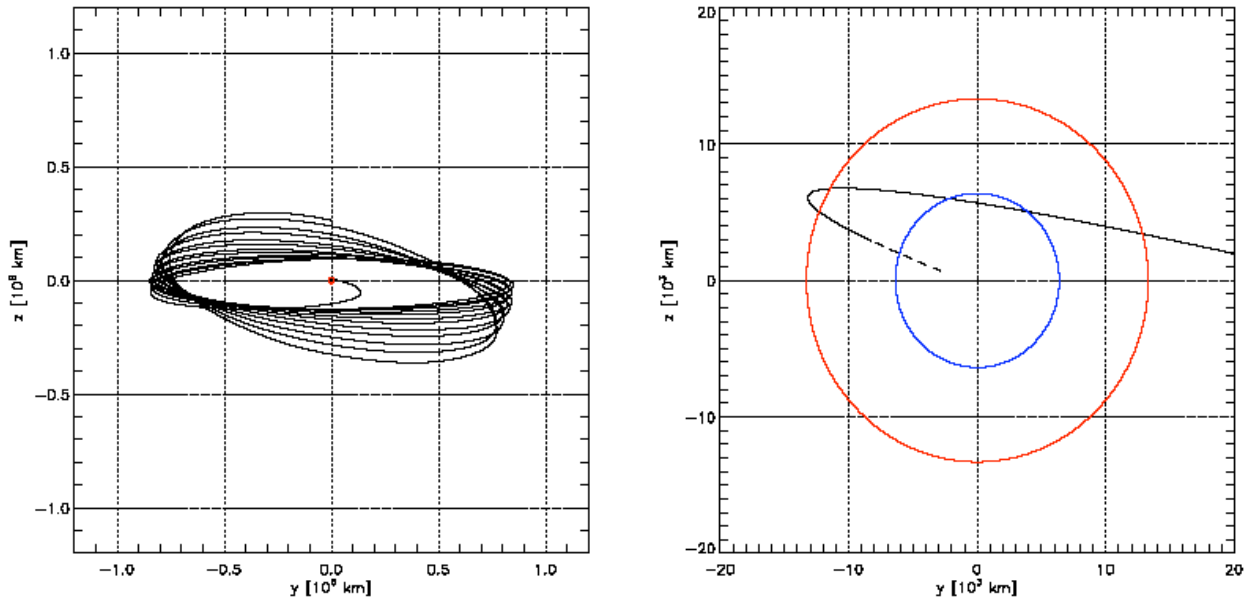


Figure 9.1: Reference orbit projected in the y - z plane of the co-rotating frame following a launch on 3 September 2017, 12:38:42UT in large (left) and small (right) scale. The red circle represents the size of the Earth's pen-umbra at L2 and the blue circle the Earth's shape. The dashed part of the trajectory is on the Earth's day-side.

9.3 Mission Scenario

The mission is foreseen to have a nominal lifetime of 6 years, which is divided into three different phases. The first two phases are used for long-duration observations, each observation focusing on a particular part of the sky which is expected to contain a high density of cool dwarfs. These sky fields are assumed to be around ecliptic longitude and latitude of 210° and -60° respectively, which is close to the galactic plane. The duration of each of these observations is several years, in order to repeatedly observe transits with orbital periods similar to the Earth. This is necessary to reduce the likelihood of flagging false transits because there can be other reasons for detection of changes in the stars brightness, either naturally occurring in the star, the stellar environment (e.g. background objects), or artificially induced in the spacecraft payload. The last phase will be a step&stare phase where several different fields with interesting scientific targets will be monitored for a period of several months each. The exact duration of each phase will be consolidated in the following phase, should PLATO be selected. The long-duration periods will be between 2-3 years with the possibility to have one long-duration observation of 3 years and the second of 2 years. The step&stare-phase will be at least one year long.

In order to continuously observe each sky field for a period of several years, the spacecraft needs to be 3-axes stabilized and needs to be able to rotate around the payload line-of-sight in order to keep the sunshield and solar arrays oriented towards the sun to avoid impinging sunlight on the payload and secure adequate power production. The communication system will also need a steerable antenna to compensate for the different angular positions of the Earth compared to the spacecraft as it orbits in the large amplitude libration orbit around L2. The foreseen ground station is New Norcia in Australia with its 35-meter antenna. Due to the large brightness range of the stellar targets ($4 < m_v < 14$) that PLATO would observe, it was decided to have dedicated telescopes or CCDs for the brighter stars in stellar sample 3 and 4. The dedicated CCDs will operate with much shorter integration times and are operated in frame-store mode. This means that only half of the active area is used for receiving flux, while the other half – the storage section – is covered with a light-shield. After the integration is completed, the charges are moved to the covered, second half, of the CCD while the first half starts receiving flux in a new integration period while the shifted charges are read out. This speeds up the read-out procedure since only half the active area is used for observation and integration and read-out occur at the same time, albeit on different halves of the CCD. As a result, twice as many CCDs are needed to cover the same area as nominal CCDs for samples 1, 2, and 5. However, since the numbers of stars needed in these bright star samples are limited, only around a dozen of the bright CCDs are needed. Observing the bright stars with the same CCDs as the other star samples would have led to

saturation of these stars. The requirement for sample 3b to observe in two different wave-bands (red and blue) simultaneously for the same targets requires the CCDs to be equipped with colour filters. These criteria can be fulfilled in a number of ways as discussed in the following sections.

9.4 Design Concept A

9.4.1 Observation Strategy

One of the proposed designs is based on a bi-annual rotation of the spacecraft around the payload line of sight in order to keep the payload protected from the sun while continuously observing the same stars. This necessary rotation is possible because this particular optical design has one axis of symmetry when the FoV is projected onto the focal plane array (FPA). It has a split field-of-view which means that half of the sub-apertures (individual telescopes) are observing one sky field (sub-field 1) and the other half is observing another sky field (sub-field 2) across the line of symmetry of the FoV. When the spacecraft is rotated after 6 months, the telescopes that observed field 1 are now observing field 2 and vice versa. In this way, the entire field (sub-field 1 + sub-field 2) can be observed simultaneously and for a long-duration, with only minor interruptions in the science operations for orbit control and bi-annual rotation manoeuvres. See section 8.1.1 for an explanation on the split-field strategy.

9.4.2 Service Module and Spacecraft Sub-systems

The Service Module (SVM) contains all sub-systems that are needed for the spacecraft to function and operate. They are the propulsion sub-system, general data handling system (DHS), AOCS, communications, power sub-system, electrical sub-system, structural design, thermal control as well as some of the data processing units belonging to the payload to facilitate thermal control of the payload (as described in relevant payload sections).

9.4.3 Structural Design

Since the SVM has to support the heavy PLM during the launch, with heavy longitudinal and lateral loads, the structural design for all proposed designs of PLATO, is important in order to optimize structural integrity while still maximizing available mass to the payload.

The SVM design is based on design heritage from GAIA and has been tailored to fit specific needs of PLATO. The SVM is connected to the payload module (PLM) via bipods which are mounted on 6 hard-points on the SVM and 12 on the PLM. Since the SVM has to support the heavy PLM during the launch, with heavy longitudinal and lateral loads, the structural design is important in order to optimize structural integrity while still maximizing available mass to the payload. One commonality from GAIA is the need for a deployable sunshield. The number of individual telescopes, as well as their physical sizes, leads to a possible large loss of FoV due to vignetting of the telescopes if a fixed sun-shield were used that would fit within the Soyuz fairing diameter. A sun-shield is required to protect the telescopes from impinging sun-light and to keep the payload assembly at the proper, cold, operating temperature. PLATO's sunshield (for design concept A) would only be partially deployable (Figure 9.2) to avoid vignetting and would therefore be fixed in a cone-shape.

9.4.4 Propulsion and Attitude and Orbit Control Sub-systems

In order to handle the attitude and orbit control sub-system (AOCS), the sub-system in this design uses several modes; orbit control mode, coarse pointing mode, normal mode and acquisition and safe mode. All modes except the Nominal Mode use the Chemical Propulsion System (CPS) as actuator. The Nominal Mode uses the micro-propulsion system (MPS) to control the attitude. The CPS is using mono-propellant Hydrazine. It is used for orbit control and for slewing between the different phases of the mission. The foreseen baseline is to perform orbit manoeuvres every 30 days to optimise the delta-v requirements as well as maximising the time allocated in science mode. The total delta-v for a 6 year mission (including 5% margin) is 69 m/s. The total fuel is 71.4 kg located in one equatorially mounted tank. There are 20 CPS thrusters (10 pairs), with 10N+10N force.

PLATO uses the micro-propulsion system of GAIA in order to fulfil the stringent pointing and stability requirements set up for the mission. A number of different sensors are used to provide input to the AOCS such as sun sensors, star trackers, IMUs. For science observations, the payload telescopes themselves are used as Fine Guidance Sensor (FGS) to be able to obtain a high pointing and stability accuracy. The current RPE requirement is ~ 0.2 arcsec (rms) or better over a period of 14 hours. The MPS is able to achieve even higher accuracies than this, in case of evolution of the requirements in possible later study phases.

9.4.5 Power and Thermal Sub-systems

Due to the bi-annual rotation, a deployable solar array is needed. The solar array is steerable (1 degree-of-freedom) to allow for maximum impinging sun-light during the six months period between spacecraft rotations. During launch it is stacked on the side of the SVM, and during operations it deploys underneath the SVM. The efficiency of solar cells have a BOL efficiency of 28% with a required area of $\sim 8 \text{ m}^2$ (current configuration allows for an area of up to 8.5 m^2). EOL power is estimated to $\sim 1770 \text{ W}$ (before slip ring; no off-pointing of solar array). The battery sizing is driven by the launch-and-early-operations-phase and the safe mode during operations. It is of Lithium-Ion type and is sized for 93Ah. The power architecture is based on a regulated 28V bus.

The SVM thermal design driver is to keep the temperature stable at PLM interface during science operations at a few degrees over ~ 14 hours (science req.). The main influences are impact of data downlink mode in the short-term perspective, and the different heat input from the sun over the course of the 6-month observation period between spacecraft rotations as well as temperature drift during lifetime due to radiator degradation. The heat transport within the SVM is done via conduction and the excess heat is expelled via radiators on cold part of the lateral area as well as a panel radiator on the bottom of the SVM.

9.4.6 Communications and Data-handling Sub-systems

One effect of the bi-annual rotation is the need for two steerable high-gain antennae (2 degrees-of-freedom) in order to guarantee contact with Earth. Due to the large out of plane angles incurred by the large amplitude orbit, the required coverage range of the steerable antennae need to be $\pm 50^\circ$ in elevation and $\pm 120^\circ$ in total azimuth due to the bi-annual rotation scheme selected. Since there are two high-gain antennae (HGA), each covering half the rotation period (3 months), each antenna need to cover $\pm 60^\circ$ in azimuth. This means that only one HGA is active at any time. The communication system includes dual transponders which can be switched between low-gain antennae (LGA) and HGA. Two LGA provide spherical coverage in case of spacecraft loss of attitude / safe mode operations. The proposed modulation is GMSK with a Reed-Solomon coding scheme. The communication system will utilize the X-band with a maximum data transfer rate of $\sim 8.7 \text{ Mbps}$.

The data handling system onboard the SVM is also based on GAIA heritage, using a standard ERC32 processor and EIU from GAIA. This could be replaced with a LEON-2 processor in the future without significant impact in mass and power budget. The DHS is the central processing platform for on-board Software (SW) and handles telemetry and telecommand to and from the transponders; controls the redundant MIL1553B buses; handles FDIR as well as AOCS SW and thermal control. There is no dedicated Mass Memory Unit in the SVM, since the science data is stored in the de-centralised data processing architecture in conjunction with the DPUs.

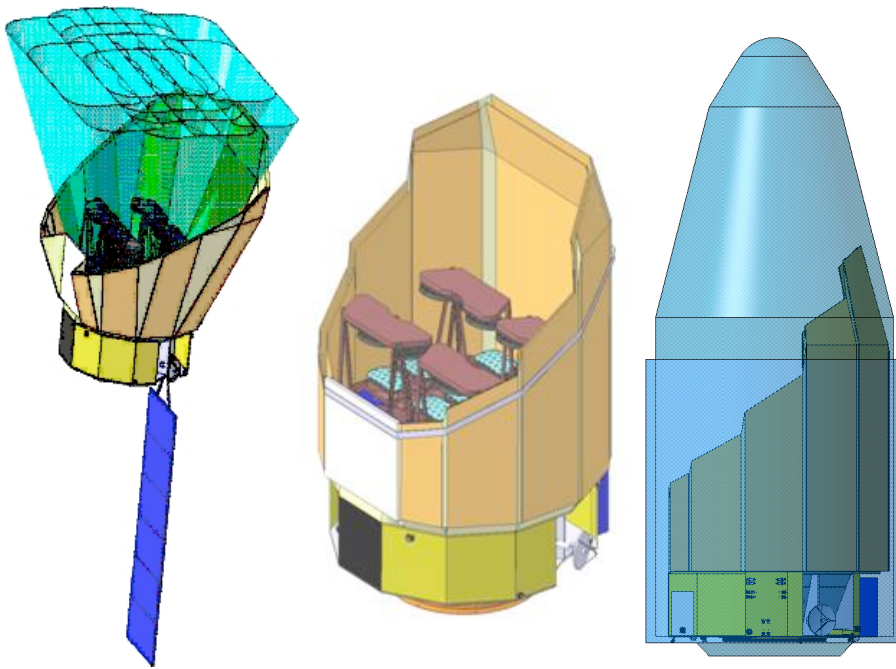


Figure 9.2: (Left) Schematic figure of PLATO design concept A, with deployed sunshield, deployed solar array and the virtual FoV cones projected on the sky. (Middle) Spacecraft during stacked launch configuration with the four telescope modules visible. (Right) Spacecraft in launch configuration inside Soyuz 2-1b fairing. The folded solar array is visible to the left in blue.

9.5 Design Concept B

9.5.1 Observation Strategy

Another proposed design is based on a monthly rotation (30°) of the spacecraft around the payload line-of-sight. This is possible because the FoV is circular and. The FoV is ultimately en-squared by the CCDs which are placed in a square configuration on the FPA. The circular FoV means that any degree of rotation around the line-of-sight is possible without interruption of the continuous observation of the stars. The monthly rotation to keep sunshield and solar arrays aligned towards the sun, means that less propellant is used for orbit control since the rotation manoeuvres are smaller.

9.5.2 Service Module and Spacecraft Sub-systems

The basic SVM structure has some design heritage from the Herschel platform, but has been modified, scaled and updated for PLATO needs. The SVM contains all sub-systems that are needed for the spacecraft to function and operate (see heading 9.4.2 for a list of the different sub-systems).

9.5.3 Structural Sub-system

Due to the different launchers used for PLATO (Soyuz 2-1b) and Herschel (Ariane 5) the SVM design need to be tailored towards the smaller dimensions in the Soyuz 2-1b launcher compared to Ariane 5. The design is based on an octagonal shape. The bulk of the payload mass is in the tilted base plate with the individual telescopes mounted on it. That structure is connected to the SVM thrust cone (a central cone that is designed to carry most of the loads from the PLM mass during launch) via three CRFP bipods with 3 connections on the SVM and 6 on the tilted base plate (see Figure 9.3). There is a bottom panel belonging to the PLM which is used to mount PLM data processing units. This panel has no structural function; it is primarily intended to simplify AIV of the data processing units onto one single panel. It is located just above the top panel of the SVM and so is also considered to be at room temperature.

Due to the circular FoV, monthly rotations around the payload LoS can be achieved. This means that the sunshield does not need to surround the entire PLM since the payload will still be protected from impinging

stray-light and excessive heat radiation using a Herschel-like sunshield shape. This also means that no deployable solar array is needed.

9.5.4 Propulsion and AOCS Sub-systems

This design uses several AOCS operating modes to fulfil the required stability and pointing during different phases of the mission. They are: sun acquisition mode, Science Mode, Orbit and Cruise Control Mode, Wheel Unloading and Safe Mode. The total delta-v including launcher injection manoeuvres and orbit correction manoeuvres is 49.3m/s including 10% margin. The CPS uses Hydrazine as mono-propellant, which is contained in two propellant tanks. The total propellant mass is 78kg, including propellant used to off-load RW. There are 8+8 thrusters of 20N coupled in 8 pairs connected to the CPS.

The sensors used to fulfil the AOCS requirements are sun acquisition sensors, gyroscope assembly, coarse rate sensor assembly and autonomous star trackers. This design also uses the payload telescopes as a FGS and feeds input to the AOCS control loop. As Science Mode actuator it uses a Reaction Wheel System. Four 30 NMs RWs are used as baseline, which need to be off-loaded not more frequently than 2 days.

9.5.5 Power and Thermal Sub-systems

The solar arrays are body-mounted on the sun-shield and SVM lateral sides at $\pm 45^\circ$ as shown in Figure 9.3. 3 panels are located on the sunshield and 3 panels on the SVM. Due to the spacecraft orbit around sun there is a $\pm 15^\circ$ difference in longitudinal angle towards the sun, since the spacecraft is reoriented every month (equal to 30°). The total area of the arrays is 13.2 m^2 in total and the collar cells provide 28% efficiency at beginning-of-life. The maximum power usage from spacecraft is $\sim 1700\text{W}$. The battery sizing is driven by LEOP and safe mode. It is of Lithium-Ion type and is sized for 22.5Ah. The power distribution is done via a regulated 28V bus.

The SVM thermal design driver is to keep the temperature stable at PLM interface during science operations at a few degrees over ~ 14 hours (science req.). The main influences are impact of data downlink mode in the short-term perspective, and the different heat input from the sun over the course of the observation period between spacecraft rotations as well as temperature drift during lifetime due to radiator degradation. The heat transport within the SVM is done via conduction and the excess heat is expelled via radiators on the SVM.

9.5.6 Communications and Data-handling Sub-systems

Due to the large out of plane angles incurred by the large amplitude orbit, the required coverage range of the steerable antenna need to be $\pm 50^\circ$ in elevation and $\pm 45^\circ$ in azimuth. Thanks to the monthly rotation, it is sufficient to have one high-gain antenna since the attitude towards the Earth is within the capability of the steering mechanism. There are two low-gain antennaes with spherical coverage in case of spacecraft loss of attitude / safe mode operations. The communication system includes dual transponders which can be switched between LGA and HGA. The proposed modulation is GMSK with a Reed-Solomon coding scheme. The communication system will utilize the X-band with a maximum data transfer rate of ~ 8.7 Mbps.

The general DHS is managed by a single CDMU based on a LEON2FT processor. It handles telemetry and telecommand to and from the transponders; controls the redundant MIL1553B buses; handles FDIR as well as AOCS SW and thermal control. There is a Spacewire link for data science acquisition and storage. There is a centralized Mass Memory Unit (MMU) based on flash memory. It is sized to store all data over a 48 hour period (if one daily ground station contact is missed).

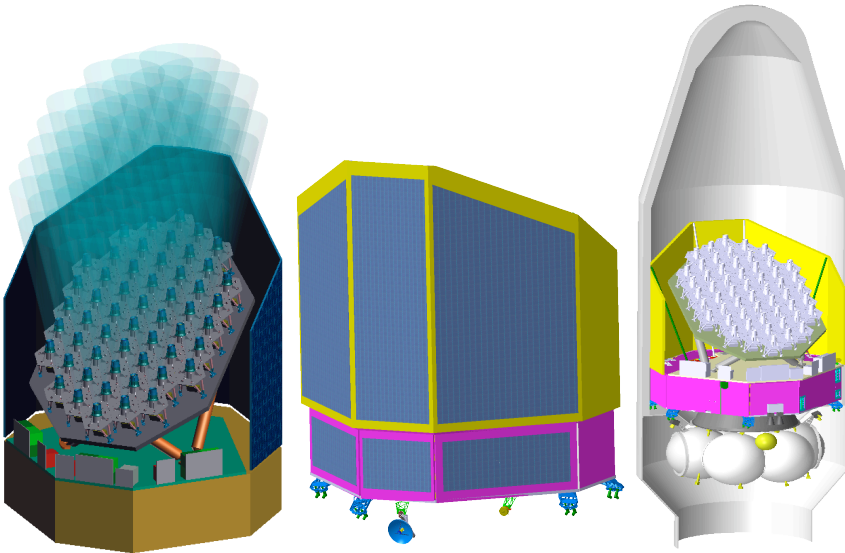


Figure 9.3: (Left) Schematic figure of PLATO design concept B, with the individual telescopes mounted on the tilted base plate Visible. (Middle) Showing the solar arrays mounted on the sunshield and on the SVM. (Right) Spacecraft in launch configuration inside Soyuz 2-1b fairing, including the Fregat upper stage below SVM.

9.6 Design Concept C

9.6.1 Observation Strategy

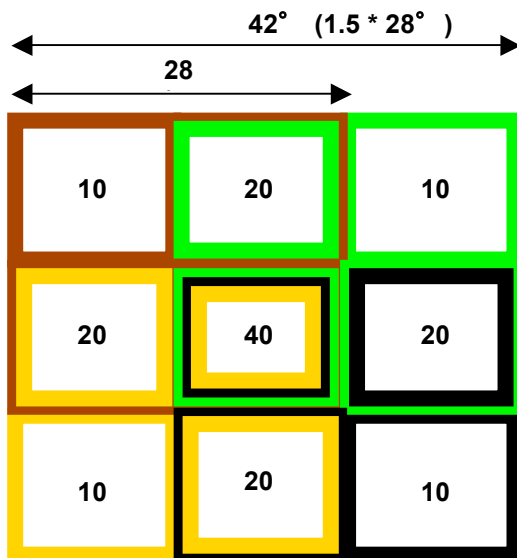


Figure 9.4: Schematic figure of the overlapping FoV for the 4 groups of telescopes. The result is 9 squares with different collecting areas depending on the number of telescopes observing that particular part of the sky. The numbers represent how many telescopes are observing that particular sky field square.

The third proposed design is based on a quarterly (90°) rotation around the LoS. This is due to the fact that the Focal Plane Array (CCDs) is square.. To be able to continuously observe the same targets, the spacecraft needs to be reoriented every 3 months to be coherent with the 90° symmetry of a square. Another difference to design concepts A and B is the fact that the telescopes are divided into four separate groups which look at partly overlapped sky fields. The FoV of each group of telescopes is offset by 50% per axis, resulting in a total FoV of $\sim 1800^\circ$. This can be divided into 9 squares with different collecting areas (Figure 9.4). Since

the central square is seen by all telescopes, it allows to re-observe interesting targets during the step&stare phase with a higher collecting area and thus with a higher photonic signal-to-noise.

9.6.2 Service Module

The scope of the instrument assessment study conducted by the PPLC only included the payload segment (see chapter 8.3). General allocations in terms of mass, power, volume and data rate were given by ESA constituting an estimated payload provision of the global spacecraft budgets. The allocated mass budget for the payload was 830 kg excluding any margin (this includes the telescopes, optical bench and all payload-related electronics). The power allocation given was ~700 W without any margins

9.7 Budgets Summary

This section summarizes the following for the 3 concepts:

- Mass budget
- Power budget

Due to differences in what is incorporated in each subsystem among the contractors and PPLC only top level figures are presented.

9.7.1 Mass Budget

The mass values listed in *Table 9.1* are the so called nominal mass values which are the basic mass values plus a “maturity mass margin” that ranges between 5-20% depending on the design maturity (if the component can be considered new development or recurring item) according to ECSS-E-10-02A. On top of this, a 20% system margin is applied on the total dry mass (excluding propellant and launch adapter). The table has divided the mass into different subsystems such that an overall comparison is possible, even though the concepts might include different elements in each subsystem or list them in another subsystem. This is why some mass values might seem low in one subsystem for a particular contractor. Since the overall PLM mass values are similar (apart from PPLC), it means that this “missing” mass is listed in another post and thus the difference will even out. Since the PPLC did not study the whole space segment, but rather just the telescopes and the optical bench, there is no total mass value listed for the PPLC concept. The propellant value for Contractor A includes both chemical propulsion system as well as the micro-propulsion systems used as actuator for attitude control. The thermal post in Contractor B is small due to the fact that each telescope has an individual integrated radiator that has been accounted for in the instrument mass. The low number for the electronics for Contractor A is due to the fact that some electronics have been accounted for in the instrument post. The mass value listed for PPLC includes a 20% design maturity margin for all posts. The mass values provided to ESA by the PPLC were excluding any margins. This is due to the fact that the mass provision for the payload of ~830kg was in turn provided without margin to the PPLC by ESA at the start of the study. This mass value was obtained by looking at initial launch mass values for the PLM provided by the contractors and then removing the system margin as well as the maturity margin.

Table 9.1: Summary of mass budgets in kilograms for each concept.

Design Concept	A [kg]	B [kg]	C [kg]
Instruments	651	571	504
Structure (excluding structure of telescopes, but including baseplate and PLM/SVM interface)	125	223	231
Thermal	67	14	44
Electronics	38	161	133
Total PLM	881	969	1094
Structure	252	236	
Thermal	23	28	
AOCS	80	54	
RCS	27	40	
Power (including photovoltaic assembly and structure)	94	49	
Harness	59	50	
Electronics/Communications	85	63	
Total SVM	620	519	
Sunshield	98	115	
Total dry mass	1599	1604	
System Margin	320	321	
Propellant	76 + 56	78	
Launch adapter 1666	90	90	
Launch mass	2141	2092	
Requirement	2146	2146	
Delta-mass	-5	-54	

9.7.2 Power budgets

This section provides an overview of the power budgets provided by the different designs. As the foreseen spacecraft modes and subsystems are not homogenous across the different designs, only an overview with the main values is listed. Two values are listed: a peak power value (maximum power usage, usually during data downlink) and during nominal science operations. They are given for the instrument (PLM) only and for the whole spacecraft (including the PLM contribution). For PPLC, only the PLM values are listed due to the fact that the SVM was outside the scope of the instrument study. The values listed **include** a 20% system margin. For Contractor A (concept A), the peak power is equal to the nominal operations mode.

Table 9.2: Peak power usage and power usage during nominal science operations for the different design concepts. [W]

Design concept		A	B	C
Peak Power	PLM	888	1142	804
	Total S/C	1497	1711	N/A
Nominal Science Mode	PLM	888	1142	804
	Total S/C	1373	1695	N/A

9.7.3 Link budgets

The downlink data rate was given to all parties to be used as a baseline. The provision for data downlink to ground, is that the X-band (10MHz bandwidth) shall be used with a maximum data rate of 8.7 Mbps using Gaussian Minimum Shift Key modulation (GMSK). This modulation is not compatible with ranging so a different modulation scheme needs to be used when performing ranging. When using the GMSK modulation, only Doppler tracking is foreseen to be used. A ground station contact of 4 hours/day is currently baselined. This includes 0.5 hours for setup, which leaves 3.5 hours for data downlink and TT&C.

9.8 Development Plan

At the end of the assessment phase, 3 different design solutions have crystallized. They each have their own development plan based on the specific details of each design concept. One point they have in common is the multi-aperture approach in which several, identical telescopes are used to obtain the required FoV and collecting area. This is reflected in the development plans such that the manufacturing of the payload elements such as optical elements, CCDs, structure etc. can be manufactured in parallel. As soon as enough elements are manufactured to complete one telescope, the assembly of that telescope can commence. There is no need to wait for components to be completed for all telescopes before the assembly and testing at individual telescope level can start.

At Payload Module sub-system level it is foreseen to have a full cycle of models (including EBB/BB, STM or EQM, PFM/FM) due to the level of new design efforts needed.

At Payload Module global level the two industrial contractors differ in their approach. One is dividing the PLM in 5 different elements (Focal Plane Array, Telescope Assemblies, Data Processing Units, Payload Interface Plate, Deployable Sunshield), on which different model philosophies are used. The development of these different payload systems can be done in parallel to maximize the efficiency. The other industrial contractor is basing the global PLM model philosophy on a STM and PFM approach. Furthermore, a PLM EQM will be developed which will in particular be focused toward securing development of critical items such as the FPA and telescope assembly process. The PLATO Payload Consortium is base-lining a PLM global model philosophy on an EM, QM and FM. For the Service Module sub-systems it is foreseen to make use of STMs and EQMs up until FM only in the case of major modifications. Otherwise a PFM approach is foreseen for recurring items with minor modifications. This is due to the fact that there is a lot of design heritage on the SVMs for both industrial contractors.

At Service Module global level it is foreseen to implement only a STM and PFM/FM since the SVM has a higher level of maturity than the PLM.

9.9 Technology Readiness Level

The requirement in terms of TRL for M-class missions is that all TRL values should be 5 or higher at the time of start of the implementation phase (2012). In terms of the SVM sub-systems, this requirement is not foreseen to be an issue.

In terms of PLM elements, a number of critical areas have been identified depending on the particular design concept.

- For design concept A, the Deployable Sunshield is identified as a critical area in which the TRL needs to be raised before a possible implementation phase. In particular, the HDRM that will need to provide structural stability during launch needs to be developed; since the GAIA approach of having it connected to the thermal tent is not possible in the case of PLATO due to different designs.
- For design concept B, the mounting of lenses in barrel segments which should in turn be assembled with a very high degree of alignment accuracy is the largest challenge in this concept. The launch would be done in a warm environment while the operating environment in space is cold, which means that there will be a shift in the de-focus since the optical design is sensitive to temperature. This will have to be

carefully measured before in order to correct for this shift in focus once in orbit. Producing a prototype in phase A/B1 will mitigate these development risks.

- For design concept C a similar activity would be needed as for design concept B, with some differences. The telescope barrel is produced in one segment only, which means that all lenses will have to be mounted in the same segment and this includes two aspherical lenses. This means that a prototype is needed to ensure the required TRL levels are reached in a timely manner.
- Common for all concepts is the need for an early CCD design activity so that there is sufficient time to produce all the CCDs needed. The specifications of the CCDs are not more complex compared to other programs such as GAIA, but the designs require many CCDs due to the large FoV. So the critical issue is rather in having enough time to produce and test all CCDs instead of new, complex CCD designs. This is why a development activity in phase A/B1 is needed to ensure that production of the FM CCDs can start as soon as possible.

10 MISSION OPERATIONS

10.1 Mission Operations Centre

10.1.1 Scope

The mission is operated by the Mission Operations Centre (MOC) at ESA/ESOC. ESOC is responsible for:

- mission operations planning
- spacecraft operations
- instrument operations execution
- mission data distribution and archiving

The science operations are organised by the Science Operations Centre (SOC) at ESAC (see section 10.2).

There is no opening of science data required by the MOC. The mission is conducted by ESA, fully relying on ESA/ESOC infrastructure, requiring no operational interfaces to non European space agencies. A close link of the project teams of PLATO, GAIA, and other Cosmic Vision Observatory missions is assumed. The PLATO mission operations will comprise Spacecraft Operations and Science instruments operations (based on operations requests from the European Space Astronomy Centre (ESAC) in Villafranca.).

The mission operations can be broken down into the following tasks:

- Mission Planning: long term, medium and short term planning (24 hours to one week time frame, it is assumed that only very limited short term planning activities are required for PLATO.)
- Spacecraft control, following the Flight Operations Plan and the short-term plan
- Spacecraft status monitoring and off line performance analysis.
- Instrument control, implementation of the observation schedules
- Collection of the instrument HKTM telemetry and instrument status monitoring.
- Orbit determination and control using tracking data and implementing orbit manoeuvres.
- Off line attitude determination and control based on the processed attitude sensors data in the spacecraft telemetry and by commanded updates of control parameters in the on-board attitude control system.
- On-board S/W maintenance (OBCP programming and maintenance, and application and payload software update management).
- Data distribution and data archiving (science data are archived at ESAC).
- Maintenance of ESA ground facilities and network.

10.1.2 Operational Concept Goals

ESA/ESOC will prepare a Ground Segment including all facilities, hardware, software, documentation, the respective validation, and trained staff, which are required to conduct the mission operations. The operations cost shall be optimised by a respective effective mission and ground segment design. The concept for the establishment of the PLATO ground segment shall be the maximum sharing of the general ESA/ESOC infrastructure and reuse of manpower, facilities and tools of the Science Observatory family of missions, customised to meet the mission specific requirements. (The sharing/reuse depends on the time phasing of the PLATO mission with the corresponding on-going projects, which could be in the exploitation or in the preparation phase). Nominal spacecraft control during the commissioning and operational phases shall be preplanned. A daily pass with only one ground station will be allocated for communications with the spacecraft during these phases. The PLATO spacecraft is assumed to provide on-board capabilities such that the satellite is able to perform corrective actions in case of single on-board anomalies and the ground segment does not need to monitor the spacecraft in real time.

10.1.3 Mission Planning, Spacecraft Monitoring and Control

The Operations support activities for PLATO can be summarized as follows:

- All operations will be conducted by ESOC according to procedures contained in the FOP (Flight Operations Plan).
- Nominal Spacecraft control during the routine mission phase will be preplanned. (Exceptions are only possible for selected operations during critical phases.) The contacts between the Mission Control Centre and the Spacecraft, except for collecting payload and housekeeping telemetry, will therefore primarily be used for pre-programming of autonomous operation functions on the Spacecraft, and for data collection for off-line status assessment. Anomalies will be normally detected with delay.
- All PLATO operations will be conducted by uplinking of a master schedule of commands for later execution on the S/C. The master schedule will be prepared by a dedicated Mission Planning System. The Mission Planning System will be also used for planning payload operations.
- During the LEOP phase operations will be conducted from the ESOC MCR (Main Control Room).
- During the transfer, commissioning and the nominal operations phase, operations will be conducted from an ESOC DCR (Dedicated Control Room), shared with other missions of the Science observatory family of missions.
- The LEOP sequence of operations is set up such that the Main Flight Control Team (A-Team) controls all critical operations that require a short reaction time (if any).
- The composition of the Flight Control Team during mission preparations and mission operations will be determined by the criticality of the operations and the possibilities of sharing the team with other missions.
- The payload commissioning activities require a collocated PI team with decision authority.
- The SCOS2000 Mission Control System Science Kernel is used. The cost for the MCS development will mainly include the customisation for PLATO.
- A PLATO Mission Planning System will be set up based on existing ESA/ESOC tools.
- Procedures are verified on a spacecraft simulator.
- The simulator is developed under ESA/ESOC responsibility.
- Operations automation and process optimisation will be employed as much as possible based on the ESOC infrastructure developments currently ongoing (MATIS, GSTVi, EKLOPS, EMS, SMF ...).
- For PLATO the mission control system shall allow for support of pass automation (e.g. on the basis of scripts). Automated procedures will be developed and used for basic and recurring activities, e.g. Initial Pass Operations/Establishing of Ground Station Link and some limited reporting capabilities..
- Hardware usage will be shared within the Science Observatory family of missions (e.g. GAIA) where possible (e.g. back-up systems).
- The use of near real time reactions is limited to exceptional cases during critical phases (minimum required feed back time: 3 h. The need for any short term reaction is clearly defined in the Flight Operations Plan and unambiguously identified in the spacecraft telemetry. Any problems are detected in the HKTM and Flight Control/ Contingency Recovery Procedures are available.
- SPACON positions will be manned according to the coverage durations (4h/day during nominal operations).
- Software maintenance includes the maintenance of existing and programming of new OBCPs as well as the uplink, validation and management of the system software versions.

10.1.4 Orbit and Attitude Control

The trajectory, attitude and coverage analyses required for mission preparation are carried out by Mission Analysis.

For the mission the Flight Dynamics support will consist of:

- Orbit determination of the satellite during the LEOP, transfer, commissioning and nominal operations phases using X-band two-way Ranging and two-way coherent Doppler data.
- Optimisation of trajectory correction and orbit maintenance manoeuvres.
- Attitude Control System Monitoring: monitoring and verification of the on-board functions such as star tracker window and sensitivity setting.
- Antenna steering.
- Manoeuvre command generation: preparation of command sequences for input to the master schedule updates related to all orbit and attitude manoeuvres.
- Manoeuvre monitoring.
- Calibration of thrusters and sensors
- The following rule will apply:

If possible, ΔV manoeuvres shall be performed under visibility. As a guideline other spacecraft activities and manoeuvres shall be performed such that the effect can be observed during a coverage thereafter.

10.1.5 Communications

Coding and Modulation

PLATO can use the same coding and modulation scheme as GAIA, i.e. GMSK and RS plus convolutional coding with a TBD level of convolutional coding. The level of convolutional coding can be chosen between level $\frac{1}{2}$ and no convolutional coding in dependence of the finally selected data rate.

The alternative is LDPC codes and QPSK modulation. This can also be accommodated by the operational concept, if the respective coding and modulation are standardised and chosen by PLATO in time for the definition of the next generation IFMS.

Ranging

The downlink modulation scheme for high data rate is based on suppressed carrier. The ranging standard, however, requires a carrier. Ranging is thus not compatible with high data rates. The maximum symbol rate compatible with standard ranging is in the order of magnitude of 700 kb/s, the achievable data rate with RS coding is in the order of magnitude of 600 kb/s.

The operational concept for PLATO is to use ranging at the start and end of a pass in connection with a medium data rate and residual carrier modulation. The rest of the pass is used for high data rate downlink. It is estimated that the time available for high data rate is reduced by $\frac{1}{2}$ h, i.e. 3.5 h are available for high data rate downlink.

10.1.6 Ground Segment Design

The ESA/ESOC ground segment will consist of:

- The Ground Stations and the Communications Network
- The Mission Control Centre (infrastructure and computer hardware)
- The Flight Control software System (data processing and Flight Dynamics Software)
- Computer Infrastructure (Mission Control System, Simulator, etc).

The ground segment preparations start 4 years prior to launch. The readiness of the ground segment is tested and validated by a series of test campaigns, e.g. Radio Frequency Compatibility Test (RFCT), Data Flow Test, Mission Sequence Test, System Validation Tests.

Ground Stations and Communications Network

Ground station(s) will be required for communications and precision orbit determination, providing different periods of visibility according to the requirements of the different mission phases.

All control telecommand and housekeeping as well as science telemetry communications with PLATO are performed via X-Band.

The ground stations network to be used for PLATO during LEOP will be composed by the 35m deep space antennas in New Norcia and Cebreros. (Availability of acquisition aids is assumed. This network might be supported or partially replaced by TBD rented external smaller antennas (e.g. 15m antennas), in particular for the first acquisition.). This network almost guarantees a >16 hours coverage of the spacecraft during this critical period.

For all subsequent phases the 35m antenna in New Norcia is the baseline. New Norcia will be replaced by Cebreros or DS3 in case of conflicts with other missions or station maintenance.

In the spirit of a deep space network a detailed schedule will be set up in order to optimise the use of the ESA network. The nominal operational coverage will be 4h/day. It is assumed that use of the network for other missions and maintenance activities of the station are possible with the above coverage times for PLATO. (A further extension of the coverage may be possible, but is subject to a detailed station utilization planning.)

The Ground Facilities Control Centre monitors and remotely controls all the ESTRACK ground tracking stations, using information provided by Flight Dynamics and the scheduling office. They are also responsible for the TM/TC links to and from the ground stations and any data retrieval of stored tracking (i.e. Doppler and Ranging) from the IFMS equipment at the ground station.

All ESA stations interface to the MOC at ESOC in Darmstadt via the OPSNET communications network. OPSNET is a closed Wide Area Network for data (telecommand, telemetry, tracking data, station monitoring and control data) and voice.

It is assumed that the communication system will support the LEOP and routine data exchanges between the Control Centre in Darmstadt and the Ground Stations identified in this section.

The connection to the SOC is implemented via an internet connection. The data delivery to SOC is via the DDS. (Science data delivery directly from the ground station is an option.)

The Mission Control Centre

The PLATO mission will be operated from ESA/ESOC by the Flight Control Team that is organisationally integrated into the Science Observatory division under OPS-OP.

The mission will be controlled from the Mission Operations Centre (MOC), which consists of the Main Control Room (MCR) augmented by the Flight Dynamics Room (FDR) and Dedicated Control Rooms (DCR's) and Project Support Rooms (PSR's). The MCR will be used for mission control during LEOP. During the subsequent phases the mission control will be conducted from a Dedicated Control Room shared with other Science Observatory missions.

The control centre is equipped with workstations giving access to the different computer systems used for different tasks of operational data processing. The control centre will be staffed by SPACONS shared within the Science Observatory missions. (The manpower assumptions for SPACONS are based on a sharing with other missions.)

The operations are defined by the FCT (Flight Control Team). The FCT consists of operations engineers, i.e. experts in S/C control dedicated to the PLATO mission. The FCT is led by the SOM (Spacecraft Operations Manager). The FCT is supported by a single analyst (backup by sharing resources within the Science Observatory missions). The routine functions on the consoles are performed by SPACONS.

Flight Dynamics and network control are available on a part time basis for the full mission duration.

Space and equipment for scientists, project and industry experts and public relations will be provided close to the MOC as required, during LEOP, transfer and commissioning (i.e. a PISA for the scientists and a project support room for the industry experts will be provided).

10.2 Science Operations

10.2.1 Concept

The major part of the data will become publicly available as soon as it is reduced. This is assured through the PLATO Data Acquisition and Analysis System (PDAAS). The PDAAS consists of a Ground Station (GS), a Mission Operations Center (MOC), a Science Operations Center (SOC) and a PLATO Data Center (PDC). Of these, the latter (PDC) is community provided, while all the former are the task of ESA. PDAAS will provide support for the validation, calibration, and scientific analysis of the PLATO observations in order to deliver the PLATO Data product.

10.2.2 Data products and processing

The baseline science telemetry budget yields a daily uncompressed data volume of 109 Gb. Over a nominal 6 year mission the total science telemetry down-linked will therefore be around 30 TB uncompressed data. The raw telemetry will be reformatted into a standard self-describing format in common use by the astronomical community (FITS). This restructuring may entail format expansion of the packed telemetry to be compatible with widely used file formats (e.g. from 24-bit to 32-bit integers), and/or duplication of some quantities which may in the raw telemetry be represented as a single value associated with a large ensemble of data points, but which must be duplicated across every object light curve if those light curves are to be fully self-describing (time-stamps are an example of this). We estimate that this reformatting may increase the data volume by 50 %.

The PLATO data products will be divided into three main categories, corresponding to three successive levels of treatment:

- L0 (Level 0) data will correspond to the data delivered by the individual telescopes. They will include individual light curves and centroid curves, as well as imagerettes for a set of selected targets. L0 data will not include instrument corrections other than those already applied on board.

Treatments at this level will also include a processing of the available imagerettes, in order to validate the performances of the on board treatment and provide elements to optimize it.

- L1 (Level 1) data will include further instrumental corrections, such as those related to temperature sensitivity, some specific CCD corrections, and most importantly jitter as posteriori correction. L1 treatment will also include the calculation of suitable averages of individual light curves and centroid curves for each star.

- L2 (Level 2) data will correspond to all further scientific treatment of the data, including transit detection and measurements, stellar oscillation mode parameters, as well as star and planet characteristics. The L2 data will have a high scientific added value, and will make use of the PLATO L1 data on one hand, and of all other information gathered on the PLATO targets on the other hand (e.g. high spectral resolution observations and radial velocity monitoring), assembled in an ancillary database.

It is foreseen that all L0 and L1 data will be delivered under responsibility of the ESA-funded SOC, while the L2 data will be produced by the nationally-funded PDC.

More precisely, there will be seven PLATO Data Products (DP0-DP6) in all, distributed among the three levels of treatment described above:

- DP0 The validated light curves and centroid curves for all individual telescopes (Level 0 or L0).

- These are all the downloaded light curves (one each from each star and from each telescope) as well as the centroid curves and validated by assessing the quality and integrity of the data.
- DP1 The calibrated light curves and centroid curves for each star (Level 1 or L1) and corrected for instrumental effects e.g. jitter. For all stars, the L1 calibrated data is the basic science-ready PLATO data. For the normal telescopes and for each star, the L1 light curves and centroid curves are (suitably) averaged, and an associated error is provided. The stars for which imagerettes are available undergo a specific treatment.
 - DP2 The planetary transit candidates and their parameters (Level 2 or L2). A list of candidates with a ranking according to planetary likelihood and an assessment of false alarm probability. The list should contain (at least) the basic characteristics of the transits (depth, duration, period, ephemeris). The list of planetary candidates is discerned from both the light curves and the analysis of the centroid curves (astrometry)
 - DP3 The asteroseismic mode parameters
 - o For solar-like pulsators: Frequencies, amplitudes, lifetimes, harmonic degrees, and azimuthal orders of individual modes of oscillation (and their associated errors). When individual modes are not resolved in frequency space, then average quantities will be provided, such as the large and small frequency separations and the average rotational splitting frequency (L2).
 - o For classical pulsators: Frequencies, amplitudes, and phases of individual modes of oscillation and associated errors (L2).
 - DP4 The stellar rotation periods and stellar activity models inferred from activity-related periodicities in the light curves. Analysis and characterization of stellar variability on various time scales from micro-variability to activity cycles. In some case, star spot models may be inferred from the light curves (L2).
 - DP5 The seismically-determined stellar masses and ages of stars, (and their formal errors), obtained from stellar model fits to the frequencies of oscillations (L2).
 - DP6 The list of confirmed planetary systems, which will be fully characterized by combining information from the planetary transits, the seismology of the planet-host stars, and the follow-up observations(L2).

DP6 represents the most important PLATO (the final and highest level PLATO science) deliverable and includes:

- A list of confirmed planets, deduced from DP2 and follow-up observations.
- The basic parameters of the confirmed planets: orbital parameters, planet size, mass, and age (from the seismology of central stars).
- Any additional characterization of the properties of the planetary systems from the long duration PLATO light curves (e.g. secondary transits) and from specific ground-based observations (e.g. planetary atmospheres, imaging, etc).

10.2.3 Observing modes

Long-duration Observation Phase

The two long-duration observation phases will take up most of the mission life time. They are each required to last for longer than two years with a goal of 3 years. Each will monitor a separate field in the sky that together will be encompassing a minimum of 20000 dwarf stars of spectral type later than F5, each of a magnitude allowing a photometric noise level below $2.7 * 10^{-5} \text{ hr}^{-1}$.

Step-and-Stare Phase

The step-and-stare phase will occur after the two 'long pointings'. It will consist of a number of separate pointings each lasting up to 5 months. The rationale is to extend the surveyed area of the sky to a large fraction of the whole sky, as well as investigate objects found to have two or more transits during the long pointings and to confirm and characterize the planets responsible.

10.2.4 Structure of the PDAAS

Ground Segment

The Ground Station (GS) and the Mission Operations Centre (MOC) are in charge of flight- operations and will both be ESA provided. They are described elsewhere in this volume.

ESA will also provide a Science Operations Centre (SOC, mission-critical) in charge of the validation of the Level 0 light curves. The SOC is responsible for monitoring and validating the integrity and quality of the light curves (L0), producing the validated light curves and centroid as well as making the PLATO data products available to the science community. The SOC will also be responsible for all preparatory activities (see below) but may delegate to the PDC. Specifically:

- Mission planning and provision to the MOC of the detailed spacecraft set-up for the next observation: pointing attitude, full list of stars to be monitored, with their coordinates, data-compression, ...
- Acquisition and distribution of spacecraft telemetry received from the MOC.
- Validation of L0 data (DP0) using PDC s/w
- Quality control: Monitoring of data integrity and quality.
- Fine tuning of instrumental set-up and on-board software observational parameters based on quick look data. The SOC will monitor the quality of the data and request MOC to apply pre-defined procedures when needed to optimize the quality of the data or recover from a payload malfunction.
- Ground support for onboard processing.: this task includes a treatment at L0 level of the available imagettes , aimed at reproducing and validating the treatment which is applied onboard. Results of these validation steps may be used to optimize the onboard treatment, by defining the best parameters to be used, e.g. photometric mask sizes, etc.
- Archiving of all PLATO data products, HK data, and ancillary data
- Distribution of the data products to the scientific community
- Development, validation, integration, operation and maintenance of the SW and HW required for the above SOC tasks. Where it is payload specific (e.g. quick-look), the SW need to be developed together with the DPC where instrument expertise lies.
- The scientific community will provide a PLATO Data Center (PDC, science-critical) in charge of the production of, the set-up and maintenance of the ancillary data base, and the computation of the

science data products (L2), as well as preparing the archive data (PLATO data products, HK data, and ancillary data). The PDC will also be responsible to develop, validate, integrate, operate and maintain all the HW and SW needed to discharge the above responsibilities. The PDC will be distributed among a few scientific institutes in Europe, which will be selected in response to a call of opportunity.

Parts of the PDC will remain operational for at least three years after the end of the PLATO space operations phase to enable the confirmation of planets with periods of up to three years. The software and hardware technologies available today would suffice to build a successful PDAAS. The complexity of the PDAAS lies mostly in the management, integration, and validation of its many hardware and software components.

It is fundamental for the efficient handling and processing of the data and in order to ensure a prompt delivery of data to the scientist community that the interaction between the teams developing the payload, the SOC and the PDC is established as early as possible during the project and then maintained all the way up to and including the archive phase. The aim is to capture as much as possible of the payload expertise from the instrument developers and transmit it to the developers of the quick-look analysis and data reduction systems.

Data policy

The goal will be to make the data available publicly as soon as possible, within the boundaries defined by the requested quality of the data products, and by the data rights policy. The deliverables are the L1 and L2 data products.

L1 products are delivered by the SOC. These are the official products of PLATO. They are made public as soon as they are validated by the SOC.

Among the several hundreds of thousand targets, a number (< 1000, TBC) are "reserved" for the Payload and DPC Principal Investigators and their collaborators. The L1 products for these reserved targets remain proprietary for one year after their validation by the SOC.

The L2 products remain the property of the payload and PDC PIs for a year (TBC) after they are validated by the PDC.

Archiving

As soon as data products have passed quality control and after suitable proprietary period the data are made accessible to the astronomical community through an archive which is managed and maintained by ESA/SOC.

The mission will deliver not only the complete set of data products but also the required software, and the interfaces (including Virtual Observatory interfaces) to all the data obtained during the mission. Results in the form of proper identification of targets, catalogues and relevant associated supporting follow-up observations will be made available through the VO registries. The external users will be able to access the Archive through a number of web interfaces as well as through fully-compliant Virtual Observatory interfaces and mission-specific tools. Cross-referencing between the mission data and external relevant data sources will also be possible. During proprietary periods, Archives access rights will be set-up to ensure that protected data can be retrieved only by the payload and PDC PIs and their collaborators.

Preparatory activities (GAIA, OGS)

PLATO will depend on GAIA for selection of the objects that will be observed.

A major task in preparation for the PLATO mission will be to identify the cool dwarfs and subgiants in the very wide field of view of the instrument. This will be done using early Gaia results. With stellar luminosities known to better than 30-40% and effective temperatures determined to within about 10% (500 K accuracy), which is well achievable using astrometry and multiband photometry in the first two years of Gaia exploitation, stellar radii will be known to within 15-20%, which is amply sufficient to distinguish dwarfs and subgiants from giants and supergiants.

What is also needed is a full catalogue of faint neighbouring sources, including their positions, magnitudes and colours, down to approximately 19th magnitude, in sub-fields of at least 1 arcmin around each PLATO

target. This information will be used to optimize the photometric algorithm for each target, and therefore will impact on the fine tuning of the onboard data treatment software. It is therefore also needed by **mid-2016**. The information that is contained in the Gaia first release (positions, G band magnitudes, and colours from the red and blue spectro-photometry) will be sufficient for this purpose.

Assuming a PLATO launch in December 2017, this is more than four years after Gaia launch, and more than two years after the expected first partial release of Gaia results. In the very unlikely case of a major delay or failure of the Gaia mission, the process can, however, be replaced by a ground based program that could be carried-out at e.g. the ESA OGS telescope in Teneriffe, Spain.

11 MANAGEMENT

This chapter gives an overview of the preliminary management approach of the PLATO mission as currently foreseen. As the mission evolves through possible later phases, this approach will be updated and possibly revised.

11.1 Preliminary Procurement Approach

This section gives an overview of the procurement philosophy for PLATO. As the actual approach has not yet been decided, the approach listed here is only one possible solution and may change depending on the funding and national involvement from member states looking to be involved in PLATO, should it go through to the next phase.

11.1.1 Industrial Organisation

After a possible down-selection of the PLATO mission to a phase A/B1, the Invitation to Tender (ITT) will be released during the spring of 2010. The scope of this contract would be to further define the ESA procured elements of the space segment, i.e. SVM. There will be two competitive industrial contracts for phase A/B1 (as in the assessment phase). The final industrial organization will be completed only in Phase B2, mostly through a process of competitive selection and according to the ESA Best Practices for subcontractor selection, by taking into account geographical distribution requirements.

It is currently foreseen that an industrial prime contractor would design, manufacture and test the Service Module. It would also be in charge of the responsibility of global assembly, integration and testing of the whole PLATO spacecraft (SVM and PLM).

Industrial contracts would be funded and placed by ESA. The responsibility for control and monitoring of the contracts and provision for liaison between partners, contractors and PI groups would be with the ESA project team. Ground segment, Launcher and Mission and Science Operations are the responsibility of ESA.

The following list is a summary of the preliminary industrial organisation, in which ESA would be responsible for the following elements:

- The overall mission design and provision of Service Module (industrial contract)
- Global Assembly/Integration/Testing and Verification of SVM and PLM (industrial contract)
- Spacecraft Launch and Operations (Arianespace, ESOC and ESAC)
- Acquisition and distribution of data to the Science Data Centre (ESOC, ESAC)

11.1.2 Payload Procurement

In conjunction to the industrial invitation-to-tender, an Announcement of Opportunity (AO) will be released to which proposals for the PLATO payload should be submitted.

The PLATO payload (PLM) would be under the responsibility of the PLATO consortium with a lead agency responsible for the assembly, integration and testing of the payload. As such, the PLATO payload would be financed via national agencies.

The responses to the AO should contain a proposal of a payload concept complete with a technical description, budget provisions (mass, power, data rates, physical sizes etc.), schedule, payload interface parameters, deliverable output etc. It should also describe the organigramme of the payload consortium and the contribution of each participating institute/organisation. A clear management structure should be described for the consortium in which the scientific, technical and data analytical management structure is detailed. Also included, should be an estimated cost including funding from participating national agencies and at least one agency being identified as the lead agency (fulfilling the Science Management Plan). Attached to the AO would be a number of ESA provided documents including the Mission Requirements Document (MRD), Payload Definition Document (PDD), Science Requirements Document (SciRD) and

Mission Assumptions Document (MAD), all of which will have been updated with the results of the assessment phase. The Science Management Plan (SMP) would also be included and will describe how the scientific objectives would be fulfilled and how the involved science institutes would be associated with the mission.

Once the contracts for phase A/B1 are in place, the first part of this phase should work to harmonize, via the ESA PLATO Study Team, a number of critical areas such as:

- SVM – PLM interface requirements
- Agree on refined resource budgets for the payload to be provided by the platform (mass, power, data rate)
- General review of payload-related requirements (e.g. required jitter-noise which would have an impact on the platform sub-systems such as AOCS)

At the end of phase A/B1 all interfaces and allocated resources shall be frozen, in order to be prepared for a possible implementation phase. At the end of Definition Phase (A/B1) a scientific evaluation by ESA’s scientific advisory bodies will provide a recommendation as to the final selection of missions to go into Implementation Phase instrumentation. This recommendation will be provided to the Science Programme Committee (SPC) for approval and the successful candidates will move into the Implementation Phase (Phase B2/C/D) and a Prime industry contract will be selected via a further ITT for start in 2012.

11.2 PLATO Schedule

The Definition Phase (A/B1) system study is expected to start in mid-2010 for a period of 15 months, with the objective to enable the mission final adoption early 2012. It will include two major reviews: the Preliminary Requirements Review (PRR), to be held by the mid-term of the study, and the System Requirements Review (SRR), which will close the Definition Phase. The Technology Development Activities (TDAs) will be initiated as soon as possible after the mission down-selection in February 2010. These activities will run in parallel with the Definition Phase and their intermediate results will be fed into the System Study as necessary. At the PRR, the mission baseline should be well established and documented. It will be critically reviewed, with the aim of confirming the technical and programmatic feasibility of the space segment, and more generally of the overall mission concept. The System Requirements Review will close the Definition Phase by consolidating the overall mission concept for enabling an efficient start of the Implementation Phase, should the mission be finally adopted.

Due to the fact that the different designs have different optical solutions, number of telescopes and critical items, which in turn impose different development plans, AIT/AIV logic etc, only a schedule overview is given here for illustration purposes. As mentioned before, the multi-aperture approach to PLATO is of benefit since individual telescopes (or groups of telescopes) can be assembled, integrated and tested as soon as enough components have been manufactured. This is important when considering the limited time available before the CV M-class launch date. An overview of the schedule is shown below in Figure 11-1.

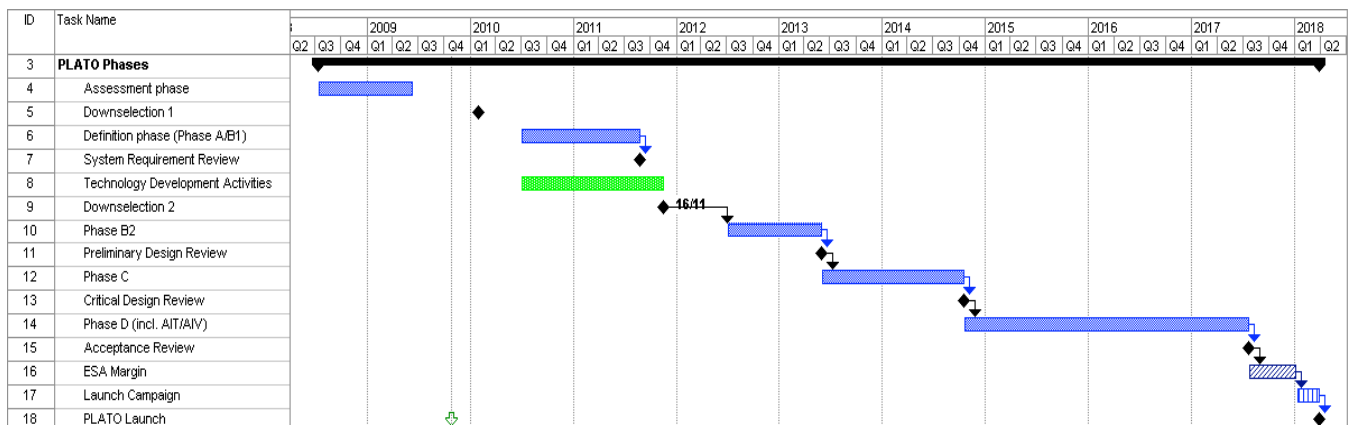


Figure 11-1. An estimated schedule of the PLATO mission.

11.3 List of acronyms

AD	Applicable Document
AOCS	Attitude and Orbit Control System
AMA	Absolute Measurement Error
APA	Absolute Pointing Accuracy
BOL	Beginning of Life
BP	Black Paint
CAN	Controller Area Network
CCD	Charge Coupled Device
CDMU	Central Data Management Unit
CFRP	Carbon-Fibre Reinforced Plastic
CoM	Centre of Mass
CPS	Chemical Propulsion System
DHS	Data Handling System
DoF	Degrees of Freedom
DPU	(Telescope) Data Processing Unit
ECSS	European Co-operation for Space Standards
EIU	Electrical Interface Unit
EOL	End of Life
ESA	European Space Agency
ESAC	European Space Astronomy Centre
FEE	Front End Electronics
FGS	Fine Guidance Sensor
FoV	Field of View
FPA	Focal Plane Assembly
FPI	Focal Plane Instrument
GFRP	Glass-Fibre Reinforced Plastic
GMSK	Gaussian Minimum Shift Key
GSE	Ground Support Equipment
HCMM	High capacity memory module
HDRM	Hold-down and Release Mechanism
HGA	High Gain Antenna
HP	Heat Pipe
ICU	Instrument Control Unit
IPPM	Integrated Processing Payload Module
LGA	Low Gain Antenna
LOS	Line Of Sight

MLI	Multi-Layer Insulation
MMU	Mass Memory Unit
MOC	Mission operations Centre
OB	Optical Bench
PDAAS	PLATO Data Acquisition and Analysis System
PDC	PLATO Data Centre
PIP	Payload Interface Plate
PLM	Payload Module
PPLC	Plato PayLoad Consortium
ppm	part per million
PRR	Preliminary Requirements Review
PSST	PLATO Study Science Team
PSF	Point Spread Function
PSU	Power Supply Unit
QE	Quantum Efficiency
RD	Reference Document
RFI	Radio Frequency Interference
RPE	Relative pointing Error
RTC	Remote Terminal Controller
S/C	Spacecraft
SiC	Silicone Carbide
SpaceWire	Space Wire
SRR	System Requirements Review
SOC	Science Operations Centre
SSM	Second Surface Mirror
SVM	Service Module
SW	SoftWare
TBC	To Be Confirmed
TBD	To Be Defined
TLS	Telescope
TMA	Three Mirror Anastigmat
WP	White Paint
WRT	With Respect To

12 REFERENCES

- Aerts C., 2008, “Core Overshoot and Nonrigid Internal Rotation of Massive Stars: Current Status from Asteroseismology”, IAU Symposium, 250, 237
- Aerts C., Christensen-Dalsgaard J., Kurtz D. W., 2009, “Asteroseismology”, Springer-Verlag, Heidelberg
- Aigrain S., Pont F., Fressin F., et al. 2009, A&A, in press
- Aigrain S., Collier Cameron A., Ollivier M., et al. 2008, A&A, 488, L43
- Alapini A., Aigrain S., 2009, A&A, in press
- Alibert A., Mordasini C., Benz W., Winisdoerffer C., 2005, A&A, 434, 343
- Alibert A., Mordasini C., Benz W., 2004, A&A, 417, L25
- Almenara J.M., Deeg H.J., 2009, A&A, in press
- Alonso R., Guillot T., Mazeh T., et al. 2009, A&A, 501, L23
- Alonso R., Auvergne M., Baglin A., et al. 2008, A&A, 482, L21
- Alonso R., et al 2007, “The Transatlantic Exoplanet Survey (TrES): A Review”, Transiting Extrapolar Planets Workshop ASP Conference Series, Vol. 366, 13. Edited by C. Afonso, D. Wel Drake, and Th. Henning. San Francisco: Astronomical Society of the Pacific.
- Appourchaux T., Michel E., Auvergne M., et al. 2008, A&A, 488, 705
- Auvergne M, et al. 2009, A&A, in press
- Bakos G., Torres W., Pal A., et al 2009, arXiv:0901.0282
- Bakos, G., Noyes, R. W., Kovács, G., Stanek, K. Z., Sasselov, D.D., & Domsa I., 2004, PASP, 116, 266
- Barge P., Baglin A., Auvergne M., et al. 2008, A&A, 482, L17
- Barnes S.A., 2007, ApJ, 669, 1167
- Bazot M., Vauclair S., 2004, A&A, 427, 965
- Beaulieu, J.-P., Bennett D., Fouqué P., et al. 2006, Nature, 439, 437
- Bennett D.P., Bond I.A., Udalski A., et al. 2008, ApJ, 684, 663
- Bonfils X., Mayor M., Delfosse X., et al. 2007, A&A, 474, 293
- Bonomo A.S., Aigrain S., Bordé P., Lanza A.F., 2009, A&A, 495, 647
- Borucki, W.J., Koch, D., Jenkins, J., Sasselov, D., Gilliland, R., et al., 2009, Science, 325, 709
- Bouchy F., Mayor M., Lovis C., et al. 2009, A&A, 496, 527
- Bouchy F., Carrier F., 2001, A&A, 374, 5
- Brown T. M., Christensen-Dalsgaard J., Mihalas B., Gilliland R., 1994, ApJ, 427, 1013
- Burrows A., Hubeny I., Budaj J., Hubbard W.B., 2007, ApJ, 661, 502
- Burrows A., Sudarsky D., Hubeny I., 2006, ApJ, 650, 1140
- Carrier F., Eggenberger P., Bouchy F., 2005, A&A, 434, 1085
- Catala C., 2009, Com. in Asteroseismology, in press
- Chaplin W. J., Appourchaux T., Arentoft T., et al., 2008, Astronomische Nachrichten, 329, 549
- Charbonneau D., Knutson H., Barman T., et al. 2008, ApJ, 686, 1341
- Charbonneau D., Allen L.E., Megeath S.T., et al. 2005, ApJ, 626, 523
- Charbonneau D., Brown T.M., Noyes R.W., Gilliland R.L., 2002, ApJ, 568, 377

Charbonneau D., Brown T.M., Latham D.W., Mayor M., 2000, *ApJ*, 529, L45

Christensen-Dalsgaard J., 1988, "A Hertzsprung-Russell diagram for stellar oscillations", *Proc. IAU Symposium No 123, Advances in helio- and asteroseismology*, Eds Christensen-Dalsgaard, J., Frandsen, S., Reidel, Dordrecht, 295

Christensen-Dalsgaard J., 2002, *Reviews of Modern Physics*, 74, 1073

Claret A., 2007, *A&A*, 475, 1019

Clementini G., Gratton R., 2002, *European Review*, 10, 237

Debosscher J., Sarro L. M., Lopez M., et al. 2009, *A&A*, in press

Degroote, P., Briquet, M., Catala, C., Uytterhoeven, K., Lefever, K., Morel, T., et al., 2009, *A & A*, 506, 111

Deheuvels S., Brunt H., Michel E., et al. 2009, *A&A*, submitted

Deming D., Harrington J., Laughlin G., et al. 2007, *ApJ*, 667, 199

Deming D., Brown T., Charbonneau D., et al. 2005, *ApJ*, 622, 1149

Demory B.-O., Gillon M., Barman T., et al. 2007, *A&A*, 475, 1125

De Mooij E.J.W., Snellen I.A.G., 2009, *A&A* 493, L35

De Ridder J., Arentoft T., Kjeldsen H., 2006, *A&A*, 365, 595

Dravins D., 1990, *A&A*, 228

Fortney J., Marley M.S., Barnes J.W., 2007, *ApJ*, 659, 1661

Fossey S., Waldmann I.P., Kipping D.M., 2009, *MNRAS*, 396, L16

Fridlund et al 2009, *A&A*, submitted

Garcia R., et al., 2009, *A&A*, 506, 41

Gillon M., Pont F., Demory B.-O., et al. 2007, *A&A*, 472, L13

Girardi L., Groenewegen M.A.T., Hatziminaoglou E., da Costa L., 2005, *A&A*, 436, 895

Gough D.O., 1990, *Progress of Seismology of the Sun and Stars*, 367, 283

Haywood M., 2009, *ApJ*, 698, L1

Hu Y., Yang D., Yang J., 2008, *Geophysical Research Letters*, 35, L19818

Ida S., Lin D.N.C., 2005, *ApJ*, 626, 1045

Ida S., Lin D.N.C., 2004, *ApJ*, 616, 567

Irwin J.B., Charbonneau D., Berta Z., et al. 2009, *ApJ*, 701, 1436

Irwin J.B., 1952, *ApJ*, 116, 211

Johnson J.A., Winn J., Narita N., et al. 2008, *ApJ*, 686, 649

Khodachenko M.L., Rucker H.O., Kislyakov A.G., Zaitsev V.V., Urpo S., 2006, *Space Science Rev.*, 122, 137

Kirsh D.R., Duncan M., Brassier R., Levison H.F., 2009, *Icarus*, 199, 197

Kjeldsen H., Bedding T. R., Christensen-Dalsgaard J.C., 2008, *ApJ*, 683, L175

Kjeldsen H., Bedding T., Butler P., et al. 2005, *ApJ*, 635, 1281

Knutson H., Charbonneau D., Allen L.E., et al. 2008, *ApJ*, 673, 526

Knutson H., Charbonneau D., Allen L.E., et al. 2007, *Nature*, 447, 183

Krauss L.M., Chaboyer B., 2003, *Science* 299, 65

Kulikov Y.N., Lammer H., Lichtenegger H., et al. 2007, *Space Science Reviews*, 129, 207

Kulikov Y.N., Lammer H., Lichtenegger H., et al. 2006, *Planetary and Space Science*, 54, 1425
 Lammer H., Bredehöft J.H., Coustenis A., et al 2009, *A&A Rev.*, 17, 181
 Lammer H., Kasting J., Caussefière E., et al. 2008, *Space Science Reviews*, 139, 399
 Lammer H., Selsis F., Ribas I., Guinan E.F., Baurer S.J., Weiss W.W., 2003, *ApJ*, 598, L121
 Latham D.W., Stefanik R.P., Mazeh T., Mayor M., Burki G., 1989, *Nature*, 339, 38
 Lebreton Y., 2008, "Stars in the age of micro-arc-second astrometry 2008, A Giant Step: from Milli- to Micro-arcsecond Astrometry", *Proceedings of the International Astronomical Union, IAU Symposium*, 248, 411 – 416
 Lecavelier des Etangs A., Vidal Madjar A., McConnell J.C., Hebrard G., 2004, *A&A*, 418, L1
 Léger A., Rouan D., Schneider J., Barge P., Fridlund M., et al., 2009, *A&A*, 506, 287
 Liu X., Burrows A., Ibgui L., 2008, *ApJ*, 687, 1191
 Lovis C., Mayor M., Pepe F., et al. 2006, *Nature*, 441, 305
 Lovis C., Mayor M., Bouchy F., et al. 2008, *IAU Symp*, 253, 502
 Marcy G.W., Butler R.P., 1996, *ApJ*, 464, L147
 Mayor M., Bonfils X., Forveille T., et al., 2009a, arXiv0906.2780M
 Mayor M., Udry S., Lovis C., et al. 2009b, *A&A*, 493, 639
 Mayor M., Queloz D., 1995, *Nature*, 378, 355
 McCullough P.R., Stys J.E., Valenti J., et al 2005, *PASP*, 117, 783
 McLaughlin D.B., 1924, *ApJ*, 60, 22
 Mermilliod J.C., Maeder A., 1986, *A&A*, 158, 45
 Metcalfe T.S., Creevey O., Christensen-Dalsgaard J., 2009, *ApJ*, 1170, 5356
 Micela G., 2002, "Second Granada Workshop: The evolving Sun and its influence on the planetary environments" Granada, Spain, Montesinos B., Gimenez A, and Guinan E. F., eds., 2002, *ASP* 269, 107
 Michel, E., *Science*, 322, 558
 Miglio A., Montalbán J., 2005, *A&A*, 441, 615 629
 Miglio A., Montalbán J., Noels A., Eggenberger P., 2008, *MNRAS*, 386, 1487
 Monteiro M J P F G., Christensen-Dalsgaard J., Thompson M. J., 1994, *A&A*, 283, 247
 Monteiro M.J.P.F.G., Christensen-Dalsgaard J., Thompson M. J., 2000, *MNRAS* 316, 165
 Mordasini C., Alibert Y., Benz W., Naef D., 2009, *A&A*, 501, 1161
 Mosser B., Appourchaux T. 2010, *A&A*, submitted
 Moutou C., Hébrard G., Bouchy F., et al. 2009, *A&A*, 498, L5
 Naef D., Mayor M., Pepe F., et al. 2001, *A&A*, 375, L27
 Namouni F., 2005, *AJ*, 130, 280
 Noyes R.W., Weiss N.O., Vaughan A.H., 1984, *ApJ*, 287, 769
 Ofek, E.O., 2008, *PASP*, 120, 1128
 Palle E., Osirio M.R.Z., Barrena R., Montanes-Rodriguez P., Martin E.L., 2009, *Nature*, 459, 814
 Palle P.L., Jimenez A., perez Hernandez F., Regulo C., Roca Cortes T., Sanchez L., 1995, *ApJ*, 441, 952
 Pepe F., Lovis C., 2008, *Phsica Scripta*, 130, 4007

Perryman M.A.C., Brown A.G.A., Lebreton Y., et al. 1998, A&A, 331, 81
Pickles A.J., 1998, PASP 110, 863
Pollacco D., Skillen I., Collier Cameron A., et al. 2006, PASP, 118, 1407
Queloz D., Bouchy F., Moutou C., et al. 2009, A&A, 506, 303
Queloz D., Henry G.W., Sivan J.-P., et al. 2001, A&A, 379, 279
Rauer H., Queloz D., Csizmadia Sz. et al 2009, arXiv:0909.3397
Ribas I., Guinan E.F., Gudel M., Audard M., 2005, ApJ, 622, 680
Robin A., Reylé C., Derrière S., Picaud S., 2003, A&A, 409, 523
Robin A., Crézé M., 1986, A&A, 157, 71
Roques, F., Moncuquet, M., 2000, Icarus, 147, 530
Rossiter R.A., 1924, ApJ, 60, 15
Roxburgh I.W., Vorontsov S.V., 1994a. MNRAS, 267, 297
Roxburgh I.W., Vorontsov S.V., 1994b. MNRAS, 268, 880
Roxburgh I.W., Vorontsov S.V., 2001, MNRAS 322, 85
Roxburgh I.W., Vorontsov S.V., 2003a, A&A, 411, 215
Roxburgh I.W., Vorontsov S.V., 2003b, Astrophysics & Space Science, 284, 187
Roxburgh I.W., Vorontsov S.V., 2006, MNRAS, 369, 1491
Roxburgh I.W., 2009a, A&A, 493, 185
Roxburgh I.W., 2009b, A&A, 506, 435
Saar S.H., Butler R.P., Marcy G.W., 1998, ApJ, 498, L153
Saar S.H., Donahue R.A., 1997, ApJ, 485, 319
Sagan C., Salpeter E.E., 1976, ApJ. Suppl., 32, 737
Santos N.C., Benz W., Mayor M., 2005, Science, 310, 251
Sarro L.M., Debosscher J., Aerts C., Lopez M., 2009, A&A, in press
Seager S., Mallén-Ornelas G., 2003, ApJ, 585, 1038
Sing D.K., Désert J.-M., Lecavelier Des Etangs A., et al. 2009, A&A, 505, 891
Snellen I.A.G., de Mooij E.J.W., Albrecht S., 2009, Nature, 459, 543
Stello D., Chaplin W. J., Bruntt H., et al. 2009, ApJ, arXiv:0906.0766v
Struve O., 1952, The Observatory, 72, 199
Swain M., Vasisth G., Tinetti G., 2008, Nature, 452, 329
Tian H., Tu C.-Y., Xia L.-D., He J.-S., 2008, A&A, 489, 1297
Tinetti G., Vidal-Madjar A., Liang M.-C., et al. 2007, Nature, 448, 169
Udry S., Bonfils X., Delfosse X., et al. 2007, A&A, 469, L43
Valencia D., Sasselov D.D., O'Connell R.J., 2007, ApJ, 665, 1413
van den Bergh S., 1995, Science, 270, 1942
Vidal Madjar A., Désert J.-M., Lecavelier des Etangs A., Hébrard G. et al. 2004, ApJ, 604, 69
Vidal Madjar A., Lecavelier des Etangs A., Desert J.-M., Ballester G.E., Ferlet R., Hébrard G., Mayor M., 2003, Nature, 422, 143

Williams, D., Pollard, D., 2003, IJAsB, 2, 1

Winn J.N., Noyes R.W., Holmann M.J., et al. 2005, ApJ, 631, 1215

Wolszczan A., Frail, D.A., 1992, Nature, 355, 145

Vorontsov S.V., 1988, "A search of the effects of magnetic field in the solar five-minute oscillations", Proc. IAU Symposium No 123, Advances in helio- and asteroseismology, Eds J. Christensen-Dalsgaard, S. Frandsen, Reidel, Dordrecht, 151

Wright J.T., Marcy G.W., Butler R.P., Vogt S.S., 2004, ApJS, 152, 261

Zahnle K.J., Walker J.C.G., 1982, Reviews of Geophysics, 20, 280